

**PHYSIOLOGICAL ROLE OF VTC4 IN POLYPHOSPHATE METABOLISM OF
TRYPANOSOMES**

by

NOELIA M. LANDER

(Under the Direction of ROBERTO DOCAMPO)

ABSTRACT

Trypanosoma brucei and *T. cruzi* are the etiologic agents of the most important human trypanosomal diseases: Sleeping sickness (human African trypanosomiasis) and Chagas disease (American trypanosomiasis). Both diseases are potentially fatal and there are no vaccines or satisfactory treatments available for them. We are interested in investigating proteins that can be used as chemotherapeutic targets to develop efficient treatments against African and American trypanosomiasis. We are particularly interested in establishing the role of proteins involved in polyphosphate (polyP) metabolism. PolyP is an anionic polymer of orthophosphate groups linked by high-energy bonds that typically accumulates in acidic, calcium-rich organelles known as acidocalcisomes. PolyP synthesis in eukaryotes was unclear until recent work demonstrated that the protein named vacuolar transporter chaperone 4 (Vtc4p) is a long chain polyP kinase localized in the yeast vacuole. Here, we report that *Vtc4* gene orthologs in *Trypanosoma brucei* (*TbVtc4*) and *T. cruzi* (*TcVtc4*) encode, in contrast, short

chain polyP kinases that localize to acidocalcisomes. The subcellular localization was demonstrated by fluorescence and electron microscopy of cell lines expressing C-terminal tagged versions of these proteins. Recombinant TbVtc4 and TcVtc4 were expressed in bacteria, and polyP kinase activity was assayed *in vitro*. A reverse genetics approach allowed us to study the physiological role of TbVtc4 in bloodstream form (BSF) and procyclic form (PCF) trypanosomes. Our results indicate the enzyme is important for parasite survival *in vitro* and *in vivo*. We conclude that TbVtc4 is required for osmoregulation and virulence. Finally, we used biotinylated polyP to obtain the polyP-binding proteome of *T. brucei* PCF and *T. cruzi* epimastigotes. We identified 73 and 60 potential polyP-binding proteins in *T. brucei* and *T. cruzi* respectively, 36 of which were observed in both datasets. The most relevant proteins found these proteomes were: glycosomal malate dehydrogenase, hexokinase, glycosomal phosphoenolpyruvate carboxykinase, snoRNP protein GAR1, and ribosomal proteins S6, S8, L36 and L38. Additional experimental work would be necessary to validate this proteomic data. *TbVtc4*-KO mutant cell line generated in BSF would be a key tool to study the role of polyP in the activity of potential polyP-binding proteins found in *T. brucei*.

INDEX WORDS: Acidocalcisomes, Osmoregulation, Polyphosphate, *Trypanosoma brucei*, *Trypanosoma cruzi*, Vacuolar transporter chaperone, PolyP-binding proteome

**PHYSIOLOGICAL ROLE OF VTC4 IN POLYPHOSPHATE METABOLISM OF
TRYPANOSOMES**

by

NOELIA M. LANDER

B.S., Universidad Simón Bolívar, Venezuela, 2002

M.S., Universidad Simón Bolívar, Venezuela, 2008

A Dissertation Submitted to the Graduate Faculty of The University of Georgia in
Partial Fulfillment of the Requirements for the Degree

DOCTOR OF PHILOSOPHY

ATHENS, GEORGIA

2013

© 2013

Noelia M. Lander

All Rights Reserved

**PHYSIOLOGICAL ROLE OF VTC4 IN POLYPHOSPHATE METABOLISM OF
TRYPANOSOMES**

by

NOELIA M. LANDER

Major Professor: Roberto Docampo

Committee: Kojo Mensa-Wilmot

Stephen Hajduk

Robert Sabatini

Electronic Version Approved:

Maureen Grasso

Dean of the Graduate School

The University of Georgia

December 2013

DEDICATION

To Marina and Miguel Angel. Thank you for your unconditional support during every single day of this adventure.

ACKNOWLEDGEMENTS

I would like to thank my mentor Dr. Roberto Docampo for giving me the opportunity of joining his laboratory and for all the advice and academic stimulus provided during this PhD. Working under his advisory has been an enriching experience that for sure will determine my professional future. I would also thank all my laboratory partners for five years of invaluable collaborative work, enthusiastic hours of scientific discussion, and great moments in and outside our work environment. I specially would like to acknowledge our laboratory manager Melina Galizzi for her diligent way of organizing things and managing situations at work, so that she made life easier every day, and also for being such a great friend. I also acknowledge Dr. Silvia Moreno for her advisory during the writing of proposals for applying to the American Heart Association pre-doctoral fellowships, and for the academic input during my PhD.

I would like to thank my Committee members, Drs. Kojo Mensa-Wilmot, Stephen Hajduk and Robert Sabatini, for the feedback and orientation provided during our annual meetings. Their input has been very important for the development of this project. Also, I should thank members of the Center for Tropical and Emerging Global Diseases, specially Dr. Boris Striepen and Dr. Rick Tarleton laboratories, for their support during every day work.

Thanks to my Venezuelan Professors Dr. José Luis Ramírez and Dr. José Bubis for supporting my applications to the Graduate School at the University of Georgia and to the American Heart Association pre-doctoral fellowship, and for the academic formation and advice provided before joining this PhD program.

Thanks to my family and friends, for the unconditional support, love, advice and patience during all these years, for giving me hope in the most difficult moments, for making me company in the distance and for letting me understand that home is the place where your beloved ones are. Without them, it would not be feasible for me to complete this journey.

TABLE OF CONTENTS

	Page
ACKNOWLEDGEMENTS	v
LIST OF TABLES	x
LIST OF FIGURES	xi
CHAPTER	
1 INTRODUCTION AND LITERATURE REVIEW	1
Purpose of the Study.....	1
Background and Significance.....	3
Life cycle of <i>T. brucei</i> and <i>T. cruzi</i>	5
The acidocalcisome	6
The physiological role of polyP	8
Enzymes involved in polyP metabolism	10
The Vacuolar Transporter Chaperone (VTC) Complex.....	11
PolyP kinase activity in <i>T. cruzi</i>	12
TbVtc1 is a subunit of the <i>T. brucei</i> VTC complex	13
2 <i>TRYPANOSOMA BRUCEI</i> VACUOLAR TRANSPORTER CHAPERONE 4 (TbVtc4) IS AN ACIDOCALCISOME POLYPHOSPHATE KINASE REQUIRED FOR <i>IN VIVO</i> INFECTION	15

Abstract.....	16
Introduction	17
Experimental procedures	20
Results	35
Discussion.....	46
3 THE ACIDOCALCISOME VACUOLAR TRANSPORTER CHAPERONE	
4 CATALYZES THE SYSTHESIS OF POLYPHOSPHATE IN INSECT-	
STAGES OF <i>TRYPANOSOMA BRUCEI</i> AND <i>T. CRUZI</i>	49
Abstract.....	50
Introduction	50
Experimental procedures	52
Results	64
Discussion.....	72
4 THE POLYPHOSPHATE-BINDING PROTEOME OF <i>T. BRUCEI</i> AND	
<i>T. CRUZI</i>	74
Introduction	74
Experimental procedures	75
Results	79
Discussion.....	86
5 CONCLUSIONS AND FUTURE DIRECTIONS	91
The role of Vtc4 in trypanosomes: what do we know now?	91
The role of polyP in trypanosomes: where do we stand now?	93

REFERENCES96

LIST OF TABLES

	Page
Table 1: Kinetic parameters of purified recombinant Vtc4 catalytic regions from <i>T. brucei</i> and <i>S. cerevisiae</i> with different substrates	40
Table 2: Primers used for molecular constructs to study Vtc4.....	56
Table 3: Morphometric analysis of acidocalcisomes of <i>T. brucei</i> PCF	70
Table 4: Potential PolyP-binding proteins identified in <i>T. brucei</i> PCF	81
Table 5: Potential PolyP-binding proteins identified in <i>T. cruzi</i> epimastigotes.....	85

LIST OF FIGURES

	Page
Figure 1: Schematic representation of a typical acidocalcisome	8
Figure 2: ScVtc4p structure	13
Figure 3: Localization of TbVtc4 in PCF and BSF trypanosomes.....	37
Figure 4: Recombinant polyP kinase activity as a function of substrate concentration	39
Figure 5: TBE-PAGE analysis of polyP produced by TbVtc4 and ScVtc4p catalytic cores	41
Figure 6: Generation of <i>TbVtc4</i> cKO cell line	42
Figure 7: Effect of inhibition of TbVtc4 expression on cell growth, PPK activity, and short and long chain polyP levels	43
Figure 8: Effect of inhibition of <i>TbVtc4</i> expression on the response of BSF trypanosomes to hyposmotic and hyperosmotic stresses	44
Figure 9: Effect of inhibition of <i>TbVtc4</i> expression on virulence in mice.....	45
Figure 10: Sequence analysis of Vtc4 proteins and western blot analysis of the tagged TcVtc4.....	66
Figure 11: Immunofluorescence analysis of TcVtc4	67
Figure 12: Immunoelectron microscopy of TcVtc4	68
Figure 13: Purification and polyP kinase activity of recombinant TcVtc4	69

Figure 14: RNA interference of <i>TbVtc4</i> in <i>T. brucei</i> procyclic forms	70
Figure 15: Morphological changes in <i>TbVtc4</i> RNAi procyclic forms	71
Figure 16: Knockdown of <i>TbVtc4</i> transcripts by RNA interference increases cellular pyrophosphate (PP _i) and decreases short chain polyP levels.....	71
Figure 17: Functional classification of proteins found in <i>T. brucei</i> polyP-binding proteome.....	80
Figure 18: Functional classification of proteins found in <i>T. cruzi</i> polyP-binding proteome.....	84

CHAPTER 1

INTRODUCTION AND LITERATURE REVIEW

Purpose of the Study

This study has been focused on investigating the physiological role of polyphosphate (polyP) in trypanosomes, a conserved and ubiquitous molecule that has been poorly studied in eukaryotic cells, as it has been historically considered a molecular fossil in living organisms. PolyP metabolism and function have been well described in prokaryotes, where long chain polyP is involved in different physiological processes, including transcription regulation, sporulation and pathogenicity (1). In eukaryotes, the role of polyP has been mainly studied in human platelets, where short chain polyP is released from activated platelets and works as a potent proinflammatory and procoagulant agent (2,3). Although this molecule is present in all cell types, where it accumulates in electron dense compartments known as acidocalcisomes (4), enzymes involved in polyP metabolism were not identified in eukaryotes until recent work demonstrated the presence of a polyP synthase in *Saccharomyces cerevisiae* (5). The enzyme (Vtc4p) is the catalytic subunit of the Vacuolar Transporter Chaperone complex, a four-protein complex present in the vacuole membrane of yeasts. Acidocalcisomes are acidic polyP- and Calcium -rich organelles that were first

described in trypanosomes (6,7). Our laboratory has been working with *Trypanosoma brucei* and *T. cruzi* as model organisms to study the role of acidocalcisomes and polyphosphate metabolism during the last two decades. These species are the causative agents of the most important human trypanosomiasis: Sleeping Sickness (African Trypanosomiasis) and Chagas Disease (American Trypanosomiasis). Both diseases are potentially fatal and there are no vaccines or satisfactory treatments available for them. We are interested in investigating proteins that can be used as chemotherapeutic targets for developing efficient treatments against African and American trypanosomiasis. Our approach is to identify metabolic pathways that are not present in human cells but are necessary for parasite survival. We are particularly interested in establishing the role of acidocalcisome proteins involved in polyphosphate (polyP) metabolism. The present work is the functional characterization of the *T. brucei* and *T. cruzi* Vtc4p homologues, both enzymes confirmed to be polyphosphate kinases present in acidocalcisomes.

We have arranged the content of this dissertation into five chapters. In order to emphasize the significance of the study a literature review is presented in Chapter 1. Chapter 2 describes the subcellular localization and enzymatic characterization of TbVtc4, as well as the physiological role of polyphosphate in the mammalian stage of the parasite by evaluating the phenotype of a TbVtc4 knockout cell line in bloodstream forms (BSF). Chapter 3 is focused on the study of Vtc4p homologues in the insect stages of *T. brucei* and *T. cruzi*. Here, the

phenotype of a TbVtc4 knockdown cell line is evaluated in *T. brucei* procyclic forms (PCF) as well as the subcellular localization and enzymatic characterization of the enzyme in *T. cruzi*. As an additional contribution to the polyP role in trypanosomes Chapter 4 summarizes the preliminary results of our polyP-binding proteome analysis in *T. brucei* and *T. cruzi*. Finally, the concluding remarks of the dissertation will be discussed in Chapter 5.

The main contribution of this dissertation is the characterization of an essential polyP kinase in trypanosomes, an enzyme without homologues in mammalian cells that could be validated as a molecular target for the rational design of alternative therapies for human trypanosomiasis. Additionally, our findings underscore the role of polyP in osmoregulation and infectivity, and show new evidences of a possible role of polyP in glycolysis, regulation of transcription/translation, and signal transduction in these organisms.

Background and Significance

T. brucei (Kinetoplastida order) is the etiologic agent of African Trypanosomiasis in humans (HAT or sleeping sickness) and also nagana disease in cattle. Continuous control efforts have decreased the number of new cases reported to about 7,000 in 2012 (8). HAT takes two forms, depending on the parasite sub-species involved: *Trypanosoma brucei gambiense* (*T.b.g.*) is found in west and central Africa. This form currently accounts for 98% of reported cases of sleeping sickness and leads to a chronic infection. An individual can be

infected for years without presenting the major symptoms of the disease. When they appear, the person is most of the times already in an advanced stage of the disease where the central nervous system is affected. *Trypanosoma brucei rhodesiense* (*T.b.r.*) is found in eastern and southern Africa. Currently, this form represents about 2% of reported cases and produces an acute infection. First signs of the disease appear a few weeks or months after infection. The disease develops very fast and affects the central nervous system (8). There is no vaccine available for this disease and chemotherapy also remains unsatisfactory, especially for advanced cases when a neurological phase is reached and the disease becomes potentially fatal.

T. cruzi is another interesting kinetoplastid to use as biological model as it is the causative agent of Chagas disease, an illness affecting an estimate of 7-8 million people worldwide, mostly in Latin America where the disease is endemic (9). Chagas disease can be cured if treated soon after infection. However, no vaccine or satisfactory treatment is available for the chronic phase (9,10). From the affected population, about 2-3 million people are chronic cases who develop serious irreversible heart damage, including cardiomegaly, altered heart rhythm, heart failure, cardiac arrest, or stroke. Although Chagas disease is considered endemic in Central and South America, the number of cases in the USA has increased during the last years. Currently it is estimated that over 300,000 people with Chagas disease are living in the USA, with more than 30,000 cases of Chagas cardiomyopathy expected per year (11).

T. brucei and *T. cruzi* have been widely used as biological models for studying cellular processes in trypanosomatids, thus many genetic tools have been developed for them. This work is a contribution to the study of specific and essential metabolic pathways in trypanosomatids, with the long-term goal of identifying drug targets and developing an efficient, non-toxic chemotherapy for these diseases.

Life cycle of *T. brucei* and *T. cruzi*

African trypanosomiasis is transmitted to humans by the *tsetse* fly, which is the insect vector for *T. brucei*. The parasite lives in the midgut of the fly (procyclic form, PCF), and eventually migrates to the salivary glands passing through epimastigote and metacyclic trypomastigote stages. Then parasites are injected to the mammalian host by biting. The parasite lives within the bloodstream (bloodstream form, BSF) where it can re-infect the fly vector after biting. Later during a *T. brucei* infection the parasite may migrate to other tissues of the host. The disease enters a neurological phase when the parasite passes through the blood-brain barrier (8). In this work we focused on the role of a polyP synthase by assessing the phenotypes associated to genetic mutant cell lines obtained in the two main stages of *T. brucei* life cycle: the procyclic and the bloodstream forms.

T. cruzi presents a digenetic life cycle that involves an invertebrate and a vertebrate host (including humans). A reduviid bug serves as the vector that

ingests trypomastigote forms by blood-feeding from the mammalian host. In the insect's gut, they differentiate into the dividing epimastigote stage and after moving to the rectal cell wall they become infectious metacyclic trypomastigotes. Then, these trypomastigotes present in parasite feces are deposited in the bite wound while the reduviid bug is taking a blood meal from the mammalian host. Once in the bloodstream, they infect almost every tissue, becoming intracellular dividing amastigotes, which differentiate into infectious trypomastigotes after several division rounds. Trypomastigotes are then released into the bloodstream where they can invade new cells from the mammalian host or get taken up by other reduviid bugs (9). As *T. cruzi* passes through its life cycle, it encounters many fluctuations in environmental conditions to which it must adapt in order to survive (12). Changes in polyP content have been reported as response to differentiation and environmental stress in *T. cruzi* (13), highlighting the importance of polyP metabolism among different *T. cruzi* life cycle stages.

The acidocalcisome

Acidocalcisomes are electron dense acidic organelles with a high concentration of polyP complexed with calcium and other inorganic (Mg^{2+} , Zn^{2+} , Fe^{2+} , Na^+ , K^+) and organic (basic amino acids, polyamines) cations (4,14). They were first described in trypanosomes (6,7) and subsequently in Apicomplexan parasites, algae, slime molds, fungi, eggs of different organisms and human platelets (14). They are currently recognized as the subcellular compartments

that were historically described as “metachromatic granules” (15), “volutin granules” (16) or “polyP bodies” (17) in different microorganisms. These granules were known to contain large amounts of calcium and polyP (18). Research work from our laboratory in trypanosomatids and Apicomplexan parasites established acidocalcisomes as real organelles (4,7,19). During the last two decades the discovery of different pumps (H^+ -vacuolar pyrophosphatase, H^+ -vacuolar ATPase, Ca^{2+} -ATPase), channels (aquaporin, inositol 1,4,5-trisphosphate receptor (InsP3R)), exchangers (Na^+/H^+ ; Ca^{2+}/H^+), and transporters, as well as enzymes involved in phosphate metabolism present in acidocalcisomes, has highlighted the physiological role of this organelle for trypanosomes survival (Fig. 1) (20). The recent discovery of an inositol 1,4,5-trisphosphate receptor (TbIP3R) on *T. brucei* acidocalcisomes provided evidence of the mechanism of Ca^{2+} release from these organelles and suggested a role for acidocalcisomes in Ca^{2+} signaling (21). The presence of acidocalcisome-like organelles in a broad variety of organisms, including bacteria (22,23) and human platelets (24) indicates that this organelle has appeared early and persisted over evolutionary time or has arisen by convergent evolution, underscoring the importance of acidocalcisomes for cell physiology (4,20,25).

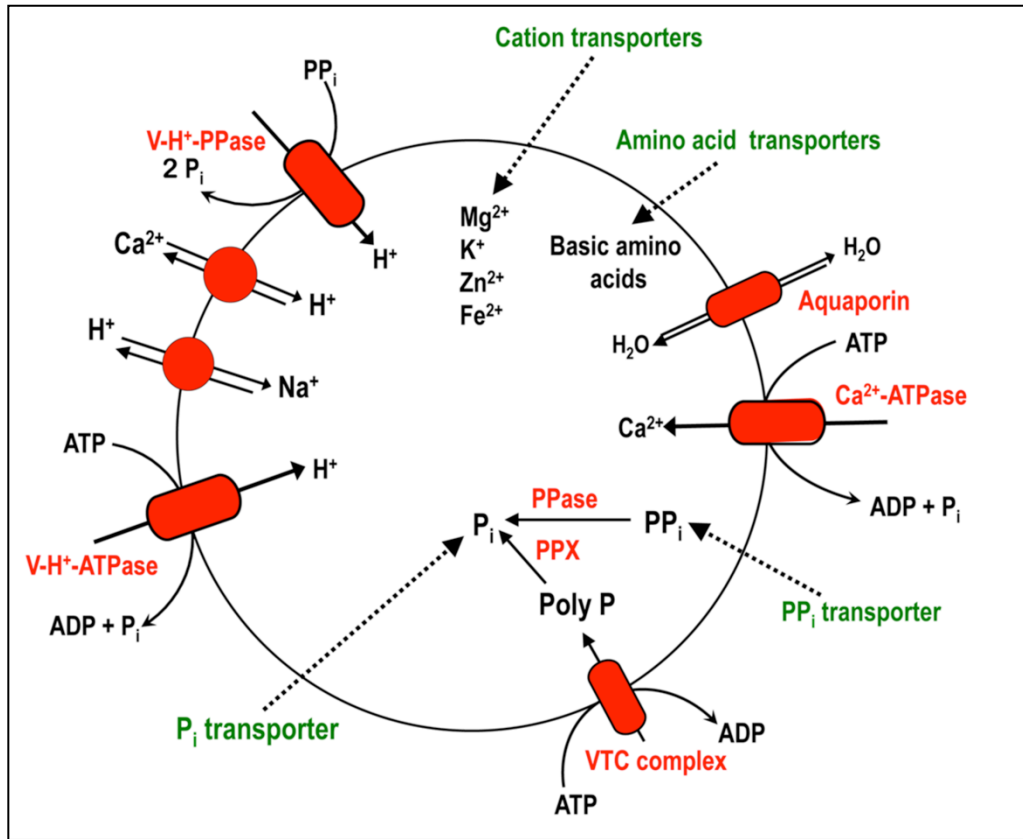


Figure 1. Schematic representation of a typical acidocalcisome. Ca^{2+} uptake occurs in exchange for H^+ by a reaction catalyzed by a vacuolar Ca^{2+} -ATPase. A H^+ gradient is established by a vacuolar H^+ -ATPase and a vacuolar H^+ -pyrophosphatase (V-H^+ -PPase). An aquaporin allows water transport. Ca^{2+} release occurs in exchange of H^+ and is favored by sodium-proton exchange. Other transporters (for example, for Mg , Zn , inorganic phosphate (P_i), pyrophosphate (PP_i), and basic amino acids) are probably present. The acidocalcisome is rich in pyrophosphate, short- and long-chain polyphosphate (poly P), magnesium, calcium, sodium and zinc. An exopolyphosphatase (PPX) and a pyrophosphatase (PPase) are also present. The VTC complex is present at the membrane of the acidocalcisome, where Vtc4 subunit presents the VTC domain, a polyP kinase catalytic core. A dashed line indicates the lack of biochemical evidence for their presence. Modified from (25).

The physiological role of polyP

PolyP is an anionic linear polymer of orthophosphate units linked by high-energy phosphoanhydride bonds. This ubiquitous molecule is abundant in nature and has been conserved during evolution (24). PolyP has been extensively studied in prokaryotes and protists, where it functions in basic metabolism, in

stress response, and as a structural component (1). PolyP is arbitrarily classified into short-chain (from 3 to ~ 300 P_i residues) and long-chain (from 300 to ~ 1000 P_i residues) polyP, based on the methodology used to extract it (14). In bacteria, long-chain polyP is involved in several essential functions as motility, pathogenesis, sporulation, germination, quorum sensing, biofilm formation, gene transcription control, regulation of enzyme activities and DNA replication (1). In eukaryotes, polyP has been found in cytosol, nucleus, lysosomes and mitochondria but it mainly accumulates in acidocalcisomes, where it reaches molar concentrations (14). However, the role of polyP in unicellular eukaryotes has not been so well established. A function in response to stress conditions, including osmotic stress, starvation and infection, has been observed in yeast, fungi, algae and trypanosomes (14,26). In trypanosomatids, drastic changes in polyP levels have been observed under osmotic stress conditions, but these studies have been carried out only in the insect stages of the parasite (27-29). In these organisms PolyP could be also important as P_i reservoir, energy source, chelator of metal ions, regulator of cell metabolism, differentiation and gene activity. An important role for polyP has been recently found in human platelets, where medium size molecules (about 100 mers) function as a new class of platelet-derived proinflammatory and procoagulant mediator, acting at four points in the blood-clotting cascade (3,30). All these new insights on the physiological role of polyP have caught again the interest of researchers for this inorganic polymer. However, the *in vivo* relevance of polyP functions in trypanosomatids

remains unknown. Our approach to understand the role of polyP is to study the enzymes involved in its metabolism in the insect and mammalian stages of *T. brucei* and *T. cruzi*.

Enzymes involved in polyP metabolism

The best studied enzyme in polyP metabolism is polyP kinase 1 (PPK1), a highly conserved enzyme in bacteria that catalyzes polyP processive synthesis by the reversible transfer of the terminal phosphate of ATP to an active-site histidine residue, the initial step in the polymerization of a long polyP chain (31). PPK1 activity has been widely described in bacteria and the slime mold *Dictyostelium discoideum* (1). Other polyP kinases (PPK2) have been described in bacteria and in *D. discoideum* (32,33). Bacterial PPK2 catalyzes polyP synthesis from ATP or GTP. *D. discoideum* PPK2 (DdPPK2) shares characteristics of actin-related proteins and is inhibited by actin inhibitors such as phalloidin and DNase I. This peculiar polyP kinase is able to combine the reversible synthesis of actin-like filaments together with polyP synthesis (33). On the other hand, polyP hydrolysis is catalyzed by exo- and endo-polyphosphatases (PPX and PPN, respectively). PPX activity has been described in bacteria, yeast, trypanosomatids and human cells (H-prune) (1,34-37). PPX removes terminal orthophosphate residues from a polyP chain, degrading the molecule in a processive way. PPNs have been found only in eukaryotic cells, where they catalyze the internal cleavage of polyP to progressively shorter lengths (1).

Another potential pathway for polyP synthesis has been recently related to inositol pyrophosphates (InsPP) metabolism (38). Yeast mutants deficient in phosphoinositide phospholipase C (PI-PLC) exhibited decreased levels of polyP and a link between both pathways (InsPP and polyP synthesis) has been postulated (38). A polyP polymerase (Vtc4p) has been recently characterized in *S. cerevisiae* (5) and the presence of Vtc4 ortholog sequences in several unicellular eukaryotes including human pathogens, has promoted research towards elucidating the role of polyphosphate in eukaryotic cells.

The Vacuolar Transporter Chaperone (VTC) Complex

Using DNA microarray methodology, four *PHM* genes that encode proteins involved in polyP synthesis were identified in *S. cerevisiae* (39). Since then protein sequence homologs from several organisms have been annotated in genome databases as polyP synthases (25). The *PHM* genes were independently identified and named vacuolar transporter chaperone (Vtc) 1–4 (*Vtc1/PHM4*; *Vtc2/PHM1*, *Vtc3/PHM2*, and *Vtc4/PHM3*) (40,41). Homolog sequences to *Vtc1* and *Vtc4* genes are present in the genome of *T. cruzi*, *T. brucei* and *Leishmania major*. TbVtc1, a protein present in *T. brucei* acidocalcisomes, is essential for polyP synthesis, acidocalcisome biogenesis and cytokinesis (42). RNA interference experiments with TbVtc1 altered acidocalcisome morphology and decreased the amount of polyP (42). However, this protein does not have a polyP synthase domain or activity.

The biochemical characterization of *S. cerevisiae* Vtc4p (here called ScVtc4p) showed that it contains the catalytic domain for polyP polymerization, using P_i or PP_i as substrate in an ATP consuming reaction (5). Using a crystallographic approach, this work established that the ScVtc4p structure contained a long chain of electron density winding through the tunnel domain, which corresponds to the generated P_i polymer from ATP during dialysis or crystallization (Fig. 2). Mutational analysis indicated that this vacuolar enzyme integrates cytoplasmic polymer synthesis with polyP membrane translocation (5). These important results opened up a broad spectrum of possibilities for the study of polyP synthases in unicellular eukaryotes. Proteomic data from our laboratory indicated that TbVtc4 is present in the acidocalcisome fraction (Huang, G., Ulrich, P.N., Johnson, D., S.N.J. Moreno, Orlando, R., and Docampo, R., unpublished data) and our preliminary results confirmed this localization. These observations suggested that TbVtc4 and also TcVtc4 are acidocalcisomes proteins that could synthesize polyP in a similar way as to ScVtc4p. The generation and phenotypic characterization of *TbVtc4* mutants provided clues to the role of this enzyme in polyP metabolism and parasite survival.

PolyP kinase activity in *T. cruzi*

A polyP kinase activity has been previously reported by Ruiz et al (13) in an isolated fraction of *T. cruzi* acidocalcisomes. This work showed that addition of ATP produced a significant time-dependent increase in short-chain (SC) and

long-chain (LC) polyP content in isolated acidocalcisomes. They also found that polyP synthesis depended on the previous acidification of the organelle produced by pre-incubation with PP_i . This activity seems to be similar to the polyP synthase activity of ScVtc4p, which catalyzes polyP synthesis using PP_i as substrate in an ATP-consuming reaction (5). The localization of the ScVtc4p homolog sequence (TcVtc4) in *T. cruzi* acidocalcisomes, strongly supports the hypothesis that TcVtc4 is the enzyme responsible for the polyP kinase activity described in *T. cruzi* acidocalcisome fraction.

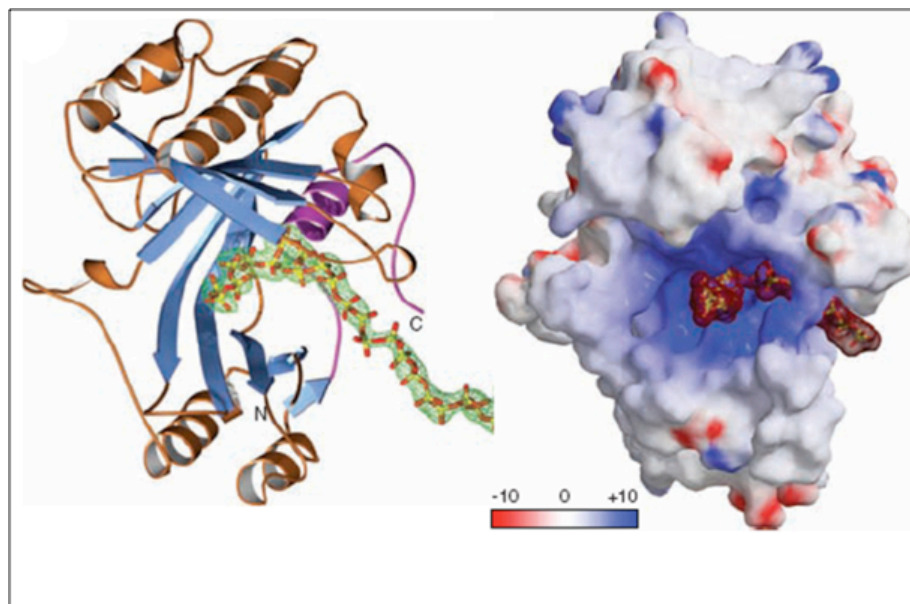


Figure 2. ScVtc4p structure. Ribbon diagram of ScVtc4p with the phosphate polymer (in bonds representation) and an omit electron difference density map contoured at 4.5 s included. The helical plug is shown in magenta. Mapping of the electrostatic potential on the surface of ScVtc4p highlights the basic tunnel center and the negatively charged poly P polymer. Modified from (5).

TbVtc1 is a subunit of the *T. brucei* VTC complex

A protein homologue to *S. cerevisiae* Vtc1p was described in *T. brucei* (42). *TbVtc1* gene encodes a 180-residues protein with a predicted molecular

mass of 19.8 kDa. In this work they demonstrated the acidocalcisome localization of TbVtc1 by C-terminal gene tagging and electron microscopy. Protein sequence alignment of TbVtc1, TcVtc1 and LmVtc1 showed that the *T. brucei* gene product has 75, 71 and 33% identity with the *T. cruzi*, *L. major* and *S. cerevisiae* deduced sequences, respectively. Ablation of *TbVtc1* expression by RNA interference and regulatory volume decrease assays (RVD) showed an essential role for this protein in polyP metabolism, osmoregulation and replication *in vitro*. RNAi ablation of *TbVtc1* caused an abnormal morphology of acidocalcisomes, indicating that their biogenesis was disturbed, with a decreased PP_i-driven H⁺ uptake and Ca²⁺ content, a significant decrease in the amount of polyP and a deficient response to hyposmotic stress (42). These results showed an essential role in polyP synthesis for a VTC complex subunit in *T. brucei*. However, this protein does not have a catalytic domain for polyP synthesis. It is known that Vtc1p and Vtc4p are present together as a complex in the vacuole of *S. cerevisiae* (5), and since TbVtc1 is found in acidocalcisomes we expected to detect TbVtc4 in the same localization. We confirmed this predicted location by immunofluorescence analysis and electron microscopy, as well as the polyP kinase nature of TbVtc4 (43).

CHAPTER 2

***TRYPANOSOMA BRUCEI* VACUOLAR TRANSPORTER CHAPERONE 4 (TbVtc4) IS AN ACIDOCALCISOME POLYPHOSPHATE KINASE REQUIRED FOR *IN VIVO* INFECTION¹**

¹ Lander, N., Ulrich, P.N. and R. Docampo. 2013. *The Journal of Biological Chemistry*. 288:34205-16.

Reprinted here with permission of the publisher.

Abstract

Polyphosphate (polyP) is an anionic polymer of orthophosphate groups linked by high-energy bonds that typically accumulates in acidic, calcium-rich organelles known as acidocalcisomes. PolyP synthesis in eukaryotes was unclear until it was demonstrated that the protein named vacuolar transporter chaperone 4 (Vtc4p) is a long chain polyP kinase that localizes to the yeast vacuole. Here, we report that the *Vtc4* ortholog of *Trypanosoma brucei* (*TbVtc4*) encodes, in contrast, a short chain polyP kinase that localizes to acidocalcisomes. The subcellular localization of *TbVtc4* was demonstrated by fluorescence and electron microscopy of cell lines expressing *TbVtc4* in its endogenous locus fused to an epitope tag and by purified polyclonal antibodies against *TbVtc4*. Recombinant *TbVtc4* was expressed in bacteria, and polyP kinase activity was assayed *in vitro*. The *in vitro* growth of conditional knockout bloodstream form (BSF) trypanosomes (*TbVtc4*-KO) was significantly affected relative to the parental cell line. This mutant had reduced polyP kinase activity and short chain polyP content, and was considerably less virulent in mice. The wild-type phenotype was recovered when an ectopic copy of *TbVtc4* gene was expressed in the presence of doxycycline. The mutant also exhibited a defect in volume recovery under osmotic stress conditions *in vitro*, underscoring the relevance of polyP in osmoregulation.

Introduction

Polyphosphate (polyP) is an inorganic, linear polymer of orthophosphate (Pi) units linked by phosphoanhydride bonds. PolyP can exist as short (3 to ~300 Pi) or long chain (~300 to ~1,000 Pi) polymers, is abundant in nature, and has been conserved during evolution (1,14). PolyP has been extensively studied in bacteria, where it is involved in several essential functions as DNA replication, sporulation, germination, motility, and pathogenesis. Much less is known of the functions of polyP in eukaryotes (1,14). The recent discoveries that polyP can be released from some mammalian cells such as blood platelets (24) and mast cells (44) and has potent modulatory activity on blood coagulation (2) and inflammation (3), have renewed interest in this polymer. Interestingly, polyP with chain lengths characteristic of microorganisms modulates coagulation and inflammation differently than polyP with chain lengths typically found in mammalian cells (30).

In many organisms polyP is mobilized primarily by the synthetic activity of polyP kinases and degradation by endo- and exopolyphosphatases, respectively. A few genes encoding exopolyphosphatases (34-37) and endopolyphosphatases (45) have been described in eukaryotes. Recently, the first eukaryotic enzyme involved in synthesis and translocation of polyP, *Saccharomyces cerevisiae* vacuolar transporter chaperone 4 (ScVtc4p), was identified (5). The Vtc complex consists of four proteins (Vtc1-4) that form hetero-oligomeric complexes and are able to synthesize and transfer polyP into the vacuole, as well as impacting

membrane trafficking and vacuole fusion (40,46,47). Vtc4 forms the catalytic core of the complex, although null mutations of each of the Vtc proteins result in reduced accumulation of polyP. Vtc proteins are present in fungi, algae, trypanosomatids, and Apicomplexan parasites but are absent in mammalian cells.

In many cells short and long chain polyP accumulate in acidocalcisomes, acidic calcium stores (48) where polyP is complexed with several cations (4,20). These organelles were first described in *Trypanosoma brucei* (6) but later identified in a broad range of organisms from bacterial to human cells (4), and are involved in Ca^{2+} signaling as inferred by the presence in them of an inositol 1,4,5- trisphosphate receptor (21). *T. brucei* belongs to the group of trypanosomes that causes Human African Trypanosomiasis (HAT, also known as sleeping sickness), an endemic disease of Sub-Saharan Africa. There is no vaccine available for this disease and chemotherapy also remains unsatisfactory, especially for advanced cases when a neurological phase has been reached and the disease becomes potentially fatal.

Previous work has shown that polyP has a critical role in survival of trypanosomes under sharp environmental changes, including osmotic stress (13,28,49). This resistance to osmotic stress is essential for digenetic trypanosomatids as they encounter drastic osmotic changes in both the insect vectors and vertebrate hosts (28,50,51). Regulation of cell volume is, in addition, a homeostatic process needed at all times by all cells. PolyP hydrolysis occurs

during hyposmotic stress of trypanosomes (13), probably increasing the osmotic pressure of the acidocalcisomes and facilitating water movement. On the other hand, an increase in long chain polyP levels has been observed in *T. cruzi* during hyperosmotic stress (13,28). This latter work suggested that polyP could play an important role at the early stages of hyperosmotic stress response by sequestering ions into the acidocalcisomes to reduce the ionic strength of the cytosol (28).

Homologs of *S. cerevisiae* *Vtc1* and *Vtc4* genes are present in the genome of *T. brucei*. TbVtc1, a protein present in *T. brucei* acidocalcisomes (42), is essential for polyP synthesis and acidocalcisome biogenesis. However, this protein does not have polyP kinase domain or PPK activity. An ScVtc4p homolog (TbVtc4) was detected in a proteomic analysis of *T. brucei* acidocalcisomes (Huang, G., Ulrich, P.N., Johnson, D., S.N.J. Moreno, Orlando, R., and Docampo, R., unpublished data). In the present study we investigated the role of this enzyme by biochemical and genetic approaches, elucidating important aspects of its physiological role in *T. brucei*, where polyP seems to be essential for parasite survival in the mammalian host. Since Vtc4 proteins are absent in vertebrates, we propose this enzyme as a potential target for drug development and disease control.

Experimental Procedures

Culture Methods. Cultivation of 29-13 procyclic form (PCF) (52) and single marker bloodstream form (BSF) (53) trypanosomes derived from *T. brucei* Lister strain 427 was carried out as previously described (54). Cell growth was followed using a Beckman® Coulter Z1 Dual Cell and Particle Counter.

Chemicals and reagents. TRIzol reagent, MagicMedia, Taq polymerase, BenchMark Protein Ladder, Alexa-conjugated secondary antibodies, and *Escherichia coli* BL21 Codon Plus (DE3)-RIPL were purchased from Invitrogen (Carlsbad, CA). Vector pET32 Ek/LIC, Benzonase® Nuclease, anti-Histidine tag antibodies, and S-protein HRP conjugate were from Novagen (EMD Millipore, Billerica, MA). [α -³²P]dCTP (3,000 Ci/mmol) and [γ -³²P]ATP (3,000 Ci/mmol) were from Perkin Elmer (Waltham, MA). Rabbit and mouse antibodies against *T. brucei* vacuolar H⁺-pyrophosphatase (TbVP1) (55) were a gift from Dr. Norbert Bakalara (Ecole Nationale Supérieure de Chimie de Montpellier, Montpellier, France). Anti-HA high affinity rat monoclonal antibody (clone 3F10) was purchased from Roche (Roche Applied Science, Mannheim, Germany). The pMOTag4H vector (56) was a gift from Dr. Thomas Seebeck (University of Bern, Bern, Switzerland). PD-10 desalting columns were from Amersham Biosciences (GE Healthcare Life Sciences, Piscataway, NJ). Pierce ECL Western blotting substrate and Pierce BCA Protein Assay Reagent were from Thermo Fisher Scientific Inc. (Rockford, IL). Zeta-Probe GT Genomic Testing blotting and nitrocellulose membranes were from Bio-Rad (Hercules, CA). AMAXA Human T-

cell Nucleofector kit was purchased from Lonza (Germany). Prime-a Gene Labeling System was from Promega (Madison, WI). QIAprep Spin Miniprep and Midiprep kits, QIquick gel extraction kit and MinElute PCR purification kit were from Qiagen (Valencia, CA). Fluorimetric ADP Assay Kit was from PhosphoWorks (AAT Bioquest, Inc., Sunnyvale, CA). The primers were purchased from Integrated DNA Technologies (Coralville, IA). Antibiotics and all other reagents of analytical grade were from Sigma (St. Louis, MO).

Sequence analysis. The analysis of *TbVtc4* sequence (gene ID Tb11.01.4040) was performed using DNAMAN software (version 7.212, Lynnon Corporation, Quebec, Canada) for alignments, the basic local alignment search tool (BLAST) for searching homologous sequences, Motif Scan algorithm for prediction of functional domains (57), and TopPred algorithm for the prediction of transmembrane domains (58). General information available for this sequence was obtained from *TriTrypDB* (59).

Gene cloning and protein heterologous expression. DNA sequence corresponding to *TbVtc4* catalytic core (nucleotides 595-1518 of the *TbVtc4* open reading frame, amino acids 199-506 of the full-length protein) was PCR-amplified from *T. brucei* 29-13 strain gDNA (forward primer: 5'-GACGACGACAAGATACC TTGTGGTACCGTTGG-3', reverse primer: 5'-GAGGAGAAGCCCGGTGTGGAA GCGCGAATGTCAA-3') and ligation-independent cloned into vector pET32 Ek/LIC for heterologous expression in bacteria. The sequence of several recombinant clones was verified and they were transformed by heat shock into *E.*

E. coli BL21 Codon Plus (DE3)-RIPL chemically competent cells. Induction of TbVtc4₁₉₉₋₅₀₆ expression was performed with MagicMedia following manufacturer's dual temperature protocol to avoid aggregation of protein in inclusion bodies for purification under native conditions. Protein expression was alternatively induced with 1 mM isopropyl-β-D-thiogalactopyranoside (IPTG) in LB broth for 3 h at 37 °C, for purification under denaturing conditions.

The catalytic domain of ScVtc4p [aa 189-480, (5)] was amplified from yeast gDNA using standard PCR protocols (forward primer: 5'-GAGCTCAAGGGAAGCAACAAAATTTTC-3', reverse primer: 5'-CACGTGTCATTGAGGTAACCAAATG-3') and Pfu Ultra HF (Stratagene). The fragment was cloned with a TOPO-TA cloning kit, verified by sequencing, and ligated into the expression vector pQE-2 (Qiagen) using SacI and PmlI sites that added to the 5' and 3' primers, respectively. *E. coli* (BL21 Codon Plus DE3 RIPL, Stratagene) were transformed with ScVtc4p₁₈₉₋₄₈₀/pQE-2. Histidine-tagged ScVtc4p₁₈₉₋₄₈₀ was induced overnight at 25 °C with 0.5 M IPTG, isolated by metal-ion affinity chromatography, and desalted on a HiTrap column (GE Life Sciences) with 25 mM Tris, 200 mM NaCl, 2 mM DTT (5).

Purification of recombinant TbVtc4 catalytic core under native conditions. Cell pellets from 200 mL culture of recombinant *E. coli* BL21 expressing TbVtc4₁₉₉₋₅₀₆ grown in MagicMedia were resuspended and incubated for 30 min on ice in 20 mL cold lysis buffer: 50 mM sodium phosphate, pH 8.0, 0.3 M sodium chloride, 10 mM imidazole, 0.1% Triton X-100, 0.1 mg/mL lysozyme, 25 U/mL Benzonase®

Nuclease and protease inhibitor cocktail for purification of histidine-tagged proteins (Sigma, 50 μ L/g cell paste). Then, three sonication pulses (40% amplitude, 30 s, on ice) were applied to ensure the complete disruption of cells. After centrifugation at 20,000 " g for 30 min at 4 °C, supernatant was passed through 0.8 μ m pore nitrocellulose filter in order to get a clarified crude protein extract that was kept on ice and used for immediate purification of recombinant TbVtc4₁₉₉₋₅₀₆. Protein purification was performed at 4 °C using HIS- Select® Cartridge (Sigma), an immobilized nickel-ion affinity chromatography, following manufacturer's protocol for histidine-tagged protein purification under native conditions. One mL fractions were eluted (elution buffer: 50 mM sodium phosphate, pH 8.0, 0.3 M sodium chloride, 250 mM imidazole) and buffer exchange was performed immediately using PD-10 desalting columns to finally obtain the protein in assay buffer (20 mM HEPES, pH 6.5). All purification steps were verified by SDS-PAGE and western blot analyses using anti-Histidine tag commercial antibodies or S-protein HRP conjugate. For antibody production, recombinant TbVtc4₁₉₉₋₅₀₆ was purified under denaturing conditions using HIS- Select® Cartridge (Sigma).

Antibody production. Polyclonal antibodies anti-TbVtc4 were generated in a guinea pig by Covance (against a synthetic peptide (CSRSRRVYARRKIRYDDRRG) that corresponds to a conserved hydrophilic region located between the second and the third predicted transmembrane domains of TbVtc4 amino acid sequence. In addition, polyclonal antibodies anti-

TbVtc4 were produced in mice using recombinant TbVtc4₁₉₉₋₅₀₆ as antigen. These antibodies were generated at the Monoclonal Antibody Facility of the College of Veterinary Medicine, University of Georgia (Athens, GA). Final bleeds from five inoculated mice were affinity purified by immunoadsorption to the recombinant protein immobilized on nitrocellulose strips. The adsorbed antibodies were eluted with 0.1 M glycine, pH 2.5, and neutral pH was restored immediately by adding 1 M Tris-HCl buffer, pH 8.0.

Fluorescence microscopy. For immunofluorescence assays (IFA), *T. brucei* PCF were centrifuged at 1,000 " g for 10 min at 25 °C, washed twice with PBS, pH 7.4, and fixed with 4% paraformaldehyde in PBS for 1 h on ice. Afterwards, cells were adhered to poly-L-lysine- coated coverslips, permeabilized with 0.3% Triton X-100 for 3 min, washed three times and blocked with PBS containing 3% BSA, 1% fish gelatin, 50 mM NH₄Cl, and 5% goat serum for 1 h. Next, cells were incubated for 1 h at room temperature (RT) with primary antibodies: polyclonal guinea pig anti-TbVtc4 (1:50) or rat anti-HA tag high affinity mAb (Roche, diluted 1:10) and polyclonal rabbit anti-TbVP1 (1:250), as acidocalcisome marker. After washing three times with 3% BSA in PBS (pH 8.0), cells were incubated for 45 min at room temperature in the dark with secondary antibodies: Alexa Fluor 488-conjugated goat anti-guinea pig or anti-rabbit (1:1,000) and Alexa Fluor 546-conjugated goat anti-rabbit or anti-mouse (1:1500). Then, cells were counterstained with 5 µg/mL DAPI to label nuclei and kinetoplast (mitochondrial DNA). Finally, all preparations were washed again three times with 3% BSA in

PBS (pH 8.0) and mounted on glass slides with Fluoromount-G (Southern Biotechnology). Differential interference contrast (DIC) and fluorescence optical images were captured under non saturating conditions and identical exposure times using an Olympus IX-71 inverted fluorescence microscope with a Photometrix CoolSnapHQ charge-coupled device (CCD) camera driven by DeltaVision software (Applied Precision).

Electron microscopy. BSF trypanosomes were washed twice in 0.1 M sodium cacodylate buffer, pH 7.4, and fixed for 1 h on ice with 0.1% glutaraldehyde, 4% paraformaldehyde and 0.1 M sodium cacodylate buffer, pH 7.4. Samples were processed for cryo-immunoelectron microscopy at the Molecular Microbiology Imaging Facility, Washington University School of Medicine. HA- fusion protein localization was detected with a polyclonal antibody against HA and anti-rabbit gold conjugated as a secondary antibody. Mouse anti-TbVP1 polyclonal antibodies and anti-mouse gold conjugated secondary antibodies were used.

Enzymatic assays for polyP synthesis

ADP assay. For determination of TbVtc4 and ScVtc4p kinetic parameters the specific activity of the enzyme was assayed using an ADP determination kit (PhosphoWorks™ Fluorimetric ADP Assay Kit, AAT Bioquest, Inc) to quantify the amount of ADP or GDP synthesized during polyP polymerization at different ATP or GTP concentrations. Analysis of ATP conversion by the recombinant catalytic domain of ScVtc4p was carried out in buffer containing 50 mM Tris-HCl (pH 7.5), 150 mM NaCl, 1 mM MnCl₂, and 1 mM ATP, at room temperature using

1 μM ScVtc4p. TbVtc4 polyP kinase activity was assayed in buffer containing 50 mM HEPES (pH 6.5), 150 mM NaCl, and 1 mM MnCl_2 , at 37 °C using 1 μM TbVtc4 and 1 mM ATP, or different concentrations of ATP, or GTP. When indicated, 1 mM PPI was included in the reactions. Twenty μL reactions were incubated 1 h at room temperature. Components A and B of ADP/GDP determination kit were added immediately, and after 30 min incubation at room temperature, fluorescence was detected at 540/590 nm excitation/emission ratio in a Molecular Devices plate reader. An ADP (or GDP) standard curve was obtained for quantification purposes. The data fit to a Michaelis-Menten equation and GraphPad Prism software version 5.0 was used for data analysis and determination of K_m , V_{max} and k_{cat} .

Coupled assay. ATP hydrolysis was also monitored via NADH oxidation enzymatically coupled to the re-phosphorylation of produced ADP. NADH concentration was measured optically at 340 nm in buffer containing 150 μM NADH, 0.15 mM phosphoenolpyruvate, 0.1 mg/mL pyruvate kinase, and 0.1 mg/mL lactate dehydrogenase. The reaction was initiated by the addition of 1 mM ATP and the incubations were done under the same conditions described above.

Radioactive assay. To visualize TbVtc4 and ScVtc4p reaction products, newly synthesized polyP chains were detected by autoradiography using $[^{32}\text{P}]\gamma\text{-ATP}$ as substrate. PolyP was separated by electrophoresis on Tris-borate- EDTA (TBE)-polyacrylamide gels. Reactions were carried out as described above using 1 mM $[^{32}\text{P}]\gamma\text{-ATP}$ (20 Ci/mmol) in a final volume of 50 μL for 8 h at room

temperature and stopped by adding EDTA (final concentration = 1 mM) and 10X sample buffer (2 mg/mL Orange G, 30% glycerol). Before loading the samples, TBE- polyacrylamide gels [0.1 x 16 x 20 cm, 1x TBE, 10% polyacrylamide (19:1 acrylamide/bis- acrylamide), 0.05% tetramethylenediamine, 0.05% (w/w) ammonium persulfate] were pre-run at 200 volts for 30 min in a cold room using a PROTEAN[®] II xi Cell (Bio-Rad). Thirty μ L sample and commercial polyP markers were loaded per well as indicated. Gels were run with a 4 mA constant current for 20 h at 4 °C. Different pH and cation requirements were assayed. Dried gels were exposed to films for at least 48 h at -80 °C for autoradiography.

Molecular constructs for *TbVtc4* mutant cell lines. For *TbVtc4* knockout construction in BSF trypanosomes, one *TbVtc4* allele was knocked out by replacement with a puromycin selectable marker in the single marker line that expresses T7 polymerase and tetracycline repressor maintained by a single G418 resistance marker (53). This puromycin cassette was obtained by PCR using a set of long primers (ultramers) containing 100- 120 nucleotides from the 5' and 3' UTRs flanking regions of the *TbVtc4* ORF (forward primer: 5'-GCTGTTGTTGTTTTCTTTTCATTATTGTTTACAAAGAAGTACGATAAGAGGAACATTAAGTGTTGAGAGGCAAGGAGAAGCAAACAACAGAGTTATAACGTGTACCGGGCCCCCCTCGAG-3', reverse primer: 5'-CGTTAAACATAGCAGAACATCAGCACATTACTGACAATCAACCAACATGTACACGTTCTTTTCCGTGAAAGCCAACATATTTCCCTGCCCCCTCCCTCAGTCTGGCGGCCGCTCTAGAACTAGTGGAT-3'), and pMOTag23M vector as template (56). To replace the second

allele we first introduced an ectopic copy of the gene (*TbVtc4_{ec}*) under the control of tet-inducible promoter and selectable by blasticidin resistance inserted at the ribosomal non-transcribed spacer. This cassette was constructed amplifying *TbVtc4* gene by PCR from *T. brucei* single marker strain gDNA (forward primer: 5'-CAGTGATCATATGCCCTTCAGCAAAGCATG-3', reverse primer: 5'-AGATGATCATCAGAAGGTGTCGCTTCCGG-3') to clone *TbVtc4_{ec}* into pLEW100v5b1d-BSD expression vector (a gift from Dr. George Cross, The Rockefeller University, New York City, NY), a modified version of the original pLEW100 vector (53). The construct was linearized with NotI restriction enzyme before cell transfection. Finally, the second *TbVtc4* allele was knocked out by replacement with a phleomycin selectable marker, while keeping the ectopic copy “on” by addition of tetracycline to the selection medium. The phleomycin cassette was also PCR amplified using a primer set containing 100-120 nucleotides from *TbVtc4* ORF 5' and 3' UTRs (forward primer: 5'-GCTGTTGTTGTTTTCTTTTTCA TTATTGTTTAAACAAAGAAGTACGATAAGAGGAACATTAAGTGTTGAGAGGCA AGGAGAAGCAAACAAACAGAGTTATAACGTATGGCCAAGTTGACCAGTGCC G-3', reverse primer: 5'-CGTTAAACATAGCAGAACATCAGCACATTA CTGACAA TCAACCAACATGTACACGTTCTTTTCCGTGAAAGCCAACATATTTCTGCCCC TCCCTCAGTCTCAGTCCTGCTCCTCGGCCA-3') and pUB39 vector, a modified version of the original pLEW82 vector (53), as DNA template. The linear constructs were used for transfection of BSF trypanosomes (single marker strain) and selection of stable resistant clones. Finally, a C-terminal HA-tagged mutant

(*TbVtc4*-HA) was generated using also ultramers (forward primer: 5'-GTAGCGTTAACATTTGTGATATTAGCCGTTATTCTTATAACTGTTATGATGCA CGTTATGGTCCGGTACGGGCCTATGCTCACCGGAAGCGACACCTTCGGTAC CGGGCCCCCCTCGAG-3', reverse primer: 5'-CGTTAAACATAGCAGAACAT CAGCACATTACTGACAATCAACCAACATGTACACGTTCTTTTCCGTGAAAGC CAACATATTTCTGCCCCTCCCTCAGTCTGGCGGCCGCTCTAGAACTAGTG GAT-3') and pMOTag4H vector (56) as DNA template to generate a linear fragment that was used to transfect *T. brucei* PCF and BSF.

Cell transfections. *T. brucei* BSF were transfected as previously described (54) with some modifications. Briefly, 3×10^7 mid-log phase cells (cell density in culture below 1×10^6 cells/mL) were harvested by centrifugation at $1,300 \times g$ for 10 min and resuspended in 100 μ L of AMAXA Human T-cell Nucleofector solution. Then, 10 μ g of NotI-linearized plasmid DNA or purified PCR product (<10 μ L) was added to cells in 2-mm gap cuvettes. Immediately, one electroporation pulse was applied using program X-001 of the AMAXA Nucleofector[®] II apparatus. Following each transfection, resistant cells were selected and cloned by limiting dilutions in HMI-9 medium containing 20% tetracycline-free FBS with appropriate antibiotics (2.5 μ g/mL G418, 0.1 μ g/mL puromycin, 2.5 μ g/mL blasticidin, 2.5 μ g/mL phleomycin or 5.0 μ g/mL hygromycin) in 24-well plates. Integration of the constructs into genomic DNA of each transfectant cell line was verified by PCR and Southern blot analysis.

For PCF transfection, mid-log phase parasites (cell density around 5×10^6 cells/mL) were harvested by centrifugation at $1,000 \times g$ for 7 min, washed with cold cytomix (2 mM EGTA, 5 mM $MgCl_2$, 120 mM KCl, 0.5% glucose, 0.15 mM $CaCl_2$, 0.01% BSA, 10 mM K_2HPO_4/KH_2PO_4 , 1 mM hypoxanthine, 25 mM HEPES, pH 7.6), and resuspended in 0.5 mL of cytomix at a cell density of 5×10^7 cells/mL. Then, cells were mixed with 10 μg of PCR product ($< 50 \mu L$) in a 0.4 cm electroporation cuvette and subjected to two pulses (1500 V, 25 μF) in a Bio-Rad Gene Pulser electroporator. The stable transfectants were obtained in SDM-79 medium supplemented with 15% FBS plus the appropriate antibiotic (50 $\mu g/mL$ hygromycin).

Southern blot analysis. Genomic DNA from parental and *TbVtc4* mutant cell lines was extracted as described (60). Two μg gDNA were digested overnight with BamHI and HindIII restriction enzymes. Digestion products were resolved by electrophoresis on a 1% agarose gel in Tris-acetate EDTA (TAE) buffer at 50 V. DNA was transferred from agarose gels onto Zeta-probe blotting membranes (Bio-Rad) by capillarity overnight using 0.4 M NaOH as transfer solution. Membranes were hybridized with a radiolabeled *TbVtc4* probe, generated by PCR (forward primer: 5'-GACGACGACAAGATACCTTGTGGTACCGTTGG-3', reverse primer: 5'- GAGGAGAAGCCCGGTGTGGAAGCGCGAATGTCAA-3') and labeled with [α - ^{32}P]dCTP using random hexanucleotide primers and the Klenow fragment of DNA polymerase I (Prime-a-Gene labeling system, Promega).

Membranes were exposed to films for 24-72 h at -80 °C and developed in dark room.

Northern blot analysis. Northern blot analysis was performed as previously described (28). Briefly, total RNA was isolated from BSF using TRI Reagent[®]. RNA samples were subjected to electrophoresis in 1% agarose gels containing 2.2 M formaldehyde, 20 mM MOPS, pH 7.0, 1 mM EDTA, and 8 mM sodium acetate, transferred to nylon membranes, and hybridized with radiolabeled probes for *TbVtc4* and *Tb-β-tubulin* gene (Tb927.1.2396). *Tb-β-tubulin* probe was also generated by PCR (forward primer: 5'- TGCGTGAGATTGTGTGCGTT CAGG-3', reverse primer: 5'-AGTGCAGACGAGGGAACGGCACCA-3') and labeled with [α -³²P]dCTP using random hexanucleotide primers and the Klenow fragment of DNA polymerase I (Prime-a-Gene labeling system, Promega). The *Tb-β-tubulin* gene was used as a loading control assuming a similar level of expression of this gene in all mutants at the same stage. Finally, membranes were exposed to films for 24-72 h at -80 °C and developed in dark room.

Western blot analysis. Parental and mutant cell lines were separately harvested. Parasites were washed twice in PBS (PCF) or buffer A with glucose (BAG, 116 mM NaCl, 5.4 mM KCl, 0.8 mM MgSO₄, 50 mM HEPES and 5.5 mM glucose, pH 7.3) for BSF and resuspended in RIPA buffer (150 mM NaCl, 20 mM Tris-HCl, pH 7.5, 1 mM EDTA, 1% SDS and 0.1% Triton X-100) plus protease inhibitors (mammalian cells protease inhibitor cocktail (Sigma P8340) diluted 1:250, 1 mM EDTA, 1 mM PMSF, 2.5 mM TPCK and 100 μM E64) and Benzonase[®] Nuclease

(25 U/mL culture). Then, cells were incubated for 30 min on ice and 5 rounds of freeze-thaw were applied (5 min on dry ice/ethanol bath, 1 min on 37 °C water bath). Cell lysis was verified under light microscope and protein concentration was determined by BCA protein assay (Pierce). Thirty µg protein from each cell lysate were mixed with 4x Laemmli sample buffer and analyzed by SDS- PAGE in 10% gels. Separated proteins were transferred onto nitrocellulose membranes (Bio- Rad) using a Bio-Rad transblot apparatus. Membranes were blocked with 5% nonfat dried skim milk in PBST (PBS containing 0.1% [vol/vol] Tween 20) overnight at 4 °C. Next, blots were incubated for 1 h at room temperature with different primary antibodies: polyclonal mouse anti-TbVtc4 (1:500), rat anti-HA tag mAb (1:100), or with anti-tubulin mAb (1:50,000). After five washes with PBST, blots were incubated with the appropriate secondary antibody: HRP-conjugated goat anti-mouse, or anti-rat IgG (1:15,000) for 1 h at RT. After washing five times with PBST, the immunoblots were visualized using ECL Western Blotting Substrate (Pierce) according to the instructions of the manufacturer.

Short chain and long chain polyphosphate quantification. Determination of polyP levels in BSF parental and mutant cell lines was performed as previously described by measuring P_i release by recombinant yeast exopolyphosphatase (27).

Regulatory volume changes under osmotic stress conditions. For osmotic stress under constant ionic strength, the following buffers described previously (27,61),

with some modifications were used: isotonic (64 mM NaCl, 4 mM KCl, 1.8 mM CaCl₂, 0.53 mM MgCl₂, 5.5 mM glucose, 5 mM Na-HEPES, pH 7.4, and 150 mM mannitol; 320 ± 5 mOsm, as determined using an Advanced Instruments 3D3 osmometer), hypotonic (the same as isotonic but without mannitol; 160 ± 5 mOsm), and hypertonic (the same as isotonic but with increased mannitol concentration to 1.2 M; 980 ± 5 mOsm). Samples of 1 " 107 BSF (single marker strain and *TbVtc4*-KO +/- tetracycline) were collected, washed with isotonic buffer pre-warmed at 37 °C, and resuspended in 100 µL isotonic buffer. Next, cells were transferred to a 96-well plate and changes in cell volume were followed monitoring absorbance at 550 nm in a plate reader with continuous agitation to avoid decantation of parasites. Osmotic stress was induced after 3 min of absorbance recording as follows: hyposmotic stress was induced by addition of 200 µL hypotonic buffer to 100 µL cells in isotonic buffer (final osmolarity: 213 mOsm), hyperosmotic stress was induced by addition of 100 µL hypertonic buffer to 100 µL cells in isotonic buffer (final osmolarity: 650 mOsm), and controls adding 100 and 200 µL isotonic buffer to the cells were carried out in parallel. After inducing osmotic stress, absorbance at 550 nm was recorded for additional 10 min. Cell viability was verified in the microscope after 10 min under osmotic stress.

In vivo studies. To evaluate the infectivity of *TbVtc4*-KO BSF trypanosomes, the cells were cultivated for 14 days in the absence of tetracycline. Exponentially growing cells (single marker and *TbVtc4*-KO +/- tetracycline) were washed once

in HMI-9 medium without selectable drugs and resuspended in the same medium. Eight-week-old Balb/c mice (5 per group) were infected with a single intraperitoneal injection of 2×10^4 BSF trypanosomes in 0.2 mL of HMI-9 medium. Mice were given either normal water or water containing 200 $\mu\text{g/mL}$ doxycycline in a 5% sucrose solution (54,55). The drinking water with or without doxycycline was provided 3 days before infection and exchanged every 2–3 days, continuing throughout the 30-day period. Animals were fed ad libitum on standard chow. Parasitemia levels were monitored 1-2 times/week during the whole experiment (62). Mice were euthanized upon attaining a parasite density over 1×10^8 cells/mL. This study was carried out in strict accordance with the recommendations in the National Institutes of Health Guide for the Care and Use of Laboratory Animals. The animal protocol was approved by the Institutional Animal Care and Use Committee (IACUC) of the University of Georgia.

Statistical analyses. For all experiments, results were expressed as mean values of three independent experiments \pm standard deviation (SD). Statistical analyses were performed using GraphPad Prism software version 5.0. Comparison of polyP kinase activity and short and long chain polyP content in different cell lines was performed by Student's t test with a significance level of 0.05. Comparison of changes in cell volume after osmotic stress in different cell lines was done by Bonferroni's multiple comparison a posteriori test of one-way ANOVA at all time points after induction of osmotic stress (significance level = 0.05). In this way, the

pattern of response to osmotic stress of all cell lines was analyzed during the entire period of observation.

Results

TbVtc4 sequence analysis. *TbVtc4* amino acid sequence (NCBI Reference Sequence: XP_829284.1; TriTrypDB sequence: Tb11.01.4040), was aligned with orthologs from other kinetoplastids and also with *ScVtc4p* (not shown). *TbVtc4* sequence shares 72.2%, 66.9% and 23.3% amino acid identity with *T. cruzi* *Vtc4* (TcCLB.511127.100), *Leishmania major* *Vtc4* (LmjF09.0220) and *ScVtc4p* (AAP21767), respectively. The ORF of *TbVtc4* encodes a protein of 793 amino acids with a predicted molecular mass of 91.3 kDa. *TbVtc4* has a VTC domain at the hydrophilic region (aa 210-482) and three predicted transmembrane domains (TMDs), one putative (aa 476-496) and two certain (aa 716-738 and aa 759-781). The catalytic domain (VTC) is highly conserved (61.5% identity) among these four orthologs.

TbVtc4 localizes to acidocalcisomes. To establish the localization of *TbVtc4*, an *in situ* tagging technique was used. We designed the tagged gene to remain under wild-type regulation, avoiding the pitfall of overexpression and consequently increased risk of abnormal distribution of the tagged protein. The linear epitope-tagging cassette was transfected into procyclic (PCF) and bloodstream form (BSF) trypanosomes, where it integrated into the original *TbVtc4* locus via homologous recombination. *TbVtc4* co-localized with the

vacuolar proton pyrophosphatase (TbVP1), an acidocalcisomal marker (31, 40), in both PCF (Fig. 3B) and BSF trypanosomes (Fig. 3C), as detected by immunofluorescence (Fig. 3B) and immunoelectron microscopy (Fig. 3C), respectively. Western blot analysis confirmed the expression of the tagged protein of the expected size and showed that TbVtc4 expression levels were higher in PCF (Fig. 3D). Similar co-localization results were observed in PCF using affinity-purified, polyclonal antibodies against synthetic peptide fragment from TbVtc4 (aa 740- 759, Fig. 3A).

TbVtc4 synthesizes short chain polyP and requires divalent cations but not pyrophosphate. To characterize the enzymatic activity of TbVtc4 we expressed its catalytic domain (TbVtc4₁₉₉₋₅₀₆) as a fusion protein with an N-terminal polyhistidine tag. In Fig. 3E, *lane rTbVtc4* shows that the recombinant protein (including the his-tag) appears as a strong single band with a molecular mass comparable to the predicted molecular mass (53.4 kDa). The catalytic core of the *S. cerevisiae* enzyme (ScVtc4p₁₈₉₋₄₈₀) (13) was used as control. We tested the activity of TbVtc4 with ATP or GTP (Fig. 4A and 4B, respectively). ScVtc4p was assayed with ATP in the absence and presence of PP_i (Figs. 4C and 4D, respectively). TbVtc4 has a higher affinity for ATP than ScVtc4p (Table 1) in the absence of PP_i (TbVtc4 $K_m = 54.8 \pm 7.3 \mu\text{M}$ vs ScVtc4p $K_m = 261.2 \pm 48.6 \mu\text{M}$). However, the yeast enzyme is much more efficient than TbVtc4 (ScVtc4p $k_{cat}/K_m = 9.3 \times 10^3 \text{ s}^{-1} \text{ M}^{-1}$ vs TbVtc4 $k_{cat}/K_m = 3.1 \times 10^3 \text{ s}^{-1} \text{ M}^{-1}$). The presence

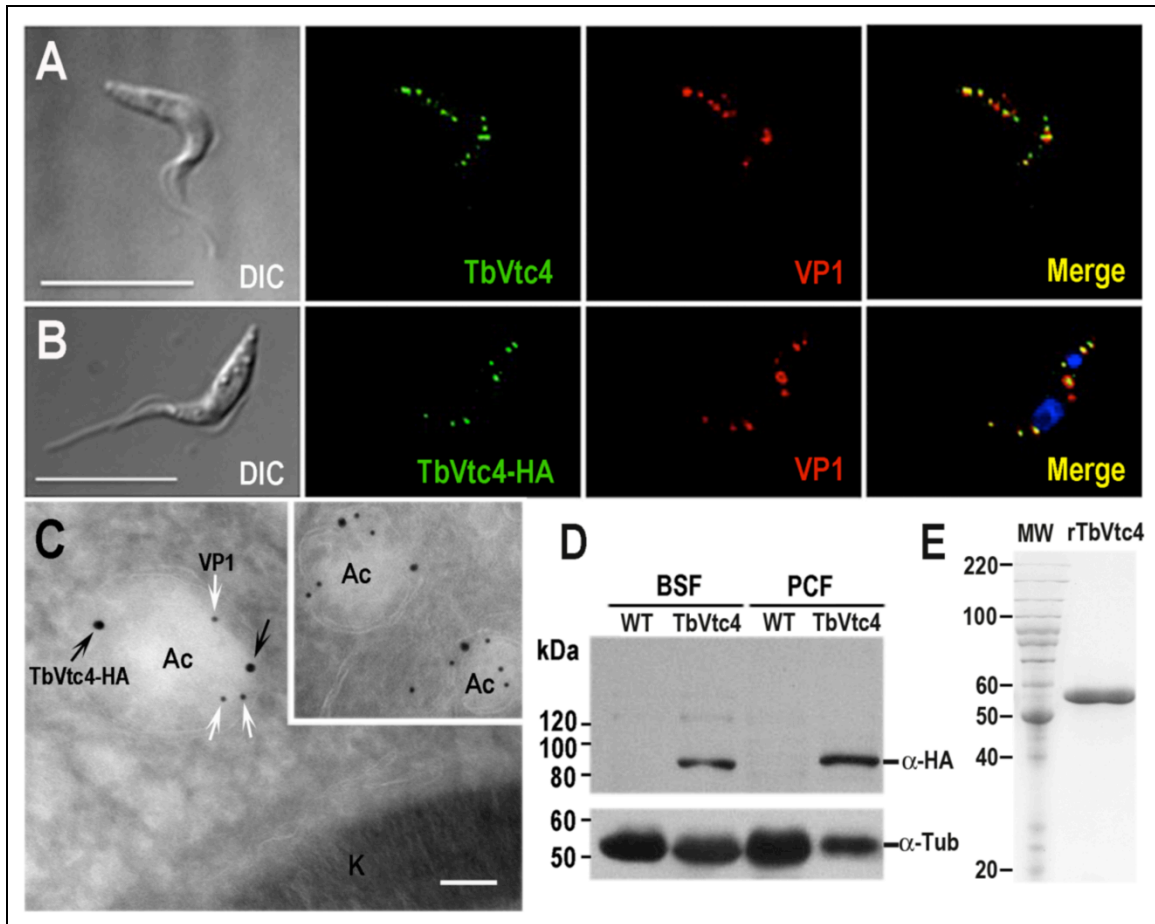


Figure 3. Localization of TbVtc4 in PCF and BSF trypanosomes. TbVtc4 co-localizes with TbVP1 in acidocalcisomes of PCF (A, B). TbVtc4 was detected with polyclonal anti-TbVtc4 antibodies in wild type trypanosomes (A) or with monoclonal anti-HA antibodies in trypanosomes expressing TbVtc4-HA (B) (green), and co-localized with antibodies against TbVP1 (red). Merge shows co-localization in yellow. Bars = 10 μ m. C, TbVtc4-HA fusion protein was also detected in BSF trypanosomes with anti-HA antibodies and gold-conjugate anti-mouse secondary antibody (18 nm) and co-localized with antibodies against TbVP1 and gold-conjugated anti-rabbit antibody (12 nm). Acidocalcisomes (Ac) and kinetoplast (k) are indicated. Bar = 100 nm. D, Western blot analysis in BSF and PCF wild type (WT) and endogenously tagged parasites (TbVtc4) using monoclonal anti-HA antibodies. Anti-tubulin antibodies were used as loading control. Molecular weights are shown on the left. E, Recombinant catalytic region of TbVtc4 (aa 199-506) affinity purified from *E. coli* (Lane rTbVtc4). Lane MW, protein molecular mass standards (kDa). The 10% SDS-PAGE gel was stained with Coomassie Brilliant Blue. A single protein band corresponds to rTbVtc4.

of PP_i did not “prime” or stimulate TbVtc4 activity (see also Fig. 5C below), as was observed with the yeast enzyme (5). On the other hand, the reported priming effect of PP_i on the polyP kinase activity of ScVtc4p was confirmed by the

increase in its efficiency in the presence of PP_i with a k_{cat}/K_m ratio of $1.7 \times 10^4 \text{ s}^{-1} \text{ M}^{-1}$ (Table 1).

PolyP produced by TbVtc4 reactions was visualized using $[^{32}P]\gamma$ -ATP as substrate followed by Tris-borate-EDTA polyacrylamide gel electrophoresis (TBE-PAGE). TbVtc4 requires divalent cations, preferentially Mg^{2+} , Mn^{2+} or Zn^{2+} (Figs. 5A and 5D) and an acidic pH (Figs. 5B and 5E) for optimal activity. The increased activity of TbVtc4 at acidic pH was corroborated using a different method based on a coupled assay that generates NADH upon polyP production. In contrast to TbVtc4 (optimal pH = 6.0), ScVtc4p exhibited pH optima at 6.0 and 7.5 (Fig. 5F). Finally, TBE-PAGE/autoradiography demonstrated that polyP chains synthesized by TbVtc4 catalytic core are much shorter (~100-300 Pi residues) than those produced by ScVtc4p (~750 Pi residues) (Fig. 5C), and TbVtc4 activity was inhibited in the presence of PP_i (Fig. 5C).

Reduced expression of TbVtc4 in BSF trypanosomes results in decreased polyP kinase activity and short chain polyP content. Previous studies demonstrated that polyP is important for trypanosome growth and osmoregulation in trypanosomes (13,27,28,42,54,55), but the length of the polyP responsible for these roles was not investigated. To investigate whether the short chain polyP synthesized by TbVtc4 is involved in these processes we analyzed the phenotypic changes of BSF trypanosomes with a conditional knockout (KO) of *TbVtc4*. In these cells, we replaced both *TbVtc4* alleles with drug resistance genes, but, since TbVtc4 could be required for growth, we introduced an ectopic copy of the *TbVtc4* gene whose

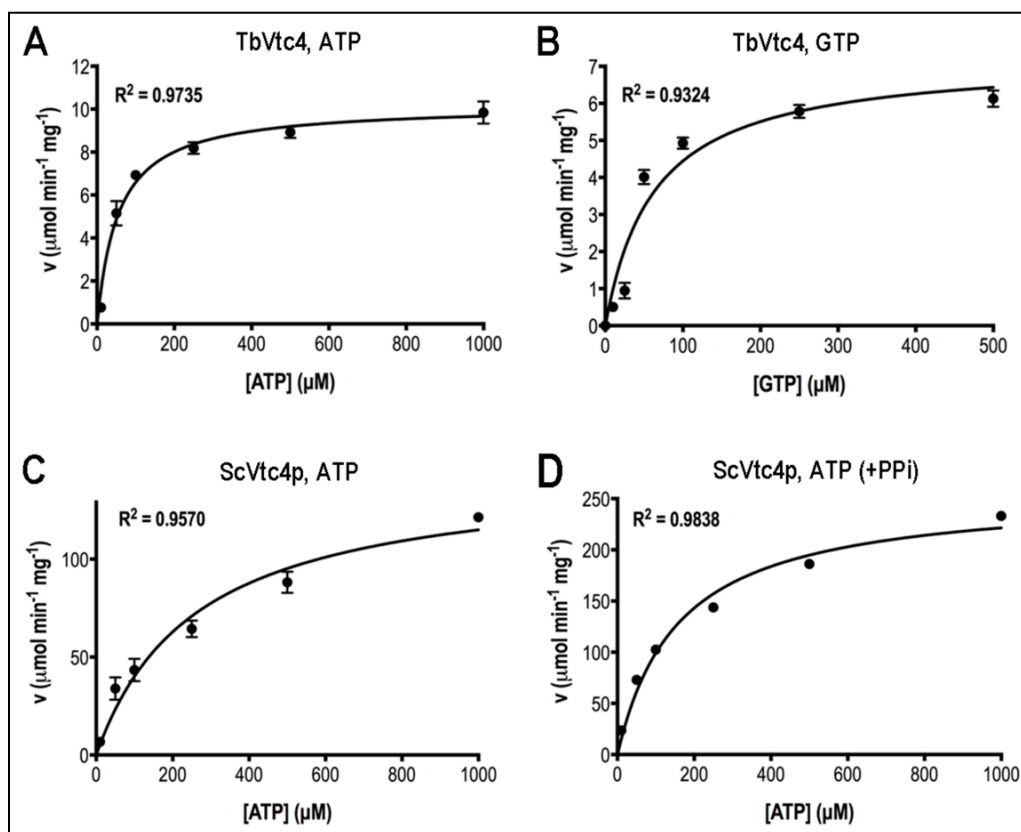


Figure 4. Recombinant polyP kinase activity as a function of substrate concentration. TbVtc4 polyP kinase activity was assayed in buffer containing 50 mM HEPES (pH 6.5), 150 mM NaCl, 1 mM MnCl₂, and different concentrations of ATP (A) or GTP (B) at room temperature, using 1 μM TbVtc4. ScVtc4p polyP kinase activity was assayed in buffer containing 50 mM Tris-HCl (pH 7.5), 150 mM NaCl, 1 mM MnCl₂, and different concentrations of ATP at room temperature, using 1 μM ScVtc4p in the absence (C) and presence (D) of 1 mM PPI. Other experimental conditions were as described under Experimental Procedures. Values are means \pm SD of three independent experiments. Error bars are smaller than the symbols used for some data points.

expression depended on presence of tetracycline or doxycycline in the culture medium (Fig. 6A). The genotype of the mutant cell line was verified by Southern blot analysis (Fig. 6B). Levels of mRNA in the presence or absence of tetracycline were analyzed by Northern blot (Fig. 6C). As expected, there was a decrease in *TbVtc4* mRNA levels in the absence of tetracycline for the KO cell

line. In the presence of tetracycline, *TbVtc4* mRNA levels of the KO mutant were normal because of the ectopic gene expression. The expression level of *TbVtc4* in these mutants was confirmed by western blot analysis using mouse polyclonal antibodies against *TbVtc4* (Fig. 6D).

Table 1. Kinetic parameters of purified recombinant Vtc4 catalytic regions from *T. brucei* and *S. cerevisiae* with different substrates.

Enzyme	Substrate	V_{max} ($\mu\text{mol} \times \text{min}^{-1} \times \text{mg}^{-1}$)	K_m (μM)	k_{cat}/K_m ($\text{s}^{-1} \times \text{M}^{-1}$)
TbVtc4	ATP	10.2 ± 0.3	54.8 ± 7.3	3.1 × 10 ³
	GTP	7.2 ± 0.5	63.0 ± 13.0	1.9 × 10 ³
ScVtc4p	ATP	145.0 ± 10.2	261.2 ± 48.6	9.3 × 10 ³
	ATP + PP _i	256.6 ± 8.6	158.5 ± 16.5	1.7 × 10 ⁴

The *in vitro* growth rate of the mutant cell line in the absence of tetracycline was monitored during 2 weeks and compared to that of the parental single marker strain (WT). The growth rate of *TbVtc4*-KO BSF progressively decreased relative to the parental cell line. *TbVtc4*-KO BSF partially recovered as escape mutants arose after 14 days (Fig. 7A). PolyP kinase activity after two weeks of withdrawal of tetracycline was significantly decreased in total cell lysates (Fig. 7B). Reduced activity was accompanied by a 35% decrease in short chain polyP (Fig. 7C), but no significant changes in long chain polyP levels (Fig. 7D). In summary, our results indicate that disruption of *TbVtc4* in BSF

trypanosomes decreases polyP kinase activity and, as a consequence, results in significantly lower levels of short chain polyP.

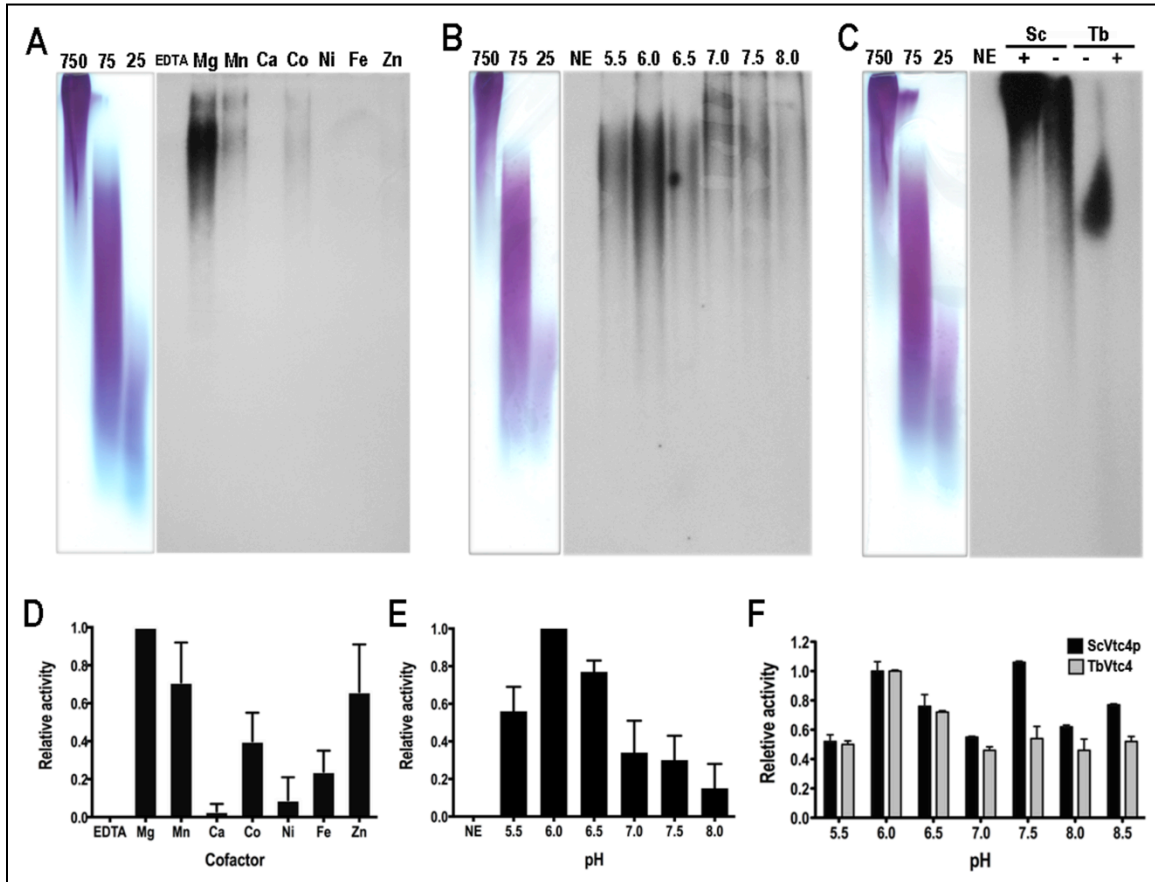


Figure 5. TBE-PAGE analysis of polyP produced by TbVtc4 and ScVtc4p catalytic cores. PolyP synthesized by recombinant TbVtc4 and ScVtc4p using [γ -³²P] ATP as substrate was analyzed by TBE- PAGE. *A*, Autoradiography of TbVtc4 reaction products in the presence of different cations. *B*, Autoradiography of TbVtc4 reaction products at different pH. *C*, Autoradiography of TbVtc4 (Tb, in the presence of Mn²⁺, pH 6.0) and ScVtc4p (Sc, in the presence of Mn²⁺, pH 7.5) reaction products in the presence (+) or absence (-) of PPI. A control without enzyme was included (NE). Lanes at the left side of each autoradiography in *A-C* show polyP of 25, 75 and 750 phosphate units loaded on the same gel and stained with toluidine blue. *D*, *E*, Results from 4 (*D*) and 3 (*E*) independent experiments similar to those shown in (*A*) and (*B*) were quantified by densitometry using SpotDenso tool of AlphamagerR gel documentation system (Proteinsimple, Santa Clara, CA), then normalized and plotted. *F*, Optimal pH of recombinant TbVtc4 and ScVtc4p was confirmed by an alternative method. Coupling the reaction to lactate synthesis from phosphoenolpyruvate allows the re-generation of ATP to the Vtc4 reaction. Absorbance (340 nm) turnover indicated NADH consumption during the coupled reaction and was used for measuring poly P kinase (PPK) activity of affinity purified recombinant Vtc4s. Results are expressed in relative activity units at different pHs. Values are means \pm SD of three independent experiments.

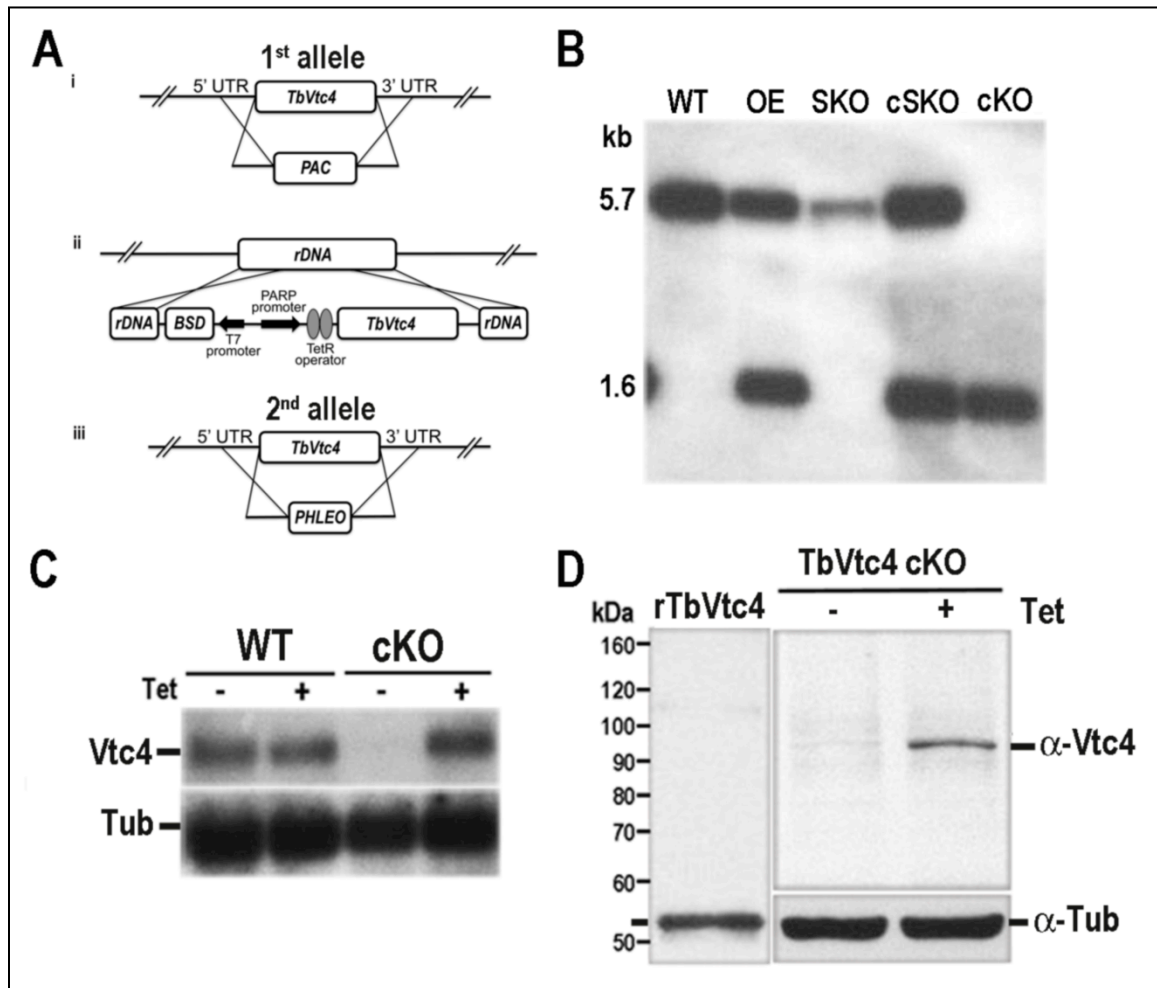


Figure 6. Generation of *TbVtc4* cKO cell line. *A*, Schematic representation of the strategy used for the generation of a stable *TbVtc4* conditional knockout mutant in *T. brucei* BSF. *i*) One allele of *TbVtc4* was replaced with the puromycin-resistance gene (*PAC*) by homologous recombination, generating the *TbVtc4* SKO cell line; *ii*) An ectopic *TbVtc4* cassette under the control of the tetracycline-inducible PARP promoter and selectable by blasticidin resistance (*BSD*), was inserted at the ribosomal non-transcribed spacer (*rDNA*), generating the *TbVtc4* cSKO cell line. This cassette was constructed using pLEW100v5b1d-*BSD* expression vector; *iii*) while keeping induced the expression of the ectopic *TbVtc4*, the second allele of the gene was replaced with a phleomycin resistance gene (*PHLEO*) by homologous recombination, resulting in conditional knockout cell line *TbVtc4* cKO. *B*, Southern blot analysis of parental cell line (Single Marker, WT), overexpressing (OE), single knockout (SKO), complemented single knockout (cSKO) and complemented double KO (cKO). *C*, Northern blot analysis of wild type (WT) and *TbVtc4*-KO mutant (cKO) in the absence or presence of tetracycline (\pm Tet), using a *Vtc4* probe. A tubulin probe was used as loading control. *D*, Western blot analysis of *TbVtc4* cKO mutant cell line in the absence or presence of tetracycline (\pm Tet), using polyclonal antibodies anti- *TbVtc4* and anti-tubulin antibodies as a loading control. Affinity purified recombinant *TbVtc4*₁₉₉₋₅₀₆ (r*TbVtc4*) was included as control. Molecular weights are shown on the left side of the blot.

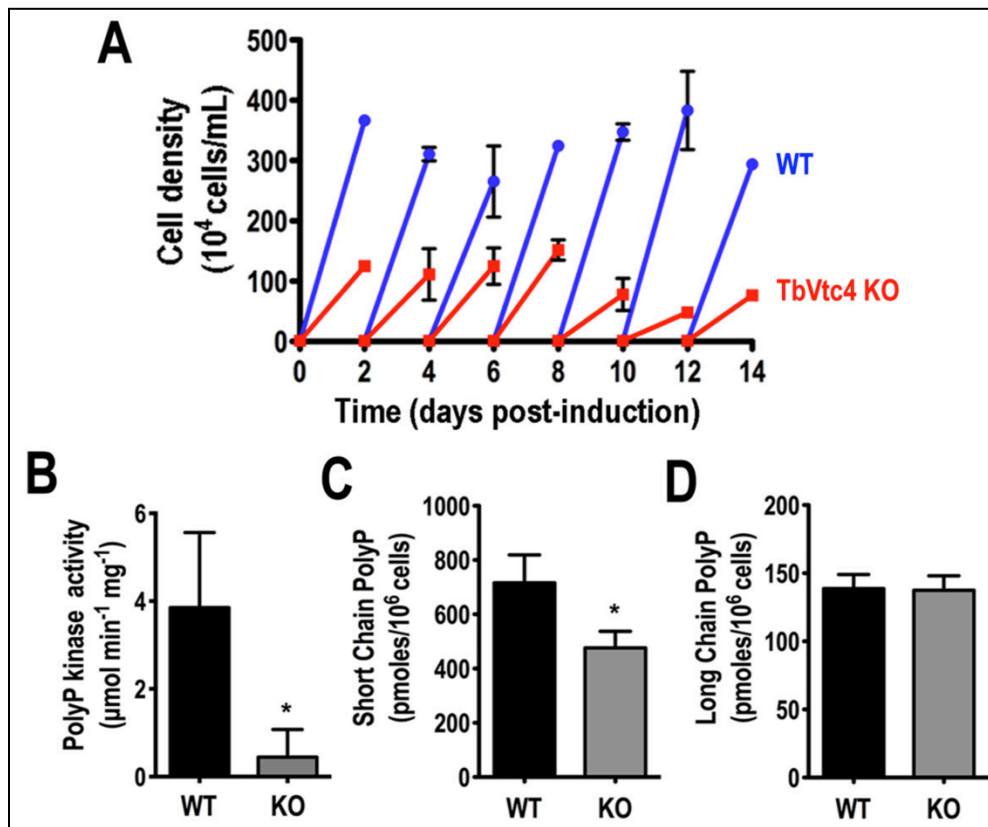


Figure 7. Effect of inhibition of TbVtc4 expression on cell growth, PPK activity, and short and long chain polyP levels. *A*, *In vitro* growth of single marker BSF (WT, full circles, blue) and *TbVtc4* conditional knockout parasites (*TbVtc4*-KO, full squares, red). *B*, Lysates from *TbVtc4*-KO BSF showed a ~8-fold lower polyP kinase activity than those from single marker BSF trypanosomes (WT). *C*, *D*, Extracts from *TbVtc4*-KO BSF trypanosomes showed a ~35% reduction in short chain polyP content (*C*) with no significant changes in long chain polyP content (*D*), as compared to the parental cell line (WT). Values are means ± SD of three different experiments. *Differences are statistically significant as compared to respective controls, $p < 0.05$ (Student's t test).

TbVtc4-KO mutant parasites display an osmoregulatory defect. To investigate the role of *TbVtc4* in osmoregulation, we exposed *TbVtc4*-deficient BSF trypanosomes to hypotonic and hypertonic conditions and evaluated changes of cell volume with time. These parasites showed a defect in the ability to recover cell volume (a process known as Regulatory Volume Decrease or RVD

(63) during hyposmotic stress when compared with parental (*WT*) and complemented (*+tet*) cell lines (Fig. 8A). Loss of water was also more pronounced in these parasites during hyperosmotic treatment compared to the single marker cell line. This defect in hyperosmotic response was overcome when we induced the expression of an ectopic copy of the gene (Fig. 8B).

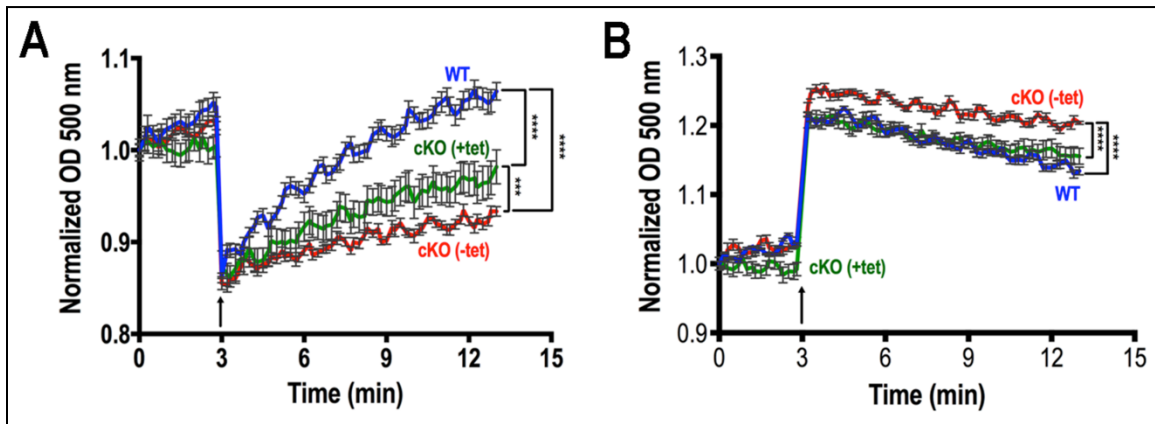


Figure 8. Effect of inhibition of *TbVtc4* expression on the response of BSF trypanosomes to hyposmotic and hyperosmotic stresses. The same amount of single marker [*WT*, blue], *TbVtc4* knockout [*cKO* (-Tet), red], and *TbVtc4* complemented knockout [*cKO* (+Tet), green] BSF trypanosomes were suspended in isotonic buffer. *TbVtc4*-KO BSF trypanosomes [*cKO* (-Tet)] were cultured in the absence of tetracycline for 14 days before de experiment. The cells were then treated as described under Experimental Procedures and relative changes in cell volume were followed by monitoring the absorbance at 550 nm. *A*, Changes in cell volume after hyposmotic stress (213 mOsm). *B*, Changes in cell volume after hyperosmotic stress (650 mOsm). Arrows indicate the time point (3 min) when osmotic stress was induced. A decrease in absorbance corresponds to an increase in cell volume and *vice versa*. Values are means \pm SD of three different experiments. Asterisks indicate statistically significant differences between cell line patterns, $p < 0.05$ (Bonferroni's multiple comparison "a posteriori" test of one-way ANOVA at all time points after induction of osmotic stress).

TbVtc4 is required for effective *in vivo* infection. We tested the infectivity of the *TbVtc4*-KO mutants *in vivo* using a mouse model and we found that the mutant cells were considerably less virulent in mice. Once again, the phenotype reverted when an ectopic copy of *TbVtc4* gene was induced by doxycycline (Fig. 9A). It is

important to mention that *TbVtc4*-KO (-dox) BSF trypanosomes were able to infect mice as verified by detection of parasites in blood at day 3-4 post- infection. However, the amount of parasites was significantly lower than that observed in the control groups, and, one week post-infection, *TbVtc4*-KO (-dox) BSF trypanosomes were no longer detected in blood of surviving animals (Fig. 9B). Thus these parasites were unable to persist in the mammalian host.

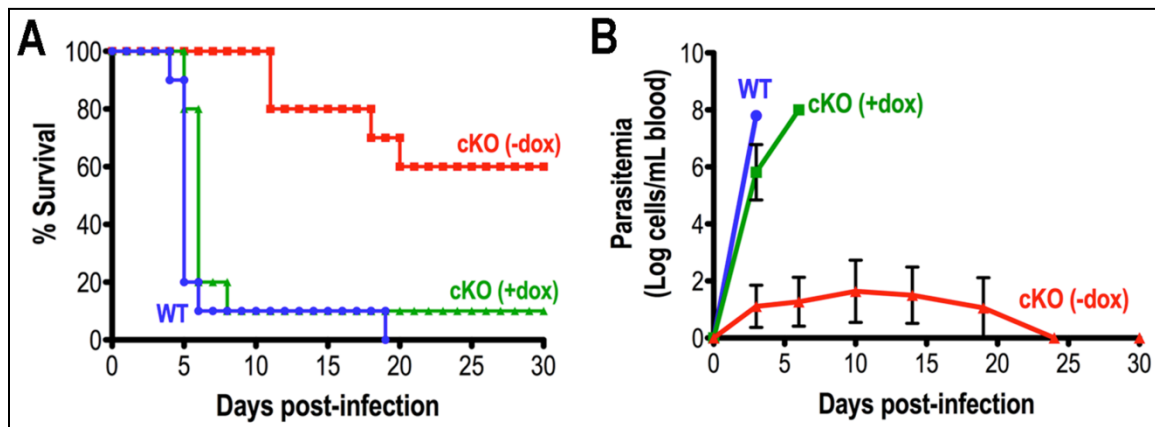


Figure 9. Effect of inhibition of *TbVtc4* expression on virulence in mice. Two experiments involving three groups of 5 mice that were infected with single marker (*WT*) and *TbVtc4*-KO mutant (*cKO*) BSF trypanosomes (-dox,+dox), were performed. 200 µg/mL doxycycline was supplied in the drinking water of one group of mice for the induction of an ectopic copy of *TbVtc4* gene in the *cKO* cell line (complemented knockout control). Percentage of mice survival (A) and parasitemia levels in the blood of infected mice (B) were monitored during 30 days post-infection. The charts combine results from two independent experiments.

Taken together, our data indicate that *TbVtc4* plays an important role in the infectivity of BSF trypanosomes and this role is possibly related to their reduced ability to survive under the osmotic stress conditions of the host.

Discussion

We report here that *TbVtc4* encodes a short chain polyP kinase that localizes to the acidocalcisomes of *T. brucei*. The enzyme is important for osmoregulation, *in vitro* growth, and infectivity of BSF trypanosomes *in vivo*. In contrast to the *S. cerevisiae* enzyme, which is a very long chain polyP kinase, *TbVtc4* catalyzes production of polyP of about 100-300 Pi units and was not activated, but inhibited, by PP_i. Despite these differences, we found some characteristics of the enzyme similar to those of *ScVtc4p* (5). Bivalent cation requirements for both enzymes are slightly different (*TbVtc4* metal ion specificity is $Mg^{2+} = Mn^{2+} > Zn^{2+} > Co^{2+} > Fe^{2+} > Ni^{2+} > Ca^{2+}$, and *ScVtc4p* metal ion specificity is $Mn^{2+} > Zn^{2+} > Co^{2+} > Mg^{2+} > Fe^{2+} > Ni^{2+}$). It is important to mention that the acidocalcisome environment of *TbVtc4* is rich in zinc, magnesium and calcium (64). Both enzymes can catalyze polyP synthesis at acidic pH. *TbVtc4* activity is highest at a pH of 6.0, but *ScVtc4p* exhibits two optimal pH values (6.0 and 7.5). Although these enzymes are located in the membrane of acidic calcium stores (the acidocalcisome and the yeast vacuole, respectively), their catalytic domains are facing the cytosol. It is possible that the microenvironment close to the outer leaflet of the acidocalcisome and vacuolar membranes has a lower pH due to the presence of Na⁺/H⁺ exchangers that move protons out from the acidocalcisome (65) and vacuole lumen (66).

A significant decrease in the level of short chain polyP was observed in the knockout BSF trypanosomes. However, a large reservoir was still present

after parasites had been cultured for two weeks without tetracycline. The persistence of short chain polyP could be due to known slow turnover of polyP (67) but more likely arises from the methodological limitations to distinguish between abundant forms of very short polyP (polyP₃, polyP₄, and polyP₅) (68), and medium size polyP (100-300 Pi), which are the main product of TbVtc4. The synthetic mechanism of very short polyP is unknown. Nevertheless, our results suggest that medium size polyP is important for osmoregulation and viability. Although previous reports have shown that polyP has important roles in growth and osmoregulation in trypanosomes (13,27,28,36,54,55) the length of the polyP responsible for these roles was not investigated. In this work we report that polyP of 100-300 Pi units, which is synthesized by TbVtc4, is required for regulatory volume decrease (RVD) during hyposmotic stress and also relevant for the response of the parasites to hyperosmotic stress conditions. Ability of these parasites to overcome such drastic changes in osmolarity is critical from their survival in the mammalian host. BSF trypanosomes in humans must be able to resist osmolality as high as 1,400 mOsm when passing through the renal medulla and rapidly accommodate a return to the isosmotic environment (300 mOsm) of the general circulation (69). Our results demonstrate that depletion of TbVtc4 in BSF trypanosomes leads to defective osmoregulation and infectivity. Both phenotypes are rescued with expression of an ectopic copy of the gene. A possible explanation for these observations is that mutant parasites, with lower short chain polyP levels, are not able to overcome the dramatic cell volume

stresses of mammalian renal circulation, and consequently cannot establish an infection. Alternatively, the increased osmotic sensitivity of TbVtc4-deficient trypanosomes weakens the parasites and makes them unable to evade the host immune response.

Long chain polyP is present in trypanosomes, but TbVtc4 is not able to synthesize these polymers, therefore other enzyme(s) could be involved in this process. We measured activity of the catalytic region of TbVtc4 because our attempts to recombinantly express the full-length protein in soluble form were unsuccessful. It is possible that the native enzyme can synthesize long chain polyP. However, this is not likely as only short chain polyP synthesis was affected in knockout parasites.

The palmitoyl proteome of *T. brucei* has recently been reported (70). Both TbVtc1 and TbVtc4 were reported to be palmitoylated. However, our attempts to demonstrate palmitoylation of TbVtc4 in PCF following established protocols (71,72) were unsuccessful (data not shown).

In summary, the essentiality of TbVtc4 for growth and establishment of an efficient infection suggest that this enzyme is a potential drug target and that it would be possible to develop inhibitors.

CHAPTER 3

THE ACIDOCALCISOME VACUOLAR TRANSPORTER CHAPERONE 4

CATALYZES THE SYNTHESIS OF POLYPHOSPHATE IN INSECT-STAGES

OF *TRYPANOSOMA BRUCEI* AND *T. CRUZI*¹

¹ Ulrich, P.N.* , Lander, N.* , Kurup, S., Reiss, L., Brewer, J., Miranda, K., Soares Madeiros, L.C. , and R. Docampo. *The Journal of Eukaryotic Microbiology*. In Press.

*These authors contributed equally to this work
Reprinted here with permission of the publisher.

Abstract

Polyphosphate (polyP) is a polymer of inorganic phosphate found in both prokaryotes and eukaryotes. PolyP typically accumulates in acidic, calcium-rich organelles known as acidocalcisomes, and recent research demonstrated that vacuolar transporter chaperone 4 (Vtc4) catalyzes its synthesis in yeast. The human pathogens *Trypanosoma brucei* and *T. cruzi* possess *Vtc4* homologs. We demonstrate that *T. cruzi* Vtc4 (*TcVtc4*) localizes to acidocalcisomes of epimastigotes by immunofluorescence and immuno-electron microscopy and that the recombinant catalytic region of *TcVtc4* is a polyP kinase. RNA interference of *T. brucei* Vtc4 (*TbVtc4*) in procyclic form (PCF) parasites reduced short chain polyP levels and resulted in accumulation of pyrophosphate (PP_i). Electron microscopy of PCF *T. brucei* in which *TbVtc4* has been ablated by RNAi exhibit 2-fold reduction in acidocalcisome number, but remaining acidocalcisomes have increased volume relative to non-induced control cells in agreement with the reduced polyP content and increased PP_i levels. These results suggest that this Vtc4 is an important component of a synthase complex that utilizes ATP as substrate for synthesis and translocation of polyP to acidocalcisomes in insect stages of these parasites.

Introduction

Polyphosphate (polyP) is a polymer of inorganic phosphate (P_i) that ranges in length from three to many hundred residues. PolyP is common to all organisms

and has a wide variety of physiological functions including transcriptional regulation (73), virulence of *Salmonella* and *Shigella* (74), blood coagulation (2), phosphorus storage (1), and cell volume regulation (14). Intracellular polyP reservoirs are strongly metachromatic, stain strongly in a reaction with methylene blue-sulfuric acid, and were initially described as metachromatic or volutin granules (15,16). Significant advances in understanding polyP have been made when volutin granules were identified as dynamic organelles now known as acidocalcisomes (4,20). Concentrations of inorganic polyP in acidocalcisomes can be as high as the molar range (in terms of P_i monomers, (13)).

While enzymes that synthesize polyP in prokaryotes have been described (31,32), a synthetic pathway of polyP in eukaryotes has only recently been elucidated. Prokaryotic polyP synthesis is driven via two distinct enzymes: polyP kinase 1 (PPK1) (31) and polyP kinase 2 (PPK2) (32). *Dictyostelium discoideum* is the only eukaryote with a known homolog to prokaryotic PPK (75) and is unique among eukaryotes in that it can also synthesize polyP through a secondary path that proceeds through a complex of actin-related proteins (33). Evidence from *Saccharomyces cerevisiae* studies suggested that a group of 4 yeast proteins known as vacuolar transporter chaperones (ScVtc1-4p) is involved in polyP metabolism (39). Fang et al (42) demonstrated that a *T. brucei* ScVtc1p homologue is localized to acidocalcisomes and that RNA interference of *TbVtc1* reduces polyP levels. Additionally, a ScVtc2p homologue in *Toxoplasma gondii* is also involved in polyP synthesis (76). Conclusive evidence of the role of Vtc's in

polyP synthesis was recently established in a structural, biological and biochemical study of ScVtc4p (5) ScVtc4p catalyzes polyP synthesis in a β -barrel structure via transfer of phosphate from ATP to a growing polyP chain. Activity of ScVtc4p is Mn^{2+} -dependent and enhanced in the presence of PP_i .

Homologues of ScVtc4p are present in *T. cruzi* (TcCLB.511127.100) and *T. brucei* (Tb927.11.12220), and, in previous work (43), we demonstrated that *TbVtc4* localizes to acidocalcisomes of procyclic (PCF) and bloodstream (BSF) forms of *T. brucei*. The recombinant catalytic region catalyzes synthesis of short chain polyP and is essential for the growth of *T. brucei* BSF *in vitro* and *in vivo*. However, the enzyme is more abundantly expressed in the PCF of *T. brucei*. We demonstrate here that Vtc4 also localizes to *T. cruzi* acidocalcisomes, is an essential enzyme in *T. brucei* PCF, and is responsible for polyP synthesis in these parasite stages. Currently, no effective and toxicity-free treatments of trypanosomatid infections exist. Given that *Vtc* genes are absent from the genomes of higher eukaryotes, drugs that target Vtc4 function are promising targets for treatments of Chagas disease and human African trypanosomiasis that do not endanger patients' lives.

Experimental Procedures

Chemicals and reagents. Superscript III reverse transcriptase, hygromycin, MagicMedia, *Taq* polymerase, BenchMark Protein Ladder, Alexa-conjugated secondary antibodies, and *Escherichia coli* BL21 Codon Plus (DE3)-RIPL and

pCRII Blunt Topo were purchased from Life Technologies (Grand Island, NY). Vector pET32 Ek/LIC, Benzonase® Nuclease, anti-Histidine tag antibodies, and S-protein HRP conjugate were from Novagen (EMD Millipore, Billerica, MA), iQ Sybr Green mix were from Bio-Rad (Hercules, CA), G418 was from Calbiochem (Darmstadt, Germany), Pfu Ultra HF polymerase was from Stratagene (La Jolla, CA), Pierce ECL Western blotting substrate and Pierce BCA Protein Assay Reagent were from Thermo Fisher Scientific Inc. (Rockford, IL), anti-HA high affinity rat monoclonal antibody (clone 3F10) was purchased from Roche (Roche Applied Science, Mannheim, Germany). T4 DNA ligase was from New England Biolabs (Ipswich, MA). Kinase-Glo® Luminescent Assay was from Promega (Madison, WI), phleomycin, protease inhibitor cocktail (Cat #P8840), HIS-Select® cartridges, polyclonal anti- GFP antibody, anti-rabbit gold conjugated secondary antibody, TriReagent, DNase, and yeast pyrophosphatase (ScPPase) were from Sigma (St. Louis, MO), rabbit and mouse antibodies against *T. brucei* vacuolar H⁺-pyrophosphatase (TbVP1) (55) were a gift from Dr. Norbert Bakalara (Ecole Nationale Supérieure de Chimie de Montpellier, Montpellier, France). The pMOTag4H vector (56) was a gift from Dr. Thomas Seebeck (University of Bern, Bern, Switzerland). PD-10 desalting columns were from Amersham Biosciences (GE Healthcare Life Sciences, Piscataway, NJ). QIAprep Spin Miniprep and Midiprep kits, QIquick gel extraction kit and MinElute PCR purification kit were from Qiagen (Valencia, CA). The primers were purchased from Integrated DNA Technologies (Coralville, IA). Antibiotics and all other reagents of analytical grade

were from Sigma (St. Louis, MO).

Cell culture. PCF of *T. brucei* (427 strain) were grown at 28 °C in SDM-79 medium supplemented with 10% heat inactivated fetal bovine serum (FBS) as reported before (54). HA-tagged *TbVtc4* cell lines were maintained in the presence of 50 µg/mL hygromycin. The PCF RNAi cell line (29-13 parent strain expressing T7 RNA polymerase and tetracycline repressor (53)) was maintained in SDM-79 medium supplemented with 10% heat inactivated FBS, 15 µg/mL G418, 50 µg/mL hygromycin, and 2.5 µg/mL phleomycin.

T. cruzi epimastigotes (Y strain) were grown at 28 °C in liver infusion tryptose (LIT) medium (77) supplemented with 10% heat-inactivated FBS. GFP-expressing cell lines were maintained in medium containing 250 µg/mL G418.

Construct design. Constructs of *Vtc4* genes were subcloned from *T. brucei* (427 and 29-13 strains) and *T. cruzi* genomic DNA (Y strain) using specific oligonucleotides (Table 2) designed with VectorNTI software (Invitrogen). Pfu Ultra HF polymerase was used to amplify *TcVtc4* and *TbVtc4*. The *TbVtc4* RNAi construct was amplified using primers designed with the RNA-iT server (<http://trypanofan.path.cam.ac.uk/software/RNAit.html>, (78)) and cloned into the tetracycline-inducible RNAi vector ^{ti}B with dual-inducible T7 promoters (79). Cloned sequences were verified by sequencing (Yale DNA Analysis Facility, Yale University, New Haven, Connecticut; Integrated Biotech Laboratories, University of Georgia, Athens, Georgia). We followed the one-step epitope-tagging protocol reported by Oberholzer et al (56) to produce the HA-pMOTag construct for *T.*

brucei. *TcVtc4a* was amplified by PCR from genomic DNA of Y strain *T. cruzi* using Pfu Ultra HF polymerase (Agilent). Briefly, we performed a total of 30 cycles at 94 °C for 30 s, 59 °C for 30 s, and an extension step at 72 °C for 1 min. The protocol was initiated with an initial denaturation step at 94 °C for 2 min and concluded with an extension step of 10 min at 72 °C. The amplicon was ligated into pCRII Blunt Topo and verified by sequencing. *TcVtc4a* was ligated with T4 DNA ligase into pTREX-GFP (72) a modified version of the original pTREX vector (80), following digestion with XbaI and HindIII.

T. cruzi Y strain epimastigotes (4×10^7 cells, at room temperature, suspended in PBS, pH 7.4 containing 0.1% glucose) were transfected in ice-cold cytomix (25 mM, 120 mM KCl, 0.15 mM CaCl₂, 10 mM K₂HPO₄, 2 mM EGTA, 5 mM MgCl₂, 0.5% glucose, 100 µg/mL BSA, 1 mM hypoxanthine, pH 7.6) containing 50 µg of each plasmid construct in 4 mm electroporation cuvettes with 3 pulses (1500 V, 25 µF) delivered by a Gene Pulser II (Bio-Rad). Stable cell lines were established and maintained under drug selection with G418 at 250 µg/mL. Until stable cell lines were established, LIT media was supplemented with 20% heat-inactivated FBS.

PCF of *T. brucei* 427 strain (2.5×10^7 cells in room temperature PBS, pH 7.4 containing 0.1% glucose) were transfected in ice-cold cytomix containing 10 µg of each plasmid construct in 4 mm cuvettes with 2 pulses (1500 V, 25 µF) with resting on ice for 15 min between pulses. Stable cell lines were established under

drug selection with addition of phleomycin (RNAi line, 2.5 µg/mL) or hygromycin (epitope-tagged line, 50 µg/mL).

Table 2. Primers used for molecular constructs to study Vtc4.

<i>TbVtc4</i> C-terminal tagging in pMOTag4H vector	
TbVtc4_pMOTag-F	GTAGCGTTAACATTTGTGATATTAGCCGTTATTCTTATAACTGT TATGATGCACGTTATGGTCCGGTACGGGCCTATGCTCACCGG AAGCGACACCTTCGGTACCGGGCCCCCCTCGAG
TbVtc4_pMOTag-R	CGTTAAACATAGCAGAACATCAGCACATTACTGACAATCAAC CAACATGTACACGTTCTTTTCCGTGAAAGCCAACATATTTCT GCCCTCCCTCAGTCTGGCGGCCGCTCTAGAACTAGTGGAT
<i>RNAi</i> in p2T7⁺B vector	
TbVTC4-RT-F	CATCGTGTGGGTTCTTTG
TbVTC4-RT-R	AATAACGGCTAATATCACAAATG
TbTub-RT-F	GCCATCGCAGAGGTGTTC
TbTub-RT-R	TCTTCGTAGTCCTTCTCAAGTG
TbRRNA-RT-F	CATCAAAGTGTGCCGATTACG
TbRRNA-RT-R	GGTCCGATCACCTGTATTGC
<i>TcVtc4</i> overexpression in pTREX vector	
TcVTC4-OEF	<u>TCTAGA</u> AATGCCGTTTAGCAAAGCATGGA
TcVTC4-OER	<u>AAGCTT</u> AAAGTTATCATCGCCGGTAAGC
<i>TcVtc4</i>₁₉₉₋₅₀₆ heterologous expression in pET32 Ek/LIC vector	
TcVTC4(199-506)-F	GACGACGACAAGATTCCAGCAGGCACCGTTGG
TcVTC4(199-506)-R	GAGGAGAAGCCCGGCGTCGAGGCACGGATATCAA

Western blot analysis. Protein was extracted from *T. cruzi* epimastigotes or *T. brucei* PCF for western blot analysis. Five milliliters (*T. cruzi*) or 16 mL (*T. brucei*) of cultured cells were washed twice with PBS (pH 7.4) and resuspended in 100 µL RIPA buffer (20 mM Tris, pH 7.5; 150 mM NaCl, 1 mM EDTA, 1% SDS, 0.1%

Triton X-100) supplemented with 2.5 mM EDTA, 2 mM PMSF, and 1:200 protease inhibitor cocktail (Sigma P8840) (*T. cruzi*) or 200 μ L RIPA buffer supplemented with 2.5 mM EDTA, 2 mM PMSF, and 1:200 protease inhibitor cocktail (same as above) (*T. brucei*). Genomic DNA was sheared by passage through a tuberculin syringe, and extracts were left on ice to solubilize for 1.5 hours (*T. cruzi*) or 15 min (*T. brucei*). Protein was quantified by BCA assay, and 30 μ g (*T. cruzi*) or 15 μ g (*T. brucei*) were separated on 10% PAGE. For *T. cruzi*, proteins were transferred to nitrocellulose for 1 h at 100 V, and the membrane was blocked overnight at 4° C in PBS-T plus 5% nonfat milk. The membrane was blotted with polyclonal α -GFP (1:5000) and developed with ECL reagent. For *T. brucei*, western blot analysis was performed in TBST (10 mM Tris-HCl, pH 7.4, 150 mM NaCl and 0.05 % Tween 20). Membranes were blocked overnight at 4° C in PBS-T containing 5% nonfat dry milk prior to blotting with high affinity α -HA antibody (diluted 1:1500). The blots were developed with ECL reagent.

Immunofluorescence Microscopy. *T. cruzi* epimastigotes were washed with PBS and fixed with 4% paraformaldehyde in PBS for one hour on ice. Cells were adhered to poly-lysine coated coverslips followed by permeabilization for 3-4 min with 0.3% triton X-100. Permeabilized cells were blocked for 1 h with 3% BSA, 1% fish gelatin, 5% goat serum, 100 mM NH₄Cl in PBS (pH 8). Cells were washed with 3% BSA in PBS and incubated with primary antibody (polyclonal rabbit α -TbVP1, 1:500; monoclonal α -GFP 3E6, 1:400; and/or high affinity rat α -HA, 1:1000) for 1 h. Excess primary antibody was removed from the cells with a

series of washes and cells were incubated with secondary antibody conjugated with various Alexa dyes at a 1:2000 dilution for 1 h. Following incubation with secondary antibody, the cells were washed and mounted to slides. DAPI (5 µg/mL) was included with the secondary antibody or the mounting medium to stain DNA. Secondary antibody controls were performed as above but in the absence of primary antibody. Differential interference contrast (DIC) and fluorescence optical images were captured under non saturating conditions using an Olympus IX-71 inverted fluorescence microscope with a Photometrix CoolSnapHQ charge-coupled device (CCD) camera driven by DeltaVision software (Applied Precision).

Electron microscopy. *T. cruzi* epimastigotes overexpressing a TcVtc4-GFP fusion protein were washed twice in 0.1 M sodium cacodylate buffer, pH 7.4, and fixed for 1 h on ice in 0.1 M sodium cacodylate buffer (pH 7.4) containing 0.1% glutaraldehyde and 4% paraformaldehyde. Samples were processed for cryo-immunoelectron microscopy at the Molecular Microbiology Imaging Facility, Washington University School of Medicine. Localization of TcVtc4a-GFP fusion protein was performed with a polyclonal antibody against GFP and anti-rabbit gold conjugated as a secondary antibody.

For imaging whole *T. brucei* PCF, cells were washed with buffer A (116 mM NaCl, 5.4 mM KCl, 0.8 mM MgSO₄, 50 mM HEPES, pH 7.3) twice, directly applied to Formvar-coated copper grids, and observed in an energy-filtering Zeiss EM 902 electron microscope operating at 80 Kv. Electron spectroscopic

images were recorded at an energy loss of 60 eV using a spectrometer slit width of 20 eV. Determination of morphometric parameters was done as described previously (42). Statistical significance was determined by Student's t test. Results were considered significant if $P < 0.05$.

Gene cloning and protein heterologous expression. The DNA sequence corresponding to TcVtc4 catalytic core (nucleotides 595-1518 of the *TcVtc4* open reading frame, amino acids 199-506 of the full-length protein) was PCR-amplified from *T. cruzi* Y strain gDNA (Table 2) and cloned with a ligation-independent protocol into vector pET32 Ek/LIC for heterologous expression in bacteria. The sequences of several recombinant clones were verified, and they were transformed by heat shock into *E. coli* BL21 Codon Plus (DE3)-RIPL chemically competent cells. Induction of TcVtc4₁₉₉₋₅₀₆ expression was performed with MagicMedia following the manufacturer's dual temperature protocol to avoid aggregation of protein in inclusion bodies for purification under native conditions.

Purification of recombinant TcVtc4 catalytic core under native conditions. Recombinant *E. coli* BL21 expressing TcVtc4₁₉₉₋₅₀₆ were grown in 200 mL MagicMedia. Cells were pelleted by centrifugation prior to resuspension and incubation for 30 min on ice in 20 mL cold lysis buffer (50 mM sodium phosphate, pH 8.0, 0.3 M sodium chloride, 10 mM imidazole, 0.1% Triton X-100, 0.1 mg/mL lysozyme, 25 U/mL Benzonase[®] Nuclease and protease inhibitor cocktail for purification of histidine-tagged proteins, 50 μ L/g cell paste). Then, cells were subjected to three sonication pulses (40% amplitude, 30 s, on ice) to ensure

complete disruption. After centrifugation at 20,000 x *g* for 30 min at 4 °C, the supernatant was clarified by passage through nitrocellulose (0.8 μm) and kept on ice. Recombinant TcVtc4₁₉₉₋₅₀₆ was immediately purified at 4 °C on an immobilized nickel-ion affinity column (HIS-Select[®] cartridges) following the manufacturer's protocol. One mL fractions were eluted with 50 mM sodium phosphate, pH 8.0; 0.3 M sodium chloride; 250 mM imidazole, and buffer exchange was performed using PD-10 desalting columns to obtain the protein in assay buffer (20 mM HEPES, pH 6.5). All purification steps were verified by SDS-PAGE and western blot analyses using anti-histidine tag commercial antibodies and S-protein HRP conjugate.

Enzymatic assay for polyP synthesis. For determination of TcVtc4 kinetic parameters, the specific activity of the enzyme was assayed quantifying the ATP consumed during polyP synthesis using the Kinase-Glo[®] Luminescent Assay in a plate-reader (Synergy[™] H1 Hybrid Microplate Reader, Biotek[®]). TcVtc4 polyP kinase activity was assayed at room temperature using 2 μM TcVtc4₁₉₉₋₅₀₆ in 50 μL reactions (50 mM HEPES pH 6.0, 150 mM NaCl, and 1 mM MnCl₂). All reactions were conducted in white, 96-well microplates. ATP (freshly prepared in 50 mM HEPES, pH 7.0) was added to the assay mixture at different concentrations to start the reaction. To determine if PP_i impacts polyP synthesis by TcVtc4₁₉₉₋₅₀₆, 1 mM PP_i was included in some cases. Negative control reactions without enzyme were included on the same plate. Reactions (50 μL) were incubated for 1 h at RT. Kinase-Glo Reagent (50 μL) was then added and

the reaction was incubated for additional 10 min before measurement of luminescence. An ATP standard curve was run on the same plate for quantification purposes. GraphPad Prism software version 5.0 was used for data analysis and determination of K_m , V_{max} and k_{cat} .

RNA Interference. Knockdown of *TbVtc4* was induced with tetracycline in PCF transfectants carrying the RNAi cassette from p2T7ⁱⁱB. Transcription of the dsRNA construct was induced by addition of 1 µg/mL tetracycline to cultures at a density of 1.15×10^6 cells/mL. Control cultures were always grown alongside for comparison. Every three days or as needed, cell cultures were passed to fresh media to a density of $\sim 1 \times 10^6$ cells/mL. Experiments were independently replicated on at least 3 different occasions. Knockdown of *TbVtc4* was confirmed using QRT-PCR. RNA was isolated from control and induced cultures ($\sim 10^7$ cells per isolation). Total RNA was isolated with TriReagent and treated with DNase. First strand cDNA was synthesized from 15 µg total RNA using Superscript III reverse transcriptase oligoDT primers. Quantitative PCR was performed in 96 well plates using iQ Sybr Green mix on an iCycler iQ instrument (Biorad). PCR was performed with an initial denaturation at 94° C for 3 min followed by 40 cycles of 94° C for 15 s, 50° C for 20 s, and 72° C for 20 s. Melting profiles were performed from 55-95 °C after each reaction. Each reaction contained cDNA derived from 30 ng of total RNA. Alongside *TbVtc4* amplification reactions, triplicate amplifications of *T. brucei* ssRRNA and tubulin genes were included as internal controls. Duplicate non-template controls using each primer set and RNA

controls (DNase-treated RNA samples using tubulin primers) were included on each plate. Threshold C_t data was extracted from quantitative PCR data using iCycler iQ software (Biorad), and C_t values for TbVtc4 were normalized to the geometric mean (81) of the C_t of *T. brucei* tubulin and ssrRNA genes amplified from the same sample simultaneously.

Polyphosphate extraction and measurement. PP_i and short chain polyP were extracted from PCF *T. brucei* using a protocol modified from previously described methods (42). Because short chain polyP extraction yield varies considerably among biological samples, extraction protocols were optimized with respect to the number of each cell type. Briefly, cells (long chain polyP extraction, 2.5×10^7 cells; short chain polyP and PP_i extraction, $\sim 6 \times 10^7$ cells) were washed two or three times with room temperature buffer A containing glucose (BAG) (116 mM NaCl, 5.4 mM KCl, 0.8 mM $MgSO_4$, 5.5 mM glucose and 50 mM HEPES, pH 7.2), resuspended in 40 μ L BAG, and carefully recounted. Approximately 6×10^7 cells were resuspended in 100 μ L BAG after washing. Two hundred microliters of fresh, ice-cold perchloric acid (0.5 M) were mixed with the cells. Lysed cells were placed on ice for 30 min. Cell debris were removed by centrifugation, and the supernatant was neutralized with a solution of 0.72 M KOH/0.6 M $KHCO_3$. After 15 min at room temperature, the precipitated salt was removed by centrifugation. Because short chain polyP extracts are unstable, assays of PP_i and short chain polyP were performed within 3 h.

Long chain polyP was extracted from each sample in quadruplicate using glass milk (QBioGene) as described elsewhere (82). Prior to extraction, PCF parasites were washed and counted as described above for short chain extractions. A sample of GITC-solubilized cells was reserved for protein determination by BCA (Pierce) before binding the polyP to glass milk. To minimize variation, long chain polyP extraction protocols were first optimized with respect to cell number. We found that it is necessary to perform quadruplicate extractions of 2.5×10^7 PCF cells from each sample to adequately control variation introduced by extraction methodology (data not shown).

Enzymatic assays of polyP and PP_i were performed in triplicate using recombinant yeast exopolyphosphatase (ScPPX, (13)) and yeast pyrophosphatase (ScPPase, Sigma), respectively. Assays for short chain polyP were incubated at 35° C for 30 min in 20 mM Tris (pH 7.5), 100 mM ammonium acetate, 5 mM magnesium acetate containing the sample and >50 U ScPPX. Background phosphate contamination of each sample was measured in triplicate wells not containing ScPPX, and positive control reactions containing a final concentration of 20 μ M sodium triphosphate were included on each plate. Reactions were stopped by addition of freshly mixed, malachite green reagent (3 parts 0.045% malachite green and 1 part 4.2% ammonium molybdate/4 M HCl), and absorbance at 660 nm was immediately read on an M2^e microplate spectrophotometer (Molecular Devices). Release of P_i from PP_i was assayed for 10 min at 35° C in 50 mM Tris (pH 7.5) containing 5 mM $MgCl_2$ and 0.1 U ScPPase.

Background phosphate controls (no ScPPase) and positive control (20-25 μ M potassium PP_i) reactions were included in triplicate. P_i was measured with malachite green as described above. On all occasions, standard curves of potassium P_i were included on each plate. P_i released from polyP and PP_i were normalized to reaction yield as determined by positive controls.

Results

Residues essential for yeast Vtc4 activity are conserved in TcVtc4 and TbVtc4.

The amino acid sequences of the catalytic regions of TbVtc4 and TcVtc4 (isoforms a and b) were compared with yeast Vtc4p characterized by Hothorn et al (5) (Fig. 10A). Two alleles of Vtc4 are present in *T. cruzi* Y strain, both of which are slightly different than the *T. cruzi* CL strain genomic sequences. The predicted primary structure of TcVtc4a and TcVtc4b differ from one another only at 3 positions. TbVtc4 and TcVtc4a/b share 72% identity. While trypanosomatid Vtc4 proteins are only 25% identical to *S. cerevisiae* Vtc4 (GenBank ID: p47075), lysine and arginine residues essential for yeast Vtc4 activity are conserved in both TbVtc4 and TcVtc4a/b. Additionally, key glutamate and serine residues (E426 and S457 in *S. cerevisiae* Vtc4, respectively) are also conserved in the trypanosomatid genes. We chose TcVtc4b for expression of the recombinant catalytic domain and activity assays, as this domain shares a slightly higher identity with the *T. brucei* homolog TbVtc4. Sequences for TcVtc4a, and TcVtc4b were submitted to GenBank.

TcVtc4 localizes to acidocalcisomes. The C-terminus of vacuolar transport chaperone 4 was tagged in *T. cruzi* with GFP. TcVtc4a was overexpressed as a fusion protein in epimastigotes. Western blot analysis confirmed expression of a protein of the expected size (Fig. 10B). Interestingly, this protein is sensitive to denaturing conditions and must not be boiled prior to loading onto polyacrylamide gels. The protein clearly co-localized with the acidocalcisomal marker vacuolar pyrophosphatase (VP1) (55) by immunofluorescence analysis (Fig. 11). To further validate this localization we performed cryo-immuno-electron microscopy and demonstrated that TcVtc4a (Fig. 12) clearly occurs in acidocalcisomes and not with any other structure in the cells.

TcVtc4b has polyP kinase activity. To characterize the enzymatic activity of TcVtc4b, we expressed its catalytic domain (TcVtc4₁₉₉₋₅₀₆) as a fusion protein with an N-terminal polyhistidine tag. The recombinant protein was purified using metal-ion affinity chromatography and the fractions were analyzed by SDS-PAGE and western blot (Fig. 13A-C). The recombinant protein (including the his-tag) appears as a strong single band with a molecular mass comparable to the predicted molecular mass (53.3 kDa, Fig. 13B). We tested polyP kinase activity of TcVtc4b with ATP (Fig. 13D). TcVtc4 has a K_m for ATP of $103.4 \pm 20 \mu\text{M}$ and a V_{max} of $5.1 \pm 0.2 \mu\text{mol min}^{-1} \text{mg protein}^{-1}$. The presence of PP_i did not “prime” or stimulate TcVtc4 activity, as was observed with the yeast enzyme (5).

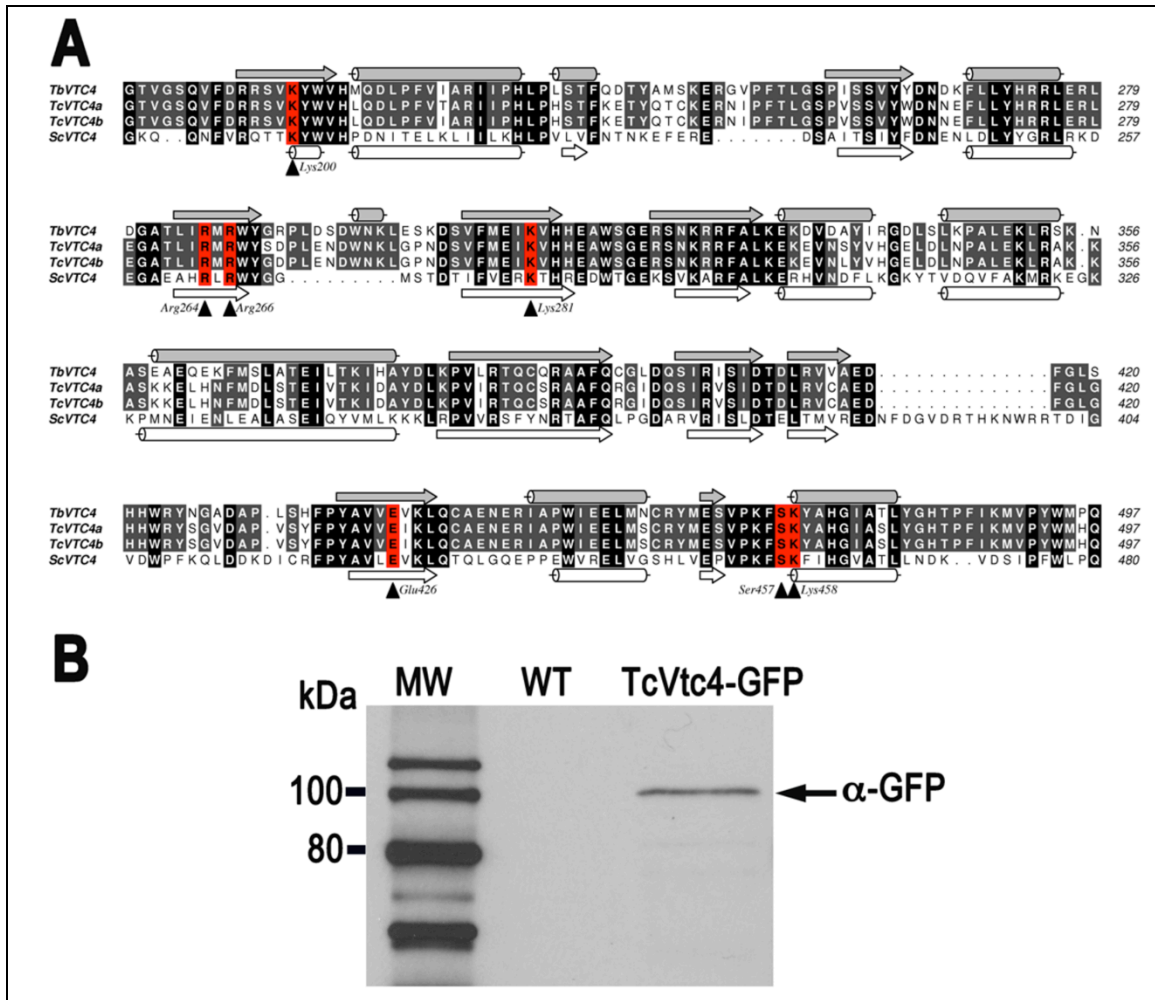


Figure 10. Sequence analysis of Vtc4 proteins and western blot analysis of the tagged TcVtc4. A. Alignment of TbVtc4 and both TcVtc4 alleles with the poly P-synthesizing domain of *S. cerevisiae* Vtc4. Secondary structure (predicted by PSIPRED v 2.6, (83,84) for TbVtc4 and ScVtc4p are shown alongside the alignment in gray and white, respectively. Essential residues of ScVtc4p are shown alongside the alignment in gray and white, respectively. Essential residues of ScVtc4p are denoted with black triangles and their residue number. Red background highlights essential residues conserved in all Vtc4 sequences. **B.** Western blot analysis of TcVtc4a-GFP in an extract from epimastigotes. TcVtc4a was overexpressed with a C-terminal GFP construct and detected with polyclonal α-GFP.

TbVtc4 is essential in *T. brucei* PCF. Knockdown of *TbVtc4* mRNA by induction of double-stranded RNAi with tetracycline resulted in growth defects and changes in acidocalcisome morphology and number. Growth defects in PCF developed after 5-6 days of RNAi (Fig. 14A). To ensure that *TbVtc4* was knocked-down, we

performed QRT-PCR on RNA isolated from treatment and control cells. *TbVtc4* RNA levels (normalized to tubulin and ssRRNA transcript abundance) were consistently knocked down >70% (Fig. 14B, C).

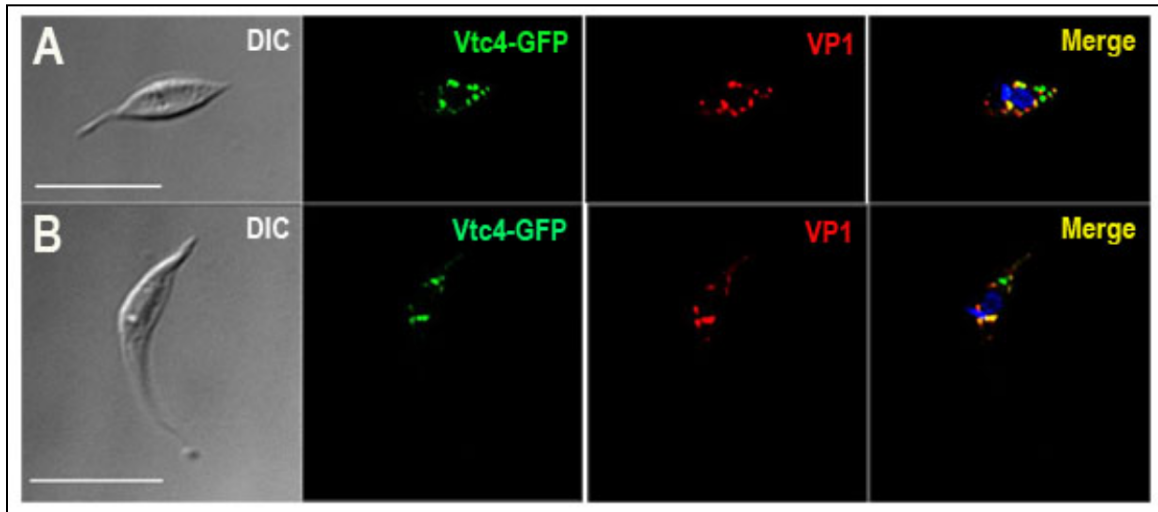


Figure 11. Immunofluorescence analysis of TcVtc4. **A, B.** Left panels are differential interference contrast (DIC) images of epimastigotes shown in the right panels. TcVtc4-GFP fusion protein (*Vtc4-GFP*, *green*) co-localizes with the vacuolar proton pyrophosphatase (*VP1*, *red*), an acidocalcisome marker, as shown in the *Merge* images. TcVtc4-GFP was detected with antibodies against GFP and VP1 was detected with antibodies against TbVP1. Scale bars = 10 μ m.

The morphology and number of acidocalcisomes changed dramatically in response to RNAi (Fig. 15A and Table 1). We quantified these changes using energy filter transmission electron microscopy (EF-TEM). The mean number of acidocalcisomes dropped by ~2-fold, but individual acidocalcisomes were considerably larger and less circular than those of un-induced cultures (Fig. 15B and C).

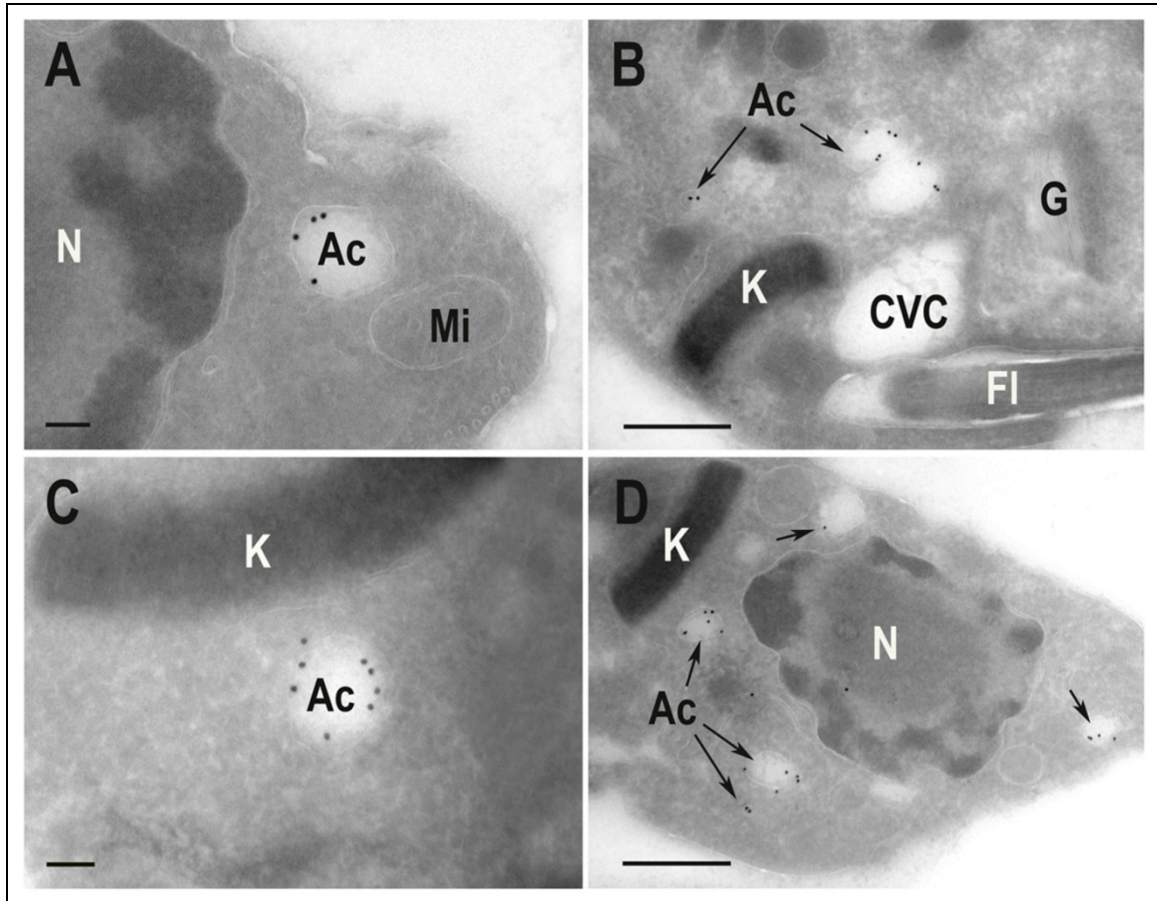


Figure 12. Immunoelectron microscopy of TcVtc4. A-D show different cells with gold-labeled antibodies against GFP localized in acidocalcisomes (Ac). CVC, contractile vacuole complex; G, Golgi; Mi: mitochondrion; N, nucleus; K, kinetoplast; FI, flagellum. Scale bars in **A** and **C** = 100 nm; **B** and **D** = 500 nm.

RNAi of TbVtc4 affects poly P balance. Knockdown of *TbVtc4* transcripts affected cellular polyP and PP_i content (Fig. 16). Short chain polyP fell almost 2-fold ($p < 0.05$, $n = 3$, Mann-Whitney test) over 6 days of RNAi while PP_i nearly doubled ($p < 0.05$, $n = 3$, ANOVA). RNAi of *TbVtc4*, however, did not significantly impact long chain polyP content during the same time frame. When experiments were extended to 9 days, long chain polyP continued to show no significant changes in total concentration ($p > 0.05$, $n = 3$, Mann-Whitney test; data not shown).

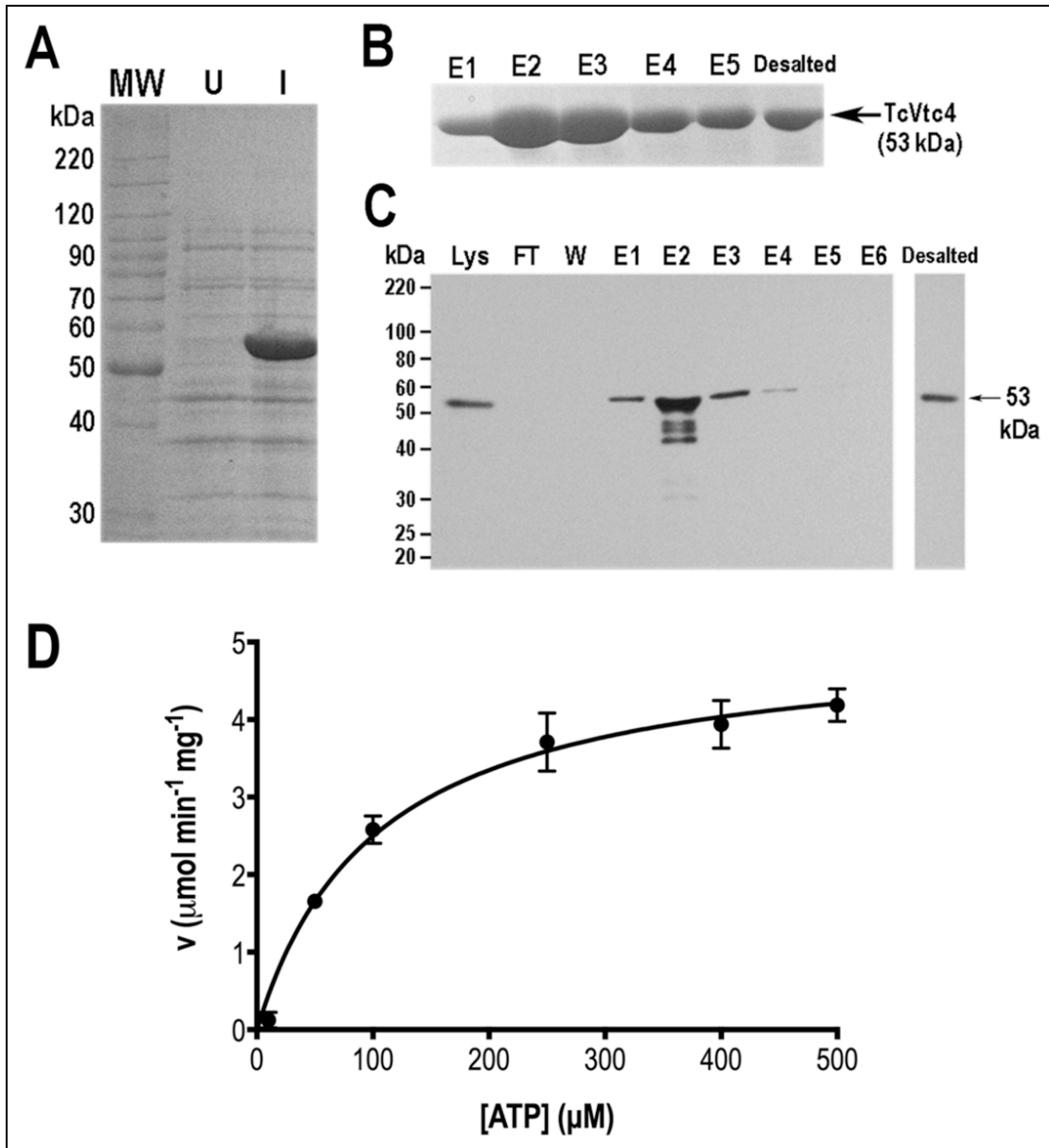


Figure 13. Purification and polyP kinase activity of recombinant TcVtc4. **A**, Bacterial lysates obtained before (U) and after induction (I) of TcVtc4b expression were analyzed by SDS-PAGE. **B**, Eluted (E1-E5) and desalted fractions obtained during TcVtc4 affinity purification as analyzed by SDS-PAGE showing a band of 53.3 kDa. **C**, Western blot analysis of lysate (Lys), flow through (FT), wash (W), eluted (E1-E6) and desalted fractions collected during TcVtc4 affinity purification, using commercial anti-histidine tag antibodies. **D**, Recombinant TcVtc4 activity as a function of ATP concentration.

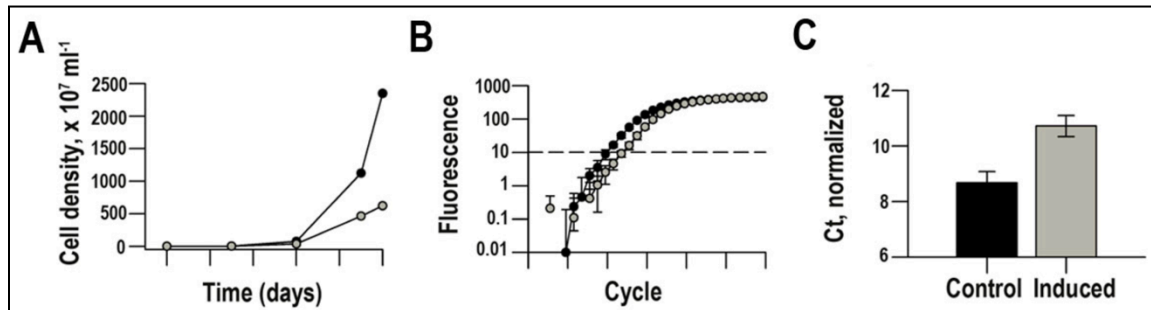


Figure 14. RNA interference of *TbVtc4* in *T. brucei* procyclic forms. **A.** Growth of procyclic *T. brucei* is reduced by knockdown of *TbVtc4* by RNAi. *Black*, uninduced control. *Gray*, PCF cultures induced with 1 $\mu\text{g}/\text{mL}$ tetracycline. Densities shown represent total cell density calculated from all dilution factors used when passing cultures during the experiment. **B.** QRT-PCR amplification curve of cDNA produced from a representative RNAi experiment six days after induction of dsRNA. *Black*, uninduced control. *Gray*, PCF cultures induced with 1 $\mu\text{g}/\text{mL}$ tetracycline. Error bars equal 1 standard deviation of the mean from duplicate assays. The dashed line denotes the threshold used for calculation of C_t . **C.** Relative abundance of *TbVtc4* transcripts in terms of threshold cycle (C_t) normalized to the geometric mean of C_t 's for *T. brucei* ssSRNA and tubulin. Error bars represent 1 standard deviation of the mean ($n = 4$).

Table 3. Morphometric analysis of acidocalcisomes of *T. brucei* PCF.

	Number of Acidocalcisomes	Mean circularity (nm)	Mean diameter (nm)	Absolute volume ($\times 10^6 \text{ nm}^3$)
WT	31 ± 2	0.99 ± 0.003	176.9 ± 6.9	3.8 ± 0.23
TbVtc4 RNAi				
≤ 10	7 ± 0	0.92 ± 0.02	$314.4 \pm 19.6^*$	$26.4 \pm 5.6^*$
11-20	14 ± 0	0.94 ± 0.01	$270.2 \pm 28.6^*$	$23.5 \pm 3.7^*$
21-40	24 ± 1	0.93 ± 0.02	$297.4 \pm 23.1^*$	$23.3 \pm 5.8^*$

The number, circularity, diameter, and absolute volume of acidocalcisomes (assuming spherical geometry) were analyzed and compared in control and *TbVtc4*-ablated cells. Cells submitted to RNAi (*TbVtc4* RNAi) were subdivided into three groups representing cells with fewer than ten, 11-20, and 21-40 acidocalcisomes per cell. Results are expressed as means \pm 1 SD. Significance as compared with wild type cells ($p < 0.05$).

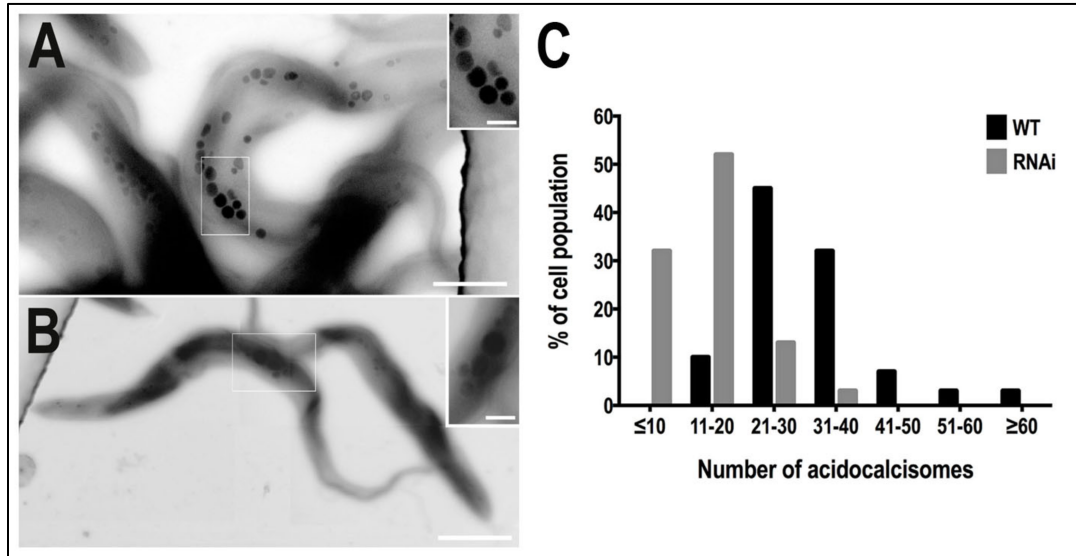


Figure 15. Morphological changes in *TbVtc4* RNAi procyclic forms. **A.** Scanning transmission electron microscopy (STEM) image from non-induced *TbVtc4* RNAi PCF trypanosomes showing the size and distribution of acidocalcisomes. Bar: 1.5 μm . Inset, inverted image showing acidocalcisomes contained in the box highlighted in A at higher magnification. Bar: 250 nm. **B.** STEM image from *TbVtc4* RNAi induced PCF trypanosomes. Bar: 3 μm . Inset, inverted image showing a high magnification of the acidocalcisomes contained in the box highlighted in B. Bar: 400 nm. **C.** Numeric distribution of acidocalcisomes in *T. brucei* PCF. Whole unfixed parasites were observed using a Zeiss EM 902 transmission electron microscope equipped with an energy filter and the number of acidocalcisomes per cell in ~50 cells was counted.

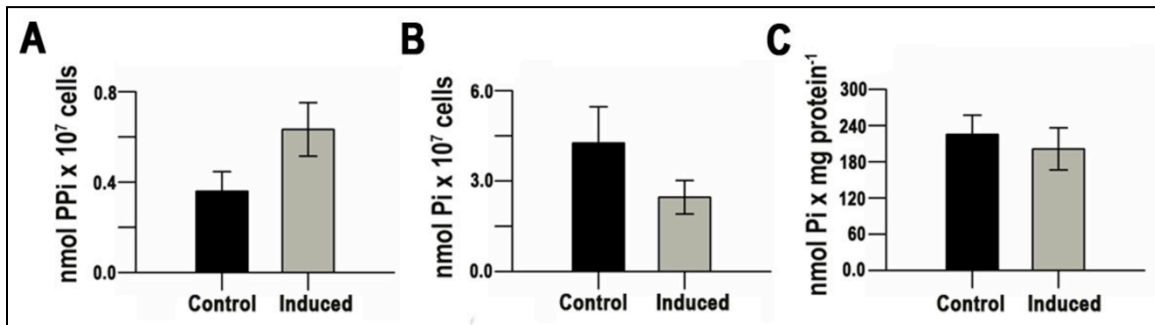


Figure 16. Knockdown of *TbVtc4* transcripts by RNA interference increases cellular pyrophosphate (PP_i) and decreases short chain polyP levels. **A.** PP_i content of cells, $p < 0.05$ (ANOVA, $n = 3$). Error bars represent 1 standard deviation of the mean. **B.** Short chain polyP content of PCF *T. brucei* after 6 days of induction with 1 $\mu\text{g mL}^{-1}$ tetracycline, $p < 0.05$ (Mann-Whitney test, $n = 3$, two-tailed). Error bars represent 1 standard deviation of the mean. **C.** Long chain polyP content of PCF *T. brucei* is unaffected by RNA interference of *TbVtc4* after 6 days of dsRNA induction. Error bars represent standard error of the mean.

Discussion

Bloodstream form (BSF) *Trypanosoma brucei* lacking detectable TbVtc4 through genetic ablation are defective in short chain polyP and exhibit growth defects *in vitro* and *in vivo* (43). In the present study, we report that insect forms of both *T. brucei* and *T. cruzi* also express a Vtc4 protein that is able to catalyze the polyP synthesis and resides in acidocalcisomes, as detected by immunofluorescence and immunoelectron microscopy. Knockdown of TbVtc4 in procyclic form (PCF) *T. brucei* inhibited growth, increased cellular levels of pyrophosphate (PP_i), and decreased levels of short chain polyP. However, RNAi of *TbVtc4* in PCF did not affect levels of long chain polyP as happens after knockout of *TbVtc4* in BSF (43). Knockdown of *TbVtc4* in PCF reduced the number of acidocalcisomes and resulted in increased acidocalcisomal size relative to wild type cells, which is consistent with the decrease in polyP content of the cells. The decreased polyP content suggests that ablation of TbVtc4 shifts the equilibrium of synthesis and degradation of the polyP pool toward hydrolysis. Increased polyP hydrolysis would increase acidocalcisome osmolyte (P_i and PP_i) concentrations and stimulate water entry, as described when polyP is hydrolyzed in trypanosomes subjected to hyposmotic conditions (28).

Although short chain polyP decreased by ~50% after 6 days of RNAi, polyP did not disappear completely. The continued presence of polyP may be the result of residual TbVtc4, or to other pathways for polyP synthesis that may be present in these parasites. Intracellular polyP is composed of different size classes, and

synthesis of very short chain polyP (polyP₃, polyP₄, and polyP₅) which are very abundant in trypanosomes (68)) may not be mediated by TbVtc4. Additionally, the extraction method we used cannot discriminate between very short and medium size polyP.

PolyP plays an important role for resistance of *T. cruzi* to osmotic stresses these parasites experience *in vivo* (13,28). The insect stages of this parasite reside in the hindgut of their insect hosts and are subjected to dramatic changes in osmolarity. Following a blood meal by host, the hindgut osmolality of *T. cruzi* hosts rises within a day from as low as 300 mOsm to as high as 1,000 mOsm as the blood meal is dehydrated (85). Much less is known about the osmotic conditions in the *tse tse* fly gut, but it is reasonable to speculate that osmolarity of the intestine changes as the blood meal is digested.

In summary, Vtc4 is essential for growth of the *T. brucei* PCF, and the *T. cruzi* enzyme is similar to *T. brucei* Vtc4 in its localization and capacity to synthesize polyP. Given that mammalian hosts lack similar enzymes, Vtc4 proteins may be promising drug targets.

CHAPTER 4

THE POLYPHOSPHATE-BINDING PROTEOME OF *T. BRUCEI* AND *T. CRUZI*

Introduction

Polyphosphate accumulation in acidocalcisomes has been evidenced from bacterial to human platelets (4). In fact, most of the polyP-interacting proteins studied to date are located to acidocalcisomes or to acidic vacuoles (yeast). However, in eukaryotic cells polyP is also present in other subcellular compartments, including nucleus, mitochondria, cytosol and lysosomes (14), where polyP is involved in biological processes that have been recently discovered but probably in many others that have not been investigated yet. For example, polyP combines with calcium and polyhydroxybutyrate to form channels in cellular membranes. That is the case of the calcium channel and potassium pump in plasma membrane, the mitochondrial permeability transition pore in mitochondria, and channels in bacterial membranes that make them competent for DNA entry (1,14,86). Some research groups have become interested in studying polyP because of its presence on a specific cell type or organelle (astrocytes, human platelets, acidocalcisomes) (2,4,87) or because they found this molecule interacting with a particular protein of interest. As an example, the role of ScVtv4p in polyP synthesis was investigated after identifying the anionic

polymer in the tunnel-like structure of the crystallized VTC domain (5). Determining polyP-protein interactions is an important step to elucidate the role of this ubiquitous molecule in different subcellular compartments. Recently, Choi et al (88) described a method to chemically modify polyP by the covalent attachment of a primary amine to the terminal phosphates of polyP via stable phosphoramidate linkages in the presence of EDAC (1-ethyl-3-[3-dimethylamino-propyl]carbodiimide). Following this strategy polyP can be biotinylated and immobilized onto solid supports, thus facilitating the study of its biological role. One of the approaches is the identification of polyP-binding proteins in different cell lines or subcellular fractions. Taking advantage of this method we used biotinylated polyP to obtain the polyP-binding proteome from total cell lysates of *T. brucei* PCF and *T. cruzi* epimastigotes. Here we report the list of potential poly-P binding proteins found in both organisms and discuss the possible role that polyP could play in some of the most abundant proteins observed in these proteomes.

Experimental Procedures

Cell culture. *T. brucei* PCF (29-13 strain) were grown at 28 °C in SM medium (89) supplemented with 10% heat-inactivated fetal bovine serum (FBS), 8 µg/mL hemin, 15 µg/mL G418 and 50 µg/mL hygromycin. Cultures were scale-up in glass sterile bottles under shaking until reaching a final volume of 3.0 L cell

culture in exponential phase ($1-1.5 \times 10^7$ cells/mL). Cell density was verified by counting parasites in a Neubauer chamber.

T. cruzi epimastigotes (Y strain) were grown at 28 °C in LIT medium (77) supplemented with 10% heat-inactivated FBS. Cultures were scale-up in glass sterile bottles under shaking until reaching a final volume of approximately 1.0 L cell culture in exponential phase ($\sim 4 \times 10^7$ cells/mL). Cell density was verified by counting parasites in a Neubauer chamber.

Cell lysis. Approximately 4×10^{10} cells (*T. brucei* PCF and *T. cruzi* epimastigotes) were harvested separately by centrifugation at $1000 \times g$ for 15 min at RT and then washed twice with buffer A with glucose (BAG, 116 mM NaCl, 5.4 mM KCl, 0.8 mM MgSO₄, 50 mM HEPES and 5.5 mM glucose, pH 7.3). Cells were resuspended in 5 mL hypotonic lysis buffer plus protease inhibitors (50 mM HEPES pH 7.0, mammalian cells protease inhibitor cocktail (Sigma P8340) diluted 1:250, 1 mM PMSF, 2.5 mM TPCK and 100 μM E64) and then incubated for 1 h on ice. Three rounds of freeze-thaw were applied to the cells (5 min on dry ice/ethanol bath, 5 min at 37 °C in water bath). Then cells were sonicated 3 times for 30 s at 40% amplitude, keeping them on ice for at least 1 min between pulses. Cell lysis was verified under light microscope and lysates were filtered through a 5 μm pore nitrocellulose membrane to remove cell ghosts. Protein concentration was determined by BCA protein assay (Pierce). Cell lysates were stored at -80°C until processed for polyP-binding protein pull down within a week after lysis.

PolyP biotinylation. Biotinylated polyP was provided by our collaborator Dr. James Morrissey (University of Illinois, Urbana, IL). Medium size polyP (<1000 mers) was end labeled by the covalent linkage of a primary biotinylated amine (amine-PEG₂-biotin) to the terminal phosphates of polyP in the presence of EDAC, as previously described (88).

PolyP-binding protein pull down. Twenty mg streptavidin-coated magnetic beads (Dynabeads MyOne Streptavidin T1, Invitrogen) were washed three times with dynabeads wash buffer (1 M LiCl, 50 mM Tris-HCl, pH 7.4) in a 15 mL tube using a DynaMag™ magnet. Beads were incubated with 1×10^{-5} moles biotinylated polyP (resuspended in 5 mL dynabeads wash buffer) for 1 h at RT under rotation. Then, beads were washed twice with 10 mL wash buffer and once with 10 mL 50 mM Tris-HCl, pH 7.4. Ten pull down rounds were performed as follows: 10 mg protein from *T. cruzi* (or *T. brucei*) total lysate were diluted in 10 mL wash buffer (50 mM Tris-HCl pH 7.4, 5 mM EDTA, 0.1% polyethylenglycol (PEG), 0.01% sodium azide) plus phosphatase inhibitors (2 mM imidazole, 1 mM sodium fluoride, 1.15 mM sodium molybdate, 1 mM sodium orthovanadate and 4 mM sodium tartrate) and filtered through a 0.22 μm pore nitrocellulose membrane. Diluted/filtered protein extracts were incubated with 10 mg polyP-coated beads on a rotator for 30 min at RT. Beads were washed 5 times with 10 mL wash buffer and polyp-binding proteins were eluted with 500 μL elution buffer (1 M NaCl, 50 mM Tris-HCl, pH 7.4). Eluates from 100 mg initial protein extract were combined and precipitated with trichloroacetic acid (TCA). Finally, polyP-binding

proteins were resuspended in 500 μ L 50 mM Tris-HCl pH 7.4 and quantified by BCA protein assay.

Sample preparation. Samples containing *T. brucei* and *T. cruzi* polyP binding proteins from 2 independent experiments were processed at the Protein Sciences Facility of University of Illinois (Urbana, IL) for liquid chromatography tandem mass spectrometry analysis (LC/MS). Sample cleanup was performed using Perfect Focus (G-Biosciences, St. Louis, MO) according to manufacturer's instruction. Protein samples were reduced in 10 mM DTT at 56 °C for 30 minutes and alkylation was performed using 20 mM iodoacetamide for 30 minutes in the dark. Samples were digested with trypsin (G-Biosciences, St. Louis, MO) at a ratio of 1:10 – 1:50 using a CEM Discover Microwave Digestor (Mathews, SC) at 55° C for 15 minutes. Digested peptides were extracted with 50% acetonitrile, 5% formic acid, dried under vacuum and resuspended in 5% acetonitrile, 0.1% formic acid for LC/MS analysis.

Mass spectrometry. LC/MS was performed using a Thermo Dionex Ultimate RSLC3000 operating in nano mode at 300 microliters/min with a gradient from 0.1% formic acid to 60% acetonitrile plus 0.1% formic acid in 120 minutes. The trap column used was a Thermo Acclaim PepMap 100 (100 μ m x 2 cm) and the analytical column was a Thermo Acclaim PepMap RSLC (75 μ m x 15 cm).

Data analysis. Xcalibur raw files were converted by Mascot Distiller interface (Matrix Science) into peaklists that were submitted to Mascot Server to search

against specific protein databases: *T. brucei* Lister 427 and *T. cruzi* CL Brener (Esmeraldo and Non-Esmeraldo-like) on *TryTripDB* (59).

Results

T. brucei polyP-binding protein identification. Mascot search against *T. brucei* Lister 427 database led to the identification of 73 potential poly-P binding proteins, from which 61 have been annotated as putative proteins with a predicted function, and 12 appear as hypothetical proteins (Figure 17 and Table 4). The biggest group of identified proteins corresponds to ribosomal proteins (translation and protein synthesis, 23 proteins), followed by glycolysis (9 proteins), DNA and RNA binding (9 and 6 proteins), and signal transduction (4 proteins). Two translation factors were also identified, as well as proteins belonging to other functional groups, accounting for less than 2% of the proteome each group (Fig. 17). The protein with highest Mascot score was a small nucleolar ribonucleoprotein (snoRNP protein GAR1) followed by proteins involved in glycolysis (hexokinase, phosphoenolpyruvate carboxykinase, fructose-bisphosphate aldolase), ribosomal proteins (S6, S15 and L10a) and signal transduction (high mobility group protein). One of the hypothetical proteins also exhibited a high (> 300) Mascot score, indicating a high relative abundance of an unknown protein in this proteome. The list of potential polyP-binding proteins found in this study is summarized in Table 4, where proteins were grouped by

metabolic pathways or cellular function and sorted from highest to lower score within each group.

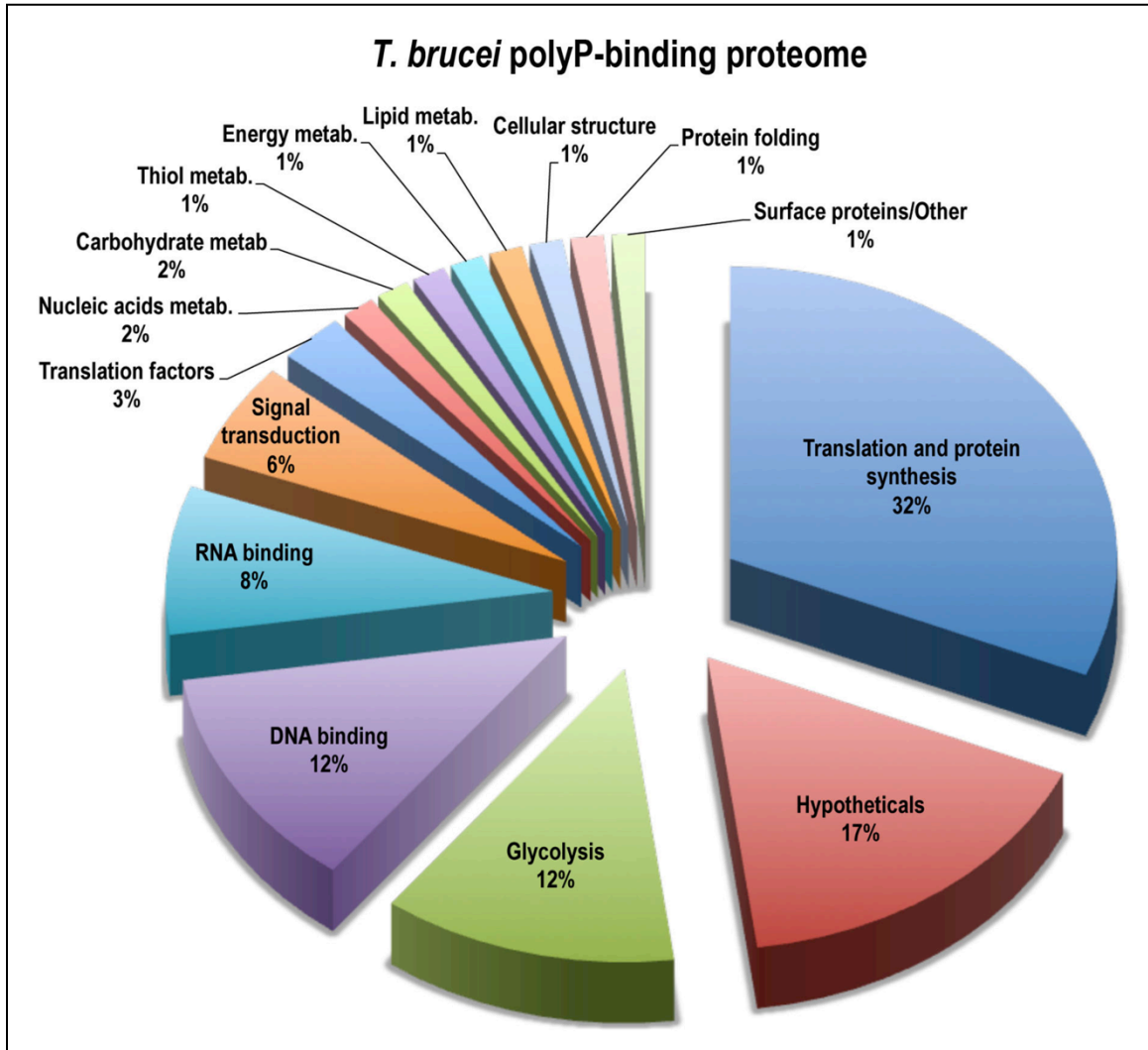


Figure 17. Functional classification of proteins found in *T. brucei* polyP-binding proteome.

Table 4. Potential PolyP-binding proteins identified in *T. brucei* PCF.

Mascot Score	Protein name	TriTrypDB ID	Length (aa)
NUCLEOSIDE, NUCLEOTIDE & NUCLEIC ACID METABOLISM			
106	hypoxanthine-guanine phosphoribosyltransferase	Tb427.10.1390	234
CARBOHYDRATE METABOLISM			
15	lipophosphoglycan biosynthetic protein, putative	Tb427.03.3580	773
THIOL METABOLISM			
37	tryparedoxin peroxidase	Tb427tmp.160.4250	199
ENERGY METABOLISM			
414	glycosomal malate dehydrogenase	Tb427.10.15410	323
GLYCOLYSIS / GLUCONEOGENESIS			
787	Hexokinase	Tb427.10.2020	471
473	glycosomal phosphoenolpyruvate carboxykinase	Tb427.02.4210	525
318	fructose-bisphosphate aldolase, glycosomal	Tb427.10.5620	372
100	glycerol-3-phosphate dehydrogenase [NAD+], glycosomal	Tb427.08.3530	354
78	Fructose-1,6-bisphosphatase, cytosolic, putative	Tb427tmp.211.0540	350
75	glyceraldehyde 3-phosphate dehydrogenase, glycosomal, putative	Tb427.06.4280	359
74	pyruvate phosphate dikinase	Tb427tmp.02.4150	913
59	glycerol kinase, glycosomal, putative	Tb427tmp.211.3540	512
47	ATP-dependent phosphofructokinase	Tb427.03.3270	487
LIPID METABOLISM			
88	acyl-CoA binding protein	Tb427.04.2010	93
CELLULAR STRUCTURE, MOTILITY AND ORGANIZATION			
38	beta tubulin, putative	Tb427.01.2330	442
REPLICATION, TRANSCRIPTION, DNA REPAIR, AND DNA BINDING			
159	histone H4, putative	Tb427.05.4170	100
88	kinetoplast DNA-associated protein, putative	Tb427.10.8890	209
80	histone H2B, putative	Tb427.10.10460	112
69	histone H3, putative	Tb427.01.2430	133
67	kinetoplast-associated protein, putative	Tb427.08.7260	1028
60	ATP-dependent DEAD/H RNA helicase, putative	Tb427.04.2630	843
53	kinetoplast DNA-associated protein, putative	Tb427.10.8950	126
41	histone H2A, putative	Tb427.07.2820	134
28	DNA repair protein, putative	Tb427tmp.01.0530	762
TRANSCRIPTION, RNA PROCESSING, AND RNA BINDING			
848	snoRNP protein GAR1, putative	Tb427.04.470	230
162	cyclophilin, putative	Tb427.08.2000	301
101	RNA-binding protein (DRBD10)	Tb427tmp.211.4120	429
52	small nuclear ribonucleoprotein SmD1	Tb427.07.3120	106
49	fibrillarin, putative	Tb427.10.14750	304
29	RNA-binding protein, putative	Tb427.10.13720	377
TRANSLATION AND PROTEIN SYNTHESIS			
660	ribosomal protein S6, putative	Tb427tmp.160.3670	126
401	40S ribosomal protein S15, putative	Tb427.07.2370	172
338	60S ribosomal protein L10a, putative	Tb427tmp.01.1470	214
287	40S ribosomal protein S24E, putative	Tb427.10.7330	137
269	ribosomal protein L36, putative	Tb427.10.1590	109
266	60S ribosomal protein L29, putative	Tb427tmp.01.1790	71
230	60S ribosomal protein L6, putative	Tb427.10.11390	192
217	40S ribosomal protein S10, putative	Tb427.10.5360	172
209	40S ribosomal protein S12, putative	Tb427.10.8430	142
185	60S ribosomal protein L23a	Tb427.07.5170	164
162	40S ribosomal protein S8, putative	Tb427.08.6160	220
149	50S ribosomal protein L7Ae, putative	Tb427.04.750	145
144	60S ribosomal protein L17, putative	Tb427.10.14580	166
131	ribosome biogenesis protein, putative	Tb427.10.14680	307
107	60S ribosomal protein L28, putative	Tb427tmp.02.4050	146
96	ubiquitin/ribosomal protein S27a, putative	Tb427.07.3680	153
85	40S ribosomal protein S14, putative	Tb427.06.4980	144
74	40S ribosomal protein S24E, putative	Tb427.10.7330	137
66	40S ribosomal protein L14, putative	Tb427tmp.01.3020	189
62	60S ribosomal protein L26, putative	Tb427.08.6180	143
27	40S ribosomal protein S15A	Tb427tmp.02.4000	130
26	60S ribosomal proteins L38, putative	Tb427.10.3280	82
24	40S ribosomal protein S17, putative	Tb427tmp.01.3675	142

Table 4. (Cont.)

Mascot Score	Protein name	TriTrypDB ID	Length (aa)
TRANSLATION FACTORS			
93	elongation factor 1-alpha	Tb427.10.2100	449
44	nascent polypeptide associated complex alpha subunit, putative	Tb427tmp.01.1465	101
PROTEIN FOLDING AND STABILIZATION			
32	TPR-repeat-containing chaperone protein DNAJ, putative	Tb427.07.3630	528
SURFACE PROTEINS/OTHER			
30	retrotransposon hot spot (RHS) protein, putative	Tb427.02.470	860
SIGNAL TRANSDUCTION			
426	high mobility group protein, putative	Tb427.03.3490	271
62	calmodulin	Tb427tmp.01.4621	149
50	Trichohyalin, putative	Tb427tmp.01.3320	658
38	casein kinase II, putative	Tb427tmp.211.4890	349
HYPOTHETICALS			
453	hypothetical protein, conserved	Tb427tmp.02.2030	117
222	hypothetical protein, conserved	Tb427.03.1820	246
200	hypothetical protein, conserved	Tb427tmp.02.1910	317
132	hypothetical protein, conserved	Tb427tmp.02.3560	206
101	hypothetical protein, conserved	Tb427tmp.01.2800	348
106	hypothetical protein, conserved	Tb427.10.8960	237
72	hypothetical protein, conserved	Tb427tmp.160.1100	198
64	hypothetical protein, conserved	Tb427tmp.03.0720	174
55	unspecified product	Tb427.05.800	332
53	hypothetical protein, conserved	Tb427tmp.211.4200	337
18	hypothetical protein, conserved	Tb427.10.10030	100

T. cruzi polyP-binding protein identification. To identify *T. cruzi* poly-P binding proteins Mascot search was performed against *T. cruzi* CL Brener (Esmeraldo and non-Esmeraldo like) databases, as the genome of *T. cruzi* Y strain is not available yet. This search led to the identification of 60 potential poly-P binding proteins, from which 57 have been annotated as putative proteins with a predicted function, and 3 correspond to hypothetical proteins (Figure 18 and Table 5). It is important to mention that many other hypothetical proteins (78 in total) were found in *T. cruzi* pull downs but we are reporting here only the three of them that were found in both *T. cruzi* experiments. A high number of proteins in *T. cruzi* polyP-binding proteome belong to the group of translation and protein synthesis (22 proteins), followed by glycolysis (8 proteins), RNA and DNA binding

(7 and 4 proteins, respectively), and cellular structure (4 proteins). Mascot scores indicate that the most abundant protein in this proteome is the hexokinase, followed by ribosomal protein S6 and histidine-ammonia-lyase. Other two proteins of the glycolysis pathway exhibited a high score (> 300): fructose1,6-biphosphatase and 6 phospho-1-fructokinase. Other high-score proteins found in this proteome were: nucleolar protein, glycosomal malate dehydrogenase, ribosomal proteins L38 and S8, retrotransposon hot spot (RHS) and casein kinase II (Table 5). Most of these high-score proteins were also found abundantly in the *T. brucei* polyP- binding proteome, eight of them being present in all four *T. brucei* and *T. cruzi* samples analyzed: glycosomal malate dehydrogenase, hexokinase, glycosomal phosphoenolpyruvate carboxykinase, snoRNP protein GAR1, and ribosomal proteins S6, S8, L36 and L38. A total number of 36 proteins were independently found in *T. brucei* and *T. cruzi* PolyP-binding proteomes, a number that represents more than 50% of the proteins on each proteome.

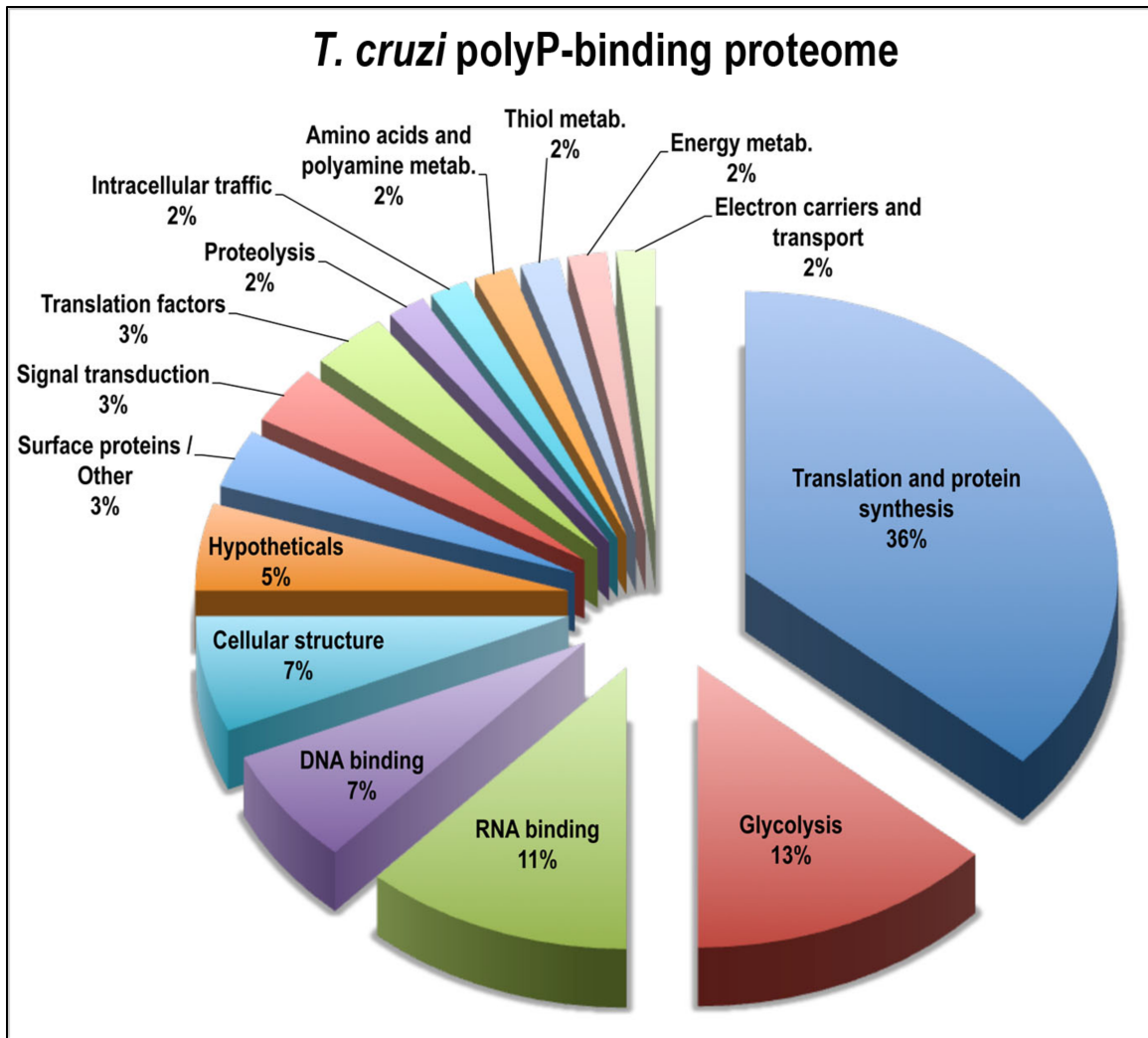


Figure 18. Functional classification of proteins found in *T. cruzi* polyP-binding proteome.

Table 5. Potential PolyP-binding proteins identified in *T. cruzi* epimastigotes.

Mascot Score	Protein name	TryTripDB ID	Length (aa)
AMINO ACID AND POLYAMINE METABOLISM			
1379	histidine ammonia-lyase, putative	Tc00.1047053506247.220	534
THIOL METABOLISM			
35	tryparedoxin peroxidase, putative	Tc00.1047053504839.28	199
ENERGY METABOLISM			
592	glycosomal malate dehydrogenase, putative	Tc00.1047053506503.69	323
ELECTRON CARRIERS AND TRANSPORT			
90	cytochrome b5 reductase, putative	Tc00.1047053503873.10	308
GLYCOLYSIS / GLUCONEOGENESIS			
1937	hexokinase, putative	Tc00.1047053508951.20	471
719	fructose-1,6-bisphosphatase, cytosolic, putative	Tc00.1047053506649.70	344
479	6-phospho-1-fructokinase, putative	Tc00.1047053508153.340	485
261	glycosomal phosphoenolpyruvate carboxykinase, putative	Tc00.1047053507547.90	525
144	pyruvate dehydrogenase E1 component alpha subunit, putative	Tc00.1047053507831.70	378
108	glyceraldehyde 3-phosphate dehydrogenase, putative	Tc00.1047053506943.50	359
36	fructose-bisphosphate aldolase, putative	Tc00.1047053510301.20	372
17	pyruvate phosphate dikinase, putative	Tc00.1047053506297.190	913
CELLULAR STRUCTURE, MOTILITY, AND ORGANIZATION			
130	beta tubulin, putative	Tc00.1047053506563.40	442
85	ARP2/3 complex subunit, putative	Tc00.1047053504215.40	383
66	ARP2/3 complex subunit, putative	Tc00.1047053508737.194	180
17	ARP2/3 complex subunit, putative	Tc00.1047053506865.10	328
REPLICATION, TRANSCRIPTION, DNA REPAIR, AND DNA BINDING			
314	histone H2B, putative	Tc00.1047053511635.10	112
236	histone H2A, putative	Tc00.1047053511817.180	135
209	kinetoplast DNA-associated protein, putative	Tc00.1047053509793.30	123
28	kinetoplast associated protein, putative	Tc00.1047053509791.120	185
TRANSCRIPTION, RNA PROCESSING, AND RNA BINDING			
1179	nucleolar protein, putative	Tc00.1047053511573.58	387
291	snoRNP protein GAR1, putative	Tc00.1047053510687.120	239
118	small nuclear ribonucleoprotein, putative (SmD1)	Tc00.1047053510531.54	98
85	fibrillarin, putative	Tc00.1047053509715.40	316
73	small nuclear ribonucleoprotein, putative	Tc00.1047053510531.54	98
41	small nuclear ribonucleoprotein SmD3, putative	Tc00.1047053508257.150	115
29	RNA binding protein, putative (DRBD10)	Tc00.1047053510747.80	421
TRANSLATION AND PROTEIN SYNTHESIS			
1582	ribosomal protein S6, putative,NPH2/RS6-like protein, putative	Tc00.1047053508277.120	126
553	ribosomal protein L38, putative	Tc00.1047053503575.34	82
462	40S ribosomal protein S8, putative	Tc00.1047053511903.110	221
297	ribosomal protein L38, putative	Tc00.1047053503881.39	82
245	40S ribosomal protein S10, putative	Tc00.1047053506679.140	161
140	60S ribosomal protein L28, putative	Tc00.1047053510101.30	146
126	60S ribosomal protein L18, putative	Tc00.1047053503395.40	323
109	60S ribosomal protein L23a, putative	Tc00.1047053508175.146	194
97	40S ribosomal protein S15, putative	Tc00.1047053511809.130	152
95	ribosomal protein L36, putative	Tc00.1047053509671.64	114
92	60S ribosomal protein L22, putative	Tc00.1047053504147.120	130
84	40S ribosomal protein S15A, putative	Tc00.1047053506297.330	130
81	60S ribosomal protein L17, putative	Tc00.1047053503449.10	166
80	40S ribosomal protein S12, putative	Tc00.1047053508231.20	142
78	40S ribosomal protein S12, putative	Tc00.1047053503395.50	141
76	ribosomal protein S20, putative	Tc00.1047053508823.120	117
71	ribosomal protein L29, putative	Tc00.1047053509749.33	71
49	50S ribosomal protein L7Ae, putative	Tc00.1047053507053.10	148
47	40S ribosomal protein S17, putative	Tc00.1047053508827.70	196
37	40S ribosomal protein S14, putative	Tc00.1047053409117.20	144
27	60S ribosomal protein L32, putative	Tc00.1047053504069.30	133
20	60S ribosomal protein L6, putative	Tc00.1047053505843.20	193

Table 5. (Cont.)

Mascot Score	Protein name	TryTripDB ID	Length (aa)
TRANSLATION FACTORS			
83	nascent polypeptide associated complex subunit, putative	Tc00.1047053510241.60	181
53	eukaryotic translation initiation factor 5, putative	Tc00.1047053504105.20	379
PROTEOLYSIS			
125	serine carboxypeptidase S28, putative	Tc00.1047053506425.10	631
TRANSPORT PROTEINS - INTRACELLULAR TRAFFIC			
52	Mu-adaptin 1, putative, adaptor complex AP-1 medium subunit, putative	Tc00.1047053510533.40	432
SURFACE PROTEINS/OTHER			
503	retrotransposon hot spot (RHS) protein, putative	Tc00.1047053503483.9	916
14	dispersed gene family protein 1 (DGF-1, pseudogene), putative	Tc00.1047053511391.24	3489
SIGNAL TRANSDUCTION			
380	casein kinase II, putative	Tc00.1047053510761.60	345
104	high mobility group protein, putative	Tc00.1047053504431.64	270
HYPOTHETICALS			
180	hypothetical protein, conserved	Tc00.1047053509207.40	1136
102	hypothetical protein, conserved	Tc00.1047053506857.30	508
28	hypothetical protein, conserved	Tc00.1047053511439.40	455

Discussion

Here we report the preliminary results of the polyP-binding proteome obtained from total lysates of *T. brucei* PCF and *T. cruzi* epimastigotes. The data has to be validated through the functional study of the most relevant proteins observed. However, the list of potential polyP-binding proteins here presented represents the first high throughput attempt to elucidate the nature of proteins interacting with polyP in these two pathogenic organisms, where polyP has been demonstrated to be important for infectivity and survival under stress conditions (13,26,28,42,43).

We identified 73 and 60 potential polyP-binding proteins in *T. brucei* and *T. cruzi* respectively, 36 of which were observed in both datasets. The high percentage of proteins independently found in both proteomes validates in some

way the data, as well as previous works reporting polyP interactions with some of the most abundant proteins found in these proteomes.

None of the proteins involved in polyP metabolism (PPN, PPX, Vtc4, described in Chapter 1) were observed in *T. brucei* and *T. cruzi* polyP-binding proteomes. The explanation for this is the low relative abundance of these proteins (most of them located to acidocalcisomes) in total lysates of the parasites. In order to catch such proteins, it would be necessary to use an acidocalcisome-enriched fraction as starting material for the pull downs. Interestingly, three actin-related proteins (ARP2/3 complex subunits) were found in the *T. cruzi* proteome (Table 5). Previous work in *D. discoideum* demonstrated that polyP kinase 2 (DdPPK2) shares characteristics of actin-related proteins and is inhibited by actin inhibitors such as phalloidin and DNase I. This peculiar polyP kinase is able to combine the reversible synthesis of actin-like filaments together with polyP synthesis (33). So, it would be interesting to explore the possible role of these actin-related proteins in polyP synthesis.

One of the proteins exhibiting a high score in both, *T. brucei* and *T. cruzi* polyP-binding proteomes is the Hexokinase (HK), an enzyme that catalyzes the first step of glycolysis to produce glucose-6-phosphate (G6P). The protein has been characterized in both organisms (90,91) and as other invertebrate HKs they are not inhibited by G6P. However, TcHK activity is inhibited by PP_i (90) and this fact provides an explanation for the relative abundance of hexokinase in these proteomes, as polyP could interact with HK through the PP_i binding site that

regulates its activity. A recent work demonstrated that inorganic polyP₃ and polyP₁₅ regulates HK activity in mitochondria of *Rhipicephalus microplus* embryo, a tick from tropical regions (92). Whether polyP is regulating TbHK and TcHK activities is something to be determined.

Another glycolytic enzyme that interacts with PP_i is the pyruvate phosphate dikinase (PPDK, found in both proteomes), an enzyme that catalyzes the conversion of phosphoenolpyruvate to pyruvate, and in trypanosomes utilizes PP_i instead of ATP as substrate (93,94). On the other hand, 6-phospho-1-fructokinase (PFK, found in *T. cruzi* polyP-binding proteome) is an enzyme that catalyzes the phosphorylation of fructose-6-phosphate to fructose-1,6-bisphosphate, a key regulatory step in the glycolytic pathway. TcPFK is an ATP-dependent enzyme that shows a high degree of sequence similarity with PP_i-dependent enzymes (95). In addition, modulators of PFK activity in other organisms, such as ATP, citrate, fructose 2,6-bis-phosphate and P_i, have no effect in TbPFK (96). Therefore, it is possible that PP_i and also polyP play a role in TcPFK regulation.

PolyP anions have been involved in stabilization of glyceraldehyde-3-phosphate dehydrogenase (GAPDH) (97), another glycolytic enzyme found in both polyP-binding proteomes. In this work the authors demonstrated that polyP suppresses thermal aggregation of the enzyme without affecting its activity. This could be a general mechanism for polyP-mediated regulation of glycolytic

enzymes and it could explain the presence of glycosomal enzymes observed in *T. brucei* and *T. cruzi* polyP-binding proteomes.

The interaction of polyP with ribosomal proteins has been previously reported in *E. coli* for two main processes: degradation of ribosomal protein through polyP-Lon protease complex (98) and as promoter of translation fidelity (99). The ATP-dependent Lon protease form a complex with polyP that degrades most of the ribosomal proteins, thereby supplying the amino acids required for response to starvation (98). On the other hand, polyP interacts with ribosomes to maintain optimal translation efficiency, as demonstrated in experiments measuring the *in vivo* translation rate in *ppk* mutants (99). These studies provide an explanation for the abundance of ribosomal proteins observed in *T. brucei* and *T. cruzi* polyP-binding proteomes. However, the specificity of these interactions should be confirmed in order to validate the presence of these proteins in polyP-binding proteomes. An initial approach could be the use of *TbVtc4*-KO cell line in BSF to measure the *in vivo* translation rate as compared with the wild type and the rescued cell lines.

Transcription factors and RNA binding proteins represent another significant functional group in the *T. brucei* and *T. cruzi* polyP-binding proteomes. A recent work reported a role for polyP in nucleolar transcription of myeloma cells (100). They found that myeloma plasma cells contain higher levels of intracellular polyP than normal plasma cells, and that polyP accumulates in the nucleolus of myeloma cells where transcription of ribosomal DNA genes is carried out by RNA

polymerase I. In this work they also confirmed that RNA polymerase I is modulated by polyP, opening up a broad spectrum of possibilities regarding the role of polyP as regulator of gene expression at the transcriptional level. In fact, another nucleolar enzyme that appeared with high score in *T. cruzi*, and also with a lower score in the *T. brucei* polyP-binding proteome, was the casein kinase II alpha subunit (CK2 α). This enzyme has been characterized in *T. brucei* (101) where it accumulates in the nucleolus, which is the site of ribosome biogenesis and where many of the CK2 substrates are present. This isoform of the catalytic subunit prefers ATP over GTP as substrate and modulators of its function are still unknown. It would be interesting to evaluate whether polyP regulates CK2 activity, as the anionic polymer and the enzyme localize to the nucleolus and are involved in transcription regulation.

Finally, we would like to mention that the *TbVtc4*-KO mutant cell line described in Chapter 2 would be a key tool to study the role of polyP on the activity of potential polyP-binding proteins found in *T. brucei*, an experimental work necessary for the validation of this proteomic data.

CHAPTER 5

CONCLUSIONS AND FUTURE DIRECTIONS

The role of Vtc4 in trypanosomes: what do we know now?

At the beginning of this project little was known about polyP synthesis in trypanosomes. In fact, the only eukaryotic polyP synthase described by that moment was the yeast ScVtc4p, a long chain polyP synthase that catalyzes polyP polymerization from ATP in a reaction enhanced by the presence of PP_i (5). However, the kinetic parameters of that enzyme were still unknown. At that point, there was proteomic data from our lab indicating the presence of a Vtc4 homologue in the acidocalcisomal fraction of *T. brucei*, as well as ortholog genes in other trypanosomatids, including *T. cruzi*. In addition, another subunit of the VTC complex, a 19 kDa protein named TbVtc1, had been characterized in our lab and the results showed an acidocalcisome localization of the protein and a role in polyP metabolism and acidocalcisome biogenesis, as RNAi experiments in PCF disturbed polyP levels, acidocalcisomes morphology, and osmoregulation, when the expression of TbVtc1 was ablated (42). However, this protein did not exhibit polyP synthase activity. The main contribution of the present study has been the characterization of TbVtc4 and TcVtc4. Our findings revealed these proteins are short chain polyP kinases located to acidocalcisomes of *T. brucei*

and *T. cruzi* in different developmental stages (in BSF and PCF of *T. brucei* and in *T. cruzi* epimastigotes). As previously observed for TbVtc1, TbVtc4 is also involved in cell growth and acidocalcisome biogenesis in PCF, but also a new role in osmoregulation and cell growth *in vivo* was disclosed for TbVtc4 in BSF, highlighting the importance of polyP for parasite survival in the infective stage of its life cycle. However, we noticed that the *in vitro* growth phenotype of TbVtc4-ablated mutant cell lines in PCF and BSF (Figs. 7 and 14) was not as dramatic as observed in RNAi-ablated TbVtc1 PCF, where cells displayed a strong growth defect from day 3 post-induction (42), even when this protein does not catalyze polyP synthesis. As TbVtc1 and TbVtc4 are expected to conform the VTC complex in the acidocalcisome membrane of *T. brucei*, we assume that the decrease in polyP levels observed in TbVtc1 is a consequence of the disruption of the VTC complex required for polyP synthesis and translocation (5). However, TbVtc1 is probably involved in other essential functions as described on its yeast homologue Vtc1p, involved in membrane trafficking and vacuole fusion (40,46,47), and that could be the explanation for the strong growth defect observed when the protein was ablated in PCF.

Another contribution of the biochemical characterization of recombinant Vtc4 catalytic domains of *T. brucei* and *T. cruzi* is the disclosure of kinetic parameters now available for both enzymes described in Chapters 2 and 3. In addition, we performed the kinetic characterization of the yeast enzyme (ScVtc4p) that allowed us to compare the features of all three enzymes and to

understand their abilities to synthesize polyphosphates of different sizes. The products of TbVtc4 are shorter (~100-300 mers) than those synthesized by ScVtc4p (>700 mers, Fig. 5) and the yeast enzyme is three times more efficient than the *T. brucei* enzyme when using ATP as substrate in the absence of PP_i (Table 1). The disclosure of TbVtc4 and TcVtc4 kinetic parameters will be useful for the search of possible inhibitors of these enzymes that could lead to the rational design of drugs to develop alternative therapies against sleeping sickness and Chagas disease, as homologues of Vtc4 enzyme have not been identified in mammalian cells.

The role of polyP in trypanosomes: where do we stand now?

The role of polyP in response to stress conditions was previously described in trypanosomes. Changes in polyP levels were observed when parasites were subjected to starvation and osmotic stress (13,26-28,42,102). In this study we confirmed the importance of polyP for parasites to overcome hyperosmotic and hyposmotic conditions and we hypothesize that the osmoregulatory defect displayed by *TbVtc4*-KO BSF is affecting their growth rate and ability to establish an efficient infection *in vivo*, as parasites were detected in the blood of mice infected with this mutant cell line but parasitemia levels were much lower than observed in mice infected with wild type BSF, or with parasites where the expression of the protein was induced back. In *T. cruzi* it has been demonstrated that polyP hydrolysis occurs when parasites are subjected to

hyposmotic conditions (13) and our explanation is that hydrolysis of polyP increases osmolyte concentration in the acidocalcisomes and facilitates water movement. On the contrary, polyP synthesis has been observed when *T. cruzi* epimastigotes are subjected to hyperosmotic stress (28). A model of metal ions sequestering by newly synthesized polyP to decrease the osmotic pressure of the cell has been proposed in that work. As the catalytic domain of yeast Vtc4p faces the cytosol and translocates polyP through its β -barrel structure to the lumen of the vacuole (5), we propose that during polyP synthesis in *T. brucei*, polyP is translocated by TbVtc4 to inside the acidocalcisome as well as metal ions through transporters in the acidocalcisome membrane, where they are chelated by newly synthesized polyP and stored in this electron dense organelle until the cell recovers the normal volume and overcome the osmotic stress situation. In the case of polyP-depleted BSF (*TbVtc4*-KO mutant cell line) we think these parasites are not able to overcome the hyperosmotic conditions when passing through the renal medulla of the mammalian host, and even though a few cells could survive, they should be weakened and unable to overcome the immune response of the host. This hypothesis has to be tested by infecting immunosuppressed mice with *TbVtc4*-KO BSF and evaluating mice survival as compared with the infection of wild-type mice.

Besides the role of polyP as a key molecule in the response of trypanosomes to stress conditions, our data from polyP-binding proteomes in *T. brucei* and *T. cruzi* revealed interesting information about functional groups of

proteins that potentially interact with polyP and could provide new clues about the polyP role in cellular physiology. As discussed in Chapter 4, proteins involved in glycolysis, translation, transcription and signal transduction, were found with a high score in both proteomes, suggesting a regulatory role of polyP through the interaction with these proteins. We consider imperative to confirm the interaction of polyP with glycosomal malate dehydrogenase, hexokinase, glycosomal phosphoenolpyruvate carboxykinase, snoRNP protein GAR1, casein kinase, actin related proteins and ribosomal proteins, to then study the nature and role of such interactions. For these experiments, TbVtc4 mutant cell lines (*TbVtc4*-KO and RNAi) generated in this study will be very useful.

REFERENCES

1. Rao, N. N., Gomez-Garcia, M. R., and Kornberg, A. (2009) *Annu Rev Biochem* **78**, 605-647
2. Smith, S. A., Mutch, N. J., Baskar, D., Rohloff, P., Docampo, R., and Morrissey, J. H. (2006) *Proc Natl Acad Sci U S A* **103**, 903-908
3. Muller, F., Mutch, N. J., Schenk, W. A., Smith, S. A., Esterl, L., Spronk, H. M., Schmidbauer, S., Gahl, W. A., Morrissey, J. H., and Renne, T. (2009) *Cell* **139**, 1143-1156
4. Docampo, R., de Souza, W., Miranda, K., Rohloff, P., and Moreno, S. N. (2005) *Nat Rev Microbiol* **3**, 251-261
5. Hothorn, M., Neumann, H., Lenherr, E. D., Wehner, M., Rybin, V., Hassa, P. O., Uttenweiler, A., Reinhardt, M., Schmidt, A., Seiler, J., Ladurner, A. G., Herrmann, C., Scheffzek, K., and Mayer, A. (2009) *Science* **324**, 513-516
6. Vercesi, A. E., Moreno, S. N., and Docampo, R. (1994) *Biochem J* **304** (Pt 1), 227-233
7. Docampo, R., Scott, D. A., Vercesi, A. E., and Moreno, S. N. (1995) *Biochem J* **310** (Pt 3), 1005-1012
8. World Health Organization. (2013) Fact sheet N°259: Human African trypanosomiasis (sleeping sickness). *WHO Media Centre*.
9. World Health Organization. (2013) Fact sheet N°340: American trypanosomiasis (Chagas disease). *WHO Media Centre*.
10. Urbina, J. A., and Docampo, R. (2003) *Trends Parasitol* **19**, 495-501
11. Bowling, J., and Walter, E. A. (2009) *Expert Rev Anti Infect Ther* **7**, 1223-1234
12. Rohloff, P., Montalvetti, A., and Docampo, R. (2004) *J Biol Chem* **279**, 52270-52281
13. Ruiz, F. A., Rodrigues, C. O., and Docampo, R. (2001) *J Biol Chem* **276**, 26114-26121
14. Moreno, S. N., and Docampo, R. (2013) *PLoS Pathog* **9**, e1003230

15. Babes, V. (1895) *Zentrabl. Bakteriolog. Parasitenkd. Infektionskr.* **20**, 412-420
16. Meyer, A. (1904) *Bot. Zeit.* **62** 113-152
17. Wiame, J. (1947) *Biochim Biophys Acta* **1**, 234-255
18. Kornberg, A. (1995) *J Bacteriol* **177**, 491-496
19. Docampo, R., and Moreno, S. N. (2001) *Mol Biochem Parasitol* **114**, 151-159
20. Docampo, R., and Moreno, S. N. (2011) *Cell Calcium* **50**, 113-119
21. Huang, G., Bartlett, P. J., Thomas, A. P., Moreno, S. N., and Docampo, R. (2013) *Proc Natl Acad Sci U S A* **110**, 1887-1892
22. Seufferheld, M., Vieira, M. C., Ruiz, F. A., Rodrigues, C. O., Moreno, S. N., and Docampo, R. (2003) *J Biol Chem* **278**, 29971-29978
23. Seufferheld, M., Lea, C. R., Vieira, M., Oldfield, E., and Docampo, R. (2004) *J Biol Chem* **279**, 51193-51202
24. Ruiz, F. A., Lea, C. R., Oldfield, E., and Docampo, R. (2004) *J Biol Chem* **279**, 44250-44257
25. Docampo, R., Ulrich, P., and Moreno, S. N. (2010) *Philos Trans R Soc Lond B Biol Sci* **365**, 775-784
26. Galizzi, M., Bustamante, J. M., Fang, J., Miranda, K., Soares Medeiros, L. C., Tarleton, R. L., and Docampo, R. (2013) *Mol Microbiol*
27. de Jesus, T. C., Tonelli, R. R., Nardelli, S. C., da Silva Augusto, L., Motta, M. C., Girard-Dias, W., Miranda, K., Ulrich, P., Jimenez, V., Barquilla, A., Navarro, M., Docampo, R., and Schenkman, S. (2010) *J Biol Chem* **285**, 24131-24140
28. Li, Z. H., Alvarez, V. E., De Gaudenzi, J. G., Sant'anna, C., Frasch, A. C., Cazzulo, J. J., and Docampo, R. (2011) *J Biol Chem* **286**, 43959-43971
29. Docampo, R., Jimenez, V., Lander, N., Li, Z. H., and Niyogi, S. (2013) *Int Rev Cell Mol Biol* **305**, 69-113
30. Morrissey, J. H., Choi, S. H., and Smith, S. A. (2012) *Blood* **119**, 5972-5979
31. Ahn, K., and Kornberg, A. (1990) *J Biol Chem* **265**, 11734-11739

32. Zhang, H., Ishige, K., and Kornberg, A. (2002) *Proc Natl Acad Sci U S A* **99**, 16678-16683
33. Gomez-Garcia, M. R., and Kornberg, A. (2004) *Proc Natl Acad Sci U S A* **101**, 15876-15880
34. Wurst, H., Shiba, T., and Kornberg, A. (1995) *J Bacteriol* **177**, 898-906
35. Rodrigues, C. O., Ruiz, F. A., Vieira, M., Hill, J. E., and Docampo, R. (2002) *J Biol Chem* **277**, 50899-50906
36. Fang, J., Ruiz, F. A., Docampo, M., Luo, S., Rodrigues, J. C., Motta, L. S., Rohloff, P., and Docampo, R. (2007) *J Biol Chem* **282**, 32501-32510
37. Tammenkoski, M., Koivula, K., Cusanelli, E., Zollo, M., Steegborn, C., Baykov, A. A., and Lahti, R. (2008) *Biochemistry* **47**, 9707-9713
38. Lonetti, A., Szigyarto, Z., Bosch, D., Loss, O., Azevedo, C., and Saiardi, A. (2011) *J Biol Chem* **286**, 31966-31974
39. Ogawa, N., DeRisi, J., and Brown, P. O. (2000) *Mol Biol Cell* **11**, 4309-4321
40. Cohen, A., Perzov, N., Nelson, H., and Nelson, N. (1999) *J Biol Chem* **274**, 26885-26893
41. Nelson, N., Perzov, N., Cohen, A., Hagai, K., Padler, V., and Nelson, H. (2000) *J Exp Biol* **203**, 89-95
42. Fang, J., Rohloff, P., Miranda, K., and Docampo, R. (2007) *Biochem J* **407**, 161-170
43. Lander, N., P.N., U., and Docampo, R. (2013) *J. Biol. Chem.* **in press**, in press
44. Moreno-Sanchez, D., Hernandez-Ruiz, L., Ruiz, F. A., and Docampo, R. (2012) *J Biol Chem* **287**, 28435-28444
45. Sethuraman, A., Rao, N. N., and Kornberg, A. (2001) *Proc Natl Acad Sci U S A* **98**, 8542-8547
46. Muller, O., Bayer, M. J., Peters, C., Andersen, J. S., Mann, M., and Mayer, A. (2002) *Embo J* **21**, 259-269
47. Muller, O., Neumann, H., Bayer, M. J., and Mayer, A. (2003) *J Cell Sci* **116**, 1107-1115

48. Patel, S., and Docampo, R. (2010) *Trends Cell Biol* **20**, 277-286
49. Docampo, R., Jimenez, V., King-Keller, S., Li, Z. H., and Moreno, S. N. (2011) *Adv Parasitol* **75**, 307-324
50. Rohloff, P., and Docampo, R. (2008) *Exp Parasitol* **118**, 17-24
51. Ulrich, P. N., Jimenez, V., Park, M., Martins, V. P., Atwood, J., 3rd, Moles, K., Collins, D., Rohloff, P., Tarleton, R., Moreno, S. N., Orlando, R., and Docampo, R. (2011) *PLoS One* **6**, e18013
52. Wirtz, E., and Clayton, C. (1995) *Science* **268**, 1179-1183
53. Wirtz, E., Leal, S., Ochatt, C., and Cross, G. A. (1999) *Mol Biochem Parasitol* **99**, 89-101
54. Huang, G., Fang, J., Sant'Anna, C., Li, Z. H., Wellems, D. L., Rohloff, P., and Docampo, R. (2011) *J Biol Chem* **286**, 36619-36630
55. Lemercier, G., Dutoya, S., Luo, S., Ruiz, F. A., Rodrigues, C. O., Baltz, T., Docampo, R., and Bakalara, N. (2002) *J Biol Chem* **277**, 37369-37376
56. Oberholzer, M., Morand, S., Kunz, S., and Seebeck, T. (2006) *Mol Biochem Parasitol* **145**, 117-120
57. Falquet, L., Pagni, M., Bucher, P., Hulo, N., Sigrist, C. J., Hofmann, K., and Bairoch, A. (2002) *Nucleic Acids Res* **30**, 235-238
58. Claros, M. G., and von Heijne, G. (1994) *Comput Appl Biosci* **10**, 685-686
59. Aslett, M., Aurrecochea, C., Berriman, M., Brestelli, J., Brunk, B. P., Carrington, M., Depledge, D. P., Fischer, S., Gajria, B., Gao, X., Gardner, M. J., Gingle, A., Grant, G., Harb, O. S., Heiges, M., Hertz-Fowler, C., Houston, R., Innamorato, F., Iodice, J., Kissinger, J. C., Kraemer, E., Li, W., Logan, F. J., Miller, J. A., Mitra, S., Myler, P. J., Nayak, V., Pennington, C., Phan, I., Pinney, D. F., Ramasamy, G., Rogers, M. B., Roos, D. S., Ross, C., Sivam, D., Smith, D. F., Srinivasamoorthy, G., Stoeckert, C. J., Jr., Subramanian, S., Thibodeau, R., Tivey, A., Treatman, C., Velarde, G., and Wang, H. (2010) *Nucleic Acids Res* **38**, D457-462
60. Medina-Acosta, E., and Cross, G. A. (1993) *Mol Biochem Parasitol* **59**, 327-329
61. Kocic, I., Hirano, Y., and Hiraoka, M. (2001) *Cardiovasc Res* **51**, 59-70
62. Herbert, W. J., and Lumsden, W. H. (1976) *Exp Parasitol* **40**, 427-431

63. Rohloff, P., Rodrigues, C. O., and Docampo, R. (2003) *Mol Biochem Parasitol* **126**, 219-230
64. Scott, D. A., Docampo, R., Dvorak, J. A., Shi, S., and Leapman, R. D. (1997) *J Biol Chem* **272**, 28020-28029
65. Rodrigues, C. O., Scott, D. A., and Docampo, R. (1999) *Mol Cell Biol* **19**, 7712-7723
66. Cagnac, O., Leterrier, M., Yeager, M., and Blumwald, E. (2007) *J Biol Chem* **282**, 24284-24293
67. Rao, N. N., and Kornberg, A. (1996) *J Bacteriol* **178**, 1394-1400
68. Moreno, B., Urbina, J. A., Oldfield, E., Bailey, B. N., Rodrigues, C. O., and Docampo, R. (2000) *J Biol Chem* **275**, 28356-28362
69. Lang, F., Busch, G. L., Ritter, M., Volkl, H., Waldegger, S., Gulbins, E., and Haussinger, D. (1998) *Physiol Rev* **78**, 247-306
70. Emmer, B. T., Nakayasu, E. S., Souther, C., Choi, H., Sobreira, T. J., Epting, C. L., Nesvizhskii, A. I., Almeida, I. C., and Engman, D. M. (2011) *Eukaryot Cell* **10**, 455-463
71. Furuya, T., Kashuba, C., Docampo, R., and Moreno, S. N. (2000) *J Biol Chem* **275**, 6428-6438
72. de Paulo Martins, V., Okura, M., Maric, D., Engman, D. M., Vieira, M., Docampo, R., and Moreno, S. N. (2010) *J Biol Chem* **285**, 30906-30917
73. Shiba, T., Tsutsumi, K., Yano, H., Ihara, Y., Kameda, A., Tanaka, K., Takahashi, H., Munekata, M., Rao, N. N., and Kornberg, A. (1997) *Proc Natl Acad Sci U S A* **94**, 11210-11215
74. Kim, K. S., Rao, N. N., Fraley, C. D., and Kornberg, A. (2002) *Proc Natl Acad Sci U S A* **99**, 7675-7680
75. Zhang, H., Gomez-Garcia, M. R., Shi, X., Rao, N. N., and Kornberg, A. (2007) *Proc Natl Acad Sci U S A* **104**, 16486-16491
76. Rooney, P. J., Ayong, L., Tobin, C. M., Moreno, S. N., and Knoll, L. J. (2011) *Mol Biochem Parasitol* **176**, 121-126
77. Bone, G. J., and Steinert, M. (1956) *Nature* **178**, 308-309
78. Redmond, S., Vadivelu, J., and Field, M. C. (2003) *Mol Biochem Parasitol* **128**, 115-118

79. LaCount, D. J., Barrett, B., and Donelson, J. E. (2002) *J Biol Chem* **277**, 17580-17588
80. Vazquez, M. P., and Levin, M. J. (1999) *Gene* **239**, 217-225
81. Vandesompele, J., De Preter, K., Pattyn, F., Poppe, B., Van Roy, N., De Paepe, A., and Speleman, F. (2002) *Genome Biol* **3**, RESEARCH0034
82. Ault-Riche, D., Fraley, C. D., Tzeng, C. M., and Kornberg, A. (1998) *J Bacteriol* **180**, 1841-1847
83. Jones, D. T. (1999) *J Mol Biol* **292**, 195-202
84. McGuffin, L. J., Bryson, K., and Jones, D. T. (2000) *Bioinformatics* **16**, 404-405
85. Kollien, A. H., and Schaub, G. A. (2000) *Parasitol Today* **16**, 381-387
86. Reusch, R. N. (2012) *Chem Biodivers* **9**, 2343-2366
87. Holmstrom, K. M., Marina, N., Baev, A. Y., Wood, N. W., Gourine, A. V., and Abramov, A. Y. (2013) *Nat Commun* **4**, 1362
88. Choi, S. H., Collins, J. N., Smith, S. A., Davis-Harrison, R. L., Rienstra, C. M., and Morrissey, J. H. (2010) *Biochemistry* **49**, 9935-9941
89. Cunningham, I. (1977) *J Protozool* **24**, 325-329
90. Caceres, A. J., Portillo, R., Acosta, H., Rosales, D., Quinones, W., Avilan, L., Salazar, L., Dubourdieu, M., Michels, P. A., and Concepcion, J. L. (2003) *Mol Biochem Parasitol* **126**, 251-262
91. Willson, M., Sanejouand, Y. H., Perie, J., Hannaert, V., and Opperdoes, F. (2002) *Chem Biol* **9**, 839-847
92. Fraga, A., Moraes, J., da Silva, J. R., Costa, E. P., Menezes, J., da Silva Vaz, I., Jr., Logullo, C., da Fonseca, R. N., and Campos, E. (2013) *Int J Biol Sci* **9**, 842-852
93. Bringaud, F., Baltz, D., and Baltz, T. (1998) *Proc Natl Acad Sci U S A* **95**, 7963-7968
94. Maldonado, R. A., and Fairlamb, A. H. (2001) *Mol Biochem Parasitol* **112**, 183-191
95. Rodriguez, E., Lander, N., and Ramirez, J. L. (2009) *Mem Inst Oswaldo Cruz* **104**, 745-748

96. Michels, P. A., Chevalier, N., Opperdoes, F. R., Rider, M. H., and Rigden, D. J. (1997) *Eur J Biochem* **250**, 698-704
97. Semenyuk, P. I., Muronetz, V. I., Haertle, T., and Izumrudov, V. A. (2013) *Biochimica et biophysica acta* **1830**, 4800-4805
98. Kuroda, A., Nomura, K., Ohtomo, R., Kato, J., Ikeda, T., Takiguchi, N., Ohtake, H., and Kornberg, A. (2001) *Science* **293**, 705-708
99. McInerney, P., Mizutani, T., and Shiba, T. (2006) *Mol Microbiol* **60**, 438-447
100. Jimenez-Nunez, M. D., Moreno-Sanchez, D., Hernandez-Ruiz, L., Benitez-Rondan, A., Ramos-Amaya, A., Rodriguez-Bayona, B., Medina, F., Brieva, J. A., and Ruiz, F. A. (2012) *Haematologica* **97**, 1264-1271
101. Park, J. H., Brekken, D. L., Randall, A. C., and Parsons, M. (2002) *Mol Biochem Parasitol* **119**, 97-106
102. Lemercier, G., Espiau, B., Ruiz, F. A., Vieira, M., Luo, S., Baltz, T., Docampo, R., and Bakalara, N. (2004) *J Biol Chem* **279**, 3420-3425